

# **The characterisation and application of bacterial nitroreductase enzymes**

**By**

**Sarah Condon**

A thesis submitted to Victoria University of Wellington  
in fulfilment of the requirements for the degree of  
Master of Science  
in Cell and Molecular Bioscience

Victoria University of Wellington  
(2013)

## **Abstract**

Cancer is an increasing global concern, with the number of people diagnosed growing rapidly each year. Gene directed enzyme prodrug therapy (GDEPT) is emerging as a front-runner of new technologies that seek to combat the growing number of cases. One developing approach to GDEPT involves the use of bacterial nitroreductase enzymes to reduce prodrug substrates, which, upon reduction to their active form, are toxic to cancer cells through DNA crosslinking.

Nitroreductases have the ability to activate a variety of nitro-quenched compounds, not only anti-cancer prodrugs, but also nil bystander antibiotics and masked fluorophores, through the reduction of strongly electron-withdrawing nitro substituents on aromatic rings. My research initially sought to exploit this capability by partnering nitroreductases with nil bystander antibiotics for targeted cell ablation, as a component of a larger gene directed enzyme prodrug therapy project. This has potential to provide important safety features for removal of viral and bacterial vectors following anti-cancer gene therapy.

From this, the main focus evolved into utilising nitroreductase enzymes for targeted cell ablation for applications in developmental and regenerative biology. This exploited the ability of nitroreductases to activate nil bystander antibiotics in partnership with masked fluorophores for imaging purposes. It has previously been shown that antibiotics can be applied to a nitroreductase under control of a tissue-specific promoter in a transgenic model organism, enabling controlled ablation of that tissue at precise stages of development. However, direct imaging of the nitroreductase location and activity, by application of masked fluorophore probes prior to ablation, has not previously been explored.

During the course of this work, several promising combinations of nitroreductases that exhibit opposing specificities for certain combinations of masked fluorophores and nil-bystander antibiotics were identified through screening in bacterial systems. In general, these results were found to translate effectively into eukaryotic cell lines. Pairs of nitroreductases that have opposite specificities for two different antibiotic substrates offer potential for the multiplexed ablation of either (or both) of two

different labelled tissues in the same transgenic model organism, according to the substrate(s) administered to that organism.

Throughout this screening process, a nitroaromatic substrate (niclosamide) was identified that is, uniquely, initially toxic to *Escherichia coli* but becomes non-toxic upon reduction of the nitro substituent. Using niclosamide, a novel strategy with potential for identification of new nitroreductases, as well as selection-based directed evolution to improve desired activities, was explored.

## Acknowledgements

Firstly I would like to thank my supervisor David Ackerley, for always being able to help with this project, and the ability to envision a clear final goal for experimental work, seeing the bigger picture and applying what you are doing to this kind of context was always hugely motivating. And thank you for putting in the enormous effort of proof reading and revision of this thesis.

I am also extremely grateful for our collaborators at the Auckland Cancer Research Society Centre for the use of compounds synthesised there, and new ideas for experimental work. Without them my project would not have evolved in the way it has as the use of their masked fluorophores has expanded the range of my thesis greatly.

I would like to thank everyone in the Ackerley lab. Working in the lab was always a good time, and anytime I needed help with anything, I knew that there would be plenty of people more than willing to help. In particular I would like to say a big thanks to Janine and Elsie, who first showed me my way around the bacterial and working with nitroreductase enzymes – your knowledge and continuing experimental guidance has been a huge help throughout this process and much appreciated.

Also, a big thanks to Claire who, with minimal time to complete her thesis, showed me the ins and outs of tissue culture in limited time. Varun and Amy have also been especially helpful when it has come to all things tissue culture, without you guys I don't think I would've got very far with any work that needed to be done in tissue culture, so thanks.

Finally I would like to thank friends and family for always being around when I needed a distraction; encouraging me to take breaks when they thought I'd been working too hard, or enabling me to focus when I needed too, and always with words of encouragement.

Thank you to everyone who has helped in any way with the completion of this thesis; every little bit has been appreciated.

## Table of Contents

Abstract.....	i
Acknowledgements .....	iii
List of figures .....	xi
List of tables.....	xvi
List of abbreviations .....	xviii
Preface .....	1
<b>1. Introduction.....</b>	<b>1</b>
<b>1.1 Current cancer treatments.....</b>	<b>1</b>
<b>1.2 Hypoxia targeted prodrugs .....</b>	<b>2</b>
<b>1.2.1 Nitroaromatic hypoxia activated prodrugs .....</b>	<b>4</b>
<b>1.3 GDEPT.....</b>	<b>6</b>
<b>1.3.1 <i>E. coli</i> nitroreductase (NfsB) and 5-aziridin-1-yl-2-4- dinitrobenzamide (CB1954).....</b>	<b>7</b>
<b>1.4 The 58-membered nitroreductase library.....</b>	<b>9</b>
<b>1.5 Nil bystander antibiotics .....</b>	<b>11</b>
<b>1.6 Masked fluorophores .....</b>	<b>12</b>
<b>1.7 Regenerative and developmental biological studies.....</b>	<b>13</b>
<b>1.7.1 Case studies utilising nitroreductase ablation technology.....</b>	<b>15</b>
<b>1.7.2 Limitations of the NfsB_Ec/ metronidazole system .....</b>	<b>17</b>

<b>1.7.3</b> Combining this technology with masked fluorophores .....	17
<b>1.7.4</b> Dual reporter/ ablation system exploiting the characteristics of nitroreductases .....	18
<b>1.8</b> Aims.....	19
<b>2. Materials and Methods</b> .....	21
<b>2.1</b> Chemicals .....	21
<b>2.1.1</b> Nil bystander antibiotics .....	21
<b>2.1.2</b> Masked fluorophores .....	23
<b>2.2</b> Enzymes .....	26
<b>2.3</b> Bacterial strains and plasmids .....	26
<b>2.4</b> Mammalian cell lines and plasmids .....	26
<b>2.5</b> Oligonucleotide primers .....	27
<b>2.6</b> Growth and maintenance of bacteria .....	31
<b>2.6.1</b> Media .....	31
<b>2.6.1.1</b> Liquid media.....	31
<b>2.6.1.2</b> Solid media.....	32
<b>2.6.2</b> Growth of bacterial strains.....	32
<b>2.7</b> Growth and maintenance of mammalian cell lines.....	32
<b>2.7.1</b> Media .....	32
<b>2.7.2</b> Antibiotics.....	33
<b>2.7.3</b> Growth of mammalian cells.....	33

<b>2.7.3.1</b> Harvesting cells .....	33
<b>2.8</b> Standard molecular biology protocols .....	34
<b>2.8.1</b> Chemically competent cells .....	34
<b>2.8.2</b> Transformation protocol .....	35
<b>2.8.3</b> Electrocompetent cells .....	35
<b>2.8.4</b> Electroporation protocol .....	35
<b>2.8.5</b> Colony screening .....	36
<b>2.8.6</b> DNA quantification .....	36
<b>2.8.7</b> Polymerase chain reaction (PCR).....	36
<b>2.8.8</b> PCR components .....	36
<b>2.8.9</b> PCR parameters .....	37
<b>2.8.10</b> Agarose gel electrophoresis .....	38
<b>2.8.11</b> Restriction digests.....	38
<b>2.8.12</b> Sequencing .....	38
<b>2.8.13</b> Miniprep protocol.....	39
<b>2.8.14</b> Midiprep protocol.....	39
<b>2.8.15</b> SDS PAGE protocol .....	39
<b>2.8.15.1</b> Recipes for SDS PAGE gels and buffers .....	40
<b>2.9</b> Bacterial cell protocols.....	41
<b>2.9.1</b> SOS assay.....	41

2.9.2 Growth inhibition assay .....	42
2.9.3 IC <sub>50</sub> analysis .....	42
2.9.4 Fluorescence assay .....	43
2.9.5 Combined growth inhibition and fluorescence assays.....	44
2.9.6 Bacterial confocal microscopy .....	44
2.9.7 Validation of liquid media protocol with potential to be used for novel nitroreductase discovery .....	45
2.9.8 Validation of solid media protocol with potential to be used for novel nitroreductase discovery .....	45
2.10 Mammalian cell protocols .....	45
2.10.1 Construction of mammalian NTR stable expression cell lines .....	45
2.10.2 Creating Gateway® constructs.....	45
2.10.3 BP recombination .....	46
2.10.4 Analysing entry clones .....	46
2.10.5 LR recombination.....	46
2.10.6 Confirming the identity of F279/ V5 destination clones .....	47
2.10.7 Stable Transfection Cell Lines .....	47
2.10.7.1 Lipofectamine™ 2000 reagent protocol .....	47
2.10.7.2 Making stocks of stable cell lines .....	48
2.10.8 MTS assay.....	48
2.10.9 Confocal microscopy in mammalian cells .....	49



2.10.10 Microscopy of challenged mammalian cells .....	49
2.10.11 Confocal microscopy of challenged mammalian cells treated with masked fluorophores .....	49
3. Nil Bystander Antibiotics .....	50
3.1 Introduction .....	50
3.1.1 Nil bystander antibiotics .....	52
3.1.2 Nitroreductase library .....	55
3.1.3 Aims.....	56
3.2 Results .....	57
3.2.1 Identification of nitroreductases with a superior activation profile with metronidazole than NfsB_Ec .....	57
3.2.2 Growth inhibition assays.....	62
3.2.3 Identification of pairs of nitroreductases / nil bystander antibiotics with opposing activation profiles .....	66
3.2.4 Nitroreductase mediated cell ablation in human cell lines .....	71
3.2.5 Gateway <sup>TM</sup> recombination system .....	72
3.2.6 Cell ablation in human cell lines .....	73
3.2.7 Niclosamide.....	77
3.2.8 Exploiting the characteristics of niclosamide .....	78
3.2.8.1 Optimisation of niclosamide selection in liquid media .....	78
3.2.8.2 Optimisation of niclosamide selection in solid media .....	82

<b>3.3 Discussion</b> .....	85
<b>4. Masked Fluorophores</b> .....	90
<b>4.1 Introduction</b> .....	90
<b>4.1.1 Masked fluorophores</b> .....	91
<b>4.1.2 Fluorescent reporter proteins</b> .....	91
<b>4.1.3 Dual ablation/ reporter system in developmental biology</b> .....	92
<b>4.1.4 6KO library</b> .....	93
<b>4.1.5 Aims</b> .....	94
<b>4.2 Results</b> .....	94
<b>4.2.1 Fluorescent screening in bacterial cells</b> .....	94
<b>4.2.2 Combined fluorescence reporting and cell ablation</b> .....	97
<b>4.2.3 Dual fluorophore screening in bacterial cells</b> .....	101
<b>4.2.4 Dual fluorophore screening in human cell lines</b> .....	105
<b>4.2.5 Dual fluorescence reporting/ nil bystander antibiotic targeted cell ablation</b> .....	110
<b>4.3 Discussion</b> .....	117
<b>5. Summary, Conclusions, and Future Directions</b> .....	120
<b>5.1 Research motivation</b> .....	120
<b>5.1.1 GDEPT</b> .....	120
<b>5.1.2 Novel developmental biology tools</b> .....	121
<b>5.2 Key Findings</b> .....	123

5.2.1 Identification of nitroreductases active with nil bystander antibiotics.....	123
5.2.2 Identification of nitroreductases superior to NfsB_Ec for metronidazole activation .....	123
5.2.3 Combined dual reporter/ ablation system .....	124
5.2.4 Niclosamide.....	126
5.3 Future Directions .....	126
5.3.1 GDEPT.....	126
5.3.2 Developmental and regenerative biological studies .....	127
5.3.3 Niclosamide as a tool for directed evolution .....	128
5.4 Concluding remarks .....	128
References .....	130

## List of Figures

<b>Figure 1.1</b>	Hypoxia prodrug mechanism of activation .....	4
<b>Figure 1.2</b>	Hypoxia activation of nitroaromatic prodrug .....	4
<b>Figure 1.3</b>	Structures of nitroaromatic anti-cancer compounds .....	5
<b>Figure 1.4</b>	Hypoxia activated nitroaromatic prodrug .....	6
<b>Figure 1.5</b>	GDEPT Overview .....	7
<b>Figure 1.6</b>	Dr Adam Patterson, University of Auckland, unpublished work.....	11
<b>Figure 1.7</b>	FSL76 and FSL178 .....	12
<b>Figure 1.8</b>	Bioreductive trigger molecule components.....	13
<b>Figure 1.9</b>	Targeted cell ablation in zebrafish.....	16
<b>Figure 1.10</b>	Live imaging of oligodendrocyte depletion and reappearance following metronidazole treatment and cessation .....	17
<b>Figure 1.11</b>	Nitroreductases with opposing specificities for both masked fluorophores and nil-bystander antibiotics .....	18
<b>Figure 3.1</b>	Map of pUCX expression plasmid .....	56
<b>Figure 3.2</b>	Metabolism of metronidazole by members of the 58 nitroreductase over-expression library as measured by growth inhibition assay .....	58
<b>Figure 3.3</b>	Metabolism of metronidazole by 6 nitroreductase enzymes from the 58 nitroreductase enzyme over-expression library over a range of concentrations as measured by IC <sub>50</sub> analysis .....	59
<b>Figure 3.4</b>	Metronidazole challenged HCT-116: NfsB_Vh cells.....	61

<b>Figure 3.5</b>	Metronidazole challenged HEK293: NfsB_Ec cells .....	62
<b>Figure 3.6</b>	Colour coded heat-map summarising activation profiles of nitroreductase/ nil bystander antibiotic combination .....	64
<b>Figure 3.7</b>	Identification of nitroreductase enzymes that exhibit opposing activation profiles with tinidazole and metronidazole .....	66
<b>Figure 3.8</b>	Identification of nitroreductase enzymes that exhibit opposing activation profiles with F-misonidazole and metronidazole .....	66
<b>Figure 3.9</b>	Identification of nitroreductase enzymes that exhibit opposing activation profiles with EF5 and dimetridazole .....	67
<b>Figure 3.10</b>	Identification of nitroreductase enzymes that exhibit opposing activation profiles with EF5/ and metronidazole .....	67
<b>Figure 3.11</b>	Metabolism of metronidazole and tinidazole by <i>E. coli</i> cells over- expressing nitroreductase NfsA_Li over a range of concentrations as measured by IC <sub>50</sub> analysis .....	68
<b>Figure 3.12</b>	Metabolism of metronidazole and tinidazole by <i>E. coli</i> cells over- expressing nitroreductase NfsA_Pp over a range of concentrations as measured by IC <sub>50</sub> analysis .....	68
<b>Figure 3.13</b>	Metabolism of metronidazole and tinidazole by <i>E. coli</i> cells over- expressing nitroreductase NfsA_Ecaro over a range of concentrations as measured by IC <sub>50</sub> analysis .....	69
<b>Figure 3.14</b>	Metabolism of metronidazole and tinidazole by <i>E. coli</i> cells over- expressing nitroreductase NfsB_Vv over a range of concentrations as measured by IC <sub>50</sub> analysis .....	70
<b>Figure 3.15</b>	Overview of the Gateway <sup>TM</sup> recombination system .....	73
<b>Figure 3.16</b>	Metronidazole and tinidazole challenged HEK293 WT cells .....	74
<b>Figure 3.17</b>	Metronidazole and tinidazole challenged HEK293: NfsA_Pp cells.....	75

<b>Figure 3.18</b>	Metronidazole and tinidazole challenged HEK293: NfsB_Vv cells .....	76
<b>Figure 3.19</b>	Metabolism of metronidazole or niclosamide by members of the 58 nitroreductase over-expression library as measured by growth inhibition assay .....	78
<b>Figure 3.20</b>	Metabolism of niclosamide by <i>E.coli</i> 6KO overexpressing NfsA_Vv or pUCX over an 8 h time period .....	80
<b>Figure 3.21</b>	Metabolism of niclosamide by <i>E.coli</i> 7KO overexpressing NfsA_Vv or pUCX over an 8 h time period .....	80
<b>Figure 3.22</b>	Metabolism of niclosamide by <i>E.coli</i> SOS-R2 overexpressing NfsA_Vv or pUCX over an 8 h time period .....	81
<b>Figure 3.23</b>	PCR confirmation of active nitroreductase enzymes from colonies picked from mixed culture NfsA_Vv/ pUCX plated on media containing metronidazole and niclosamide.....	84
<b>Figure 3.24</b>	FSL41 fluorescence visualised on UV trans-illuminator as confirmation of active nitroreductase enzymes from colonies picked from mixed culture NfsA_Vv/ pUCX plated on media containing metronidazole and niclosamide .....	84
<b>Figure 3.25</b>	FSL41 fluorescence plate reader ex 355 nm/ em 460 nm values as confirmation of active nitroreductase enzymes from colonies picked from mixed culture NfsA_Vv/ pUCX plated on media containing metronidazole and niclosamide ....	85
<b>Figure 4.1</b>	Heat-map of 23 nitroreductase 6KO library with different masked fluorophores .....	96
<b>Figure 4.2</b>	UV Trans-illuminator image of FSL41-treated cultures of <i>E. coli</i> 6KO over-expressing different candidate nitroreductases, with (top) or without (bottom) antibiotic challenge .....	97
<b>Figure 4.3</b>	6KO <i>E. coli</i> empty plasmid (pUCX) control strain treated with FSL41 .....	98
<b>Figure 4.4</b>	6KO <i>E. coli</i> over-expressing NfsB_Vh, treated with FSL41 .....	98

<b>Figure 4.5</b>	6KO <i>E. coli</i> over-expressing NfsB_Vh treated with FSL41 and metronidazole.....	99
<b>Figure 4.6</b>	HCT116: NfsB_Vh treated with FSL41 .....	100
<b>Figure 4.7</b>	HCT116: NfsB_Vh treated with FSL41 and challenged with metronidazole.....	100
<b>Figure 4.8</b>	Identification of candidate nitroreductase enzymes that exhibit opposing activation profiles for two nil bystander antibiotics, and two masked fluorophores .....	102
<b>Figure 4.9</b>	6KO <i>E. coli</i> over-expressing NfsA_Pp treated with FSL76 .....	102
<b>Figure 4.10</b>	6KO <i>E. coli</i> over-expressing NfsA_Pp treated with FSL178 .....	103
<b>Figure 4.11</b>	6KO <i>E. coli</i> over-expressing NfsB_Vv treated with FSL178 .....	103
<b>Figure 4.12</b>	6KO <i>E. coli</i> over-expressing NfsB_Vv treated with FSL76 .....	103
<b>Figure 4.13</b>	6KO <i>E. coli</i> mixed culture multiplex fluorescence imaging .....	104
<b>Figure 4.14</b>	6KO <i>E. coli</i> pUCX treated with FSL76 and FSL178 .....	104
<b>Figure 4.15</b>	HEK293 WT cells treated with either FSL41, FSL76, or FSL178 .....	106
<b>Figure 4.16</b>	HEK293: NfsB_Ec treated with FSL41 .....	106
<b>Figure 4.17</b>	HEK293: NfsB_Vv treated with FSL41 .....	107
<b>Figure 4.18</b>	HEK293: NfsA_Pp treated with FSL41 .....	107
<b>Figure 4.19</b>	HEK293: NfsA_Pp treated with FSL76.....	108
<b>Figure 4.20</b>	HEK293: NfsA_Pp treated with FSL178 .....	108
<b>Figure 4.21</b>	HEK293: NfsB_Vv treated with FSL178 .....	109
<b>Figure 4.22</b>	HEK293: NfsB_Vv treated with FSL76 .....	109

<b>Figure 4.23</b>	HEK293 mixed culture multiplex fluorescence imaging.....	110
<b>Figure 4.24</b>	6KO <i>E. coli</i> over-expressing NfsA_Pp treated with FSL76 and challenged with metronidazole .....	111
<b>Figure 4.25</b>	6KO <i>E. coli</i> over-expressing NfsA_Pp treated with FSL76 and challenged with tinidazole .....	111
<b>Figure 4.26</b>	6KO <i>E. coli</i> over-expressing NfsB_Vv treated with FSL178 and challenged with tinidazole .....	111
<b>Figure 4.27</b>	6KO <i>E. coli</i> over-expressing NfsB_Vv treated with FSL178 and challenged with metronidazole .....	112
<b>Figure 4.28</b>	6KO <i>E. coli</i> mixed culture multiplex fluorescence imaging and ablation challenged with metronidazole .....	113
<b>Figure 4.29</b>	6KO <i>E. coli</i> mixed culture multiplex fluorescence imaging and ablation challenged with tinidazole .....	113
<b>Figure 4.30</b>	6KO <i>E. coli</i> mixed culture multiplex fluorescence imaging and ablation challenged with metronidazole and tinidazole.....	114
<b>Figure 4.31</b>	HEK293: NfsA_Pp treated with FSL76 and challenged with tinidazole.....	115
<b>Figure 4.32</b>	HEK293: NfsB_Vv treated with FSL178 and challenged with metronidazole .....	115
<b>Figure 4.33</b>	HEK293 mixed culture multiplex fluorescence imaging and ablation challenged with metronidaazole.....	116
<b>Figure 4.34</b>	HEK293 mixed culture multiplex fluorescence imaging and ablation challenged with tinidazole .....	117



## List of Tables

<b>Table 1.1</b> Complete 58 nitroreductase library .....	9
<b>Table 2.1</b> Nil bystander antibiotics .....	21
<b>Table 2.2</b> Masked fluorophores.....	24
<b>Table 2.3</b> Bacterial Strains .....	26
<b>Table 2.4</b> Plasmids.....	26
<b>Table 2.5</b> Mammalian cell lines .....	26
<b>Table 2.6</b> Plasmids.....	27
<b>Table 2.7</b> Oligonucleotide Primers .....	27
<b>Table 2.8</b> Growth media supplements and antibiotics.....	32
<b>Table 2.9</b> Antibiotics used in the growth of mammalian cell lines .....	33
<b>Table 2.10</b> Recipes for chemically competent cell buffers .....	34
<b>Table 2.11</b> PCR components.....	36
<b>Table 2.12</b> PCR parameters.....	37
<b>Table 2.13</b> Restriction digest parameters.....	38
<b>Table 2.14</b> Recipes for SOS assay buffers .....	41
<b>Table 2.15</b> BP recombination reaction components .....	45
<b>Table 2.16</b> LR recombination reaction components.....	46
<b>Table 3.1</b> IC <sub>50</sub> results of 6 nitroreductase enzymes from the 58 nitroreductase enzyme over-expression library .....	59

<b>Table 4.1</b> 23 nitroreductase 6KO library .....	93
--	----

## List of Abbreviations

<b>2M5NI</b>	2-Methyl-5-Nitroimidazole
<b>4NI</b>	4-Nitroimidazole
<b>ACSRC</b>	Auckland Cancer Society Research Centre
<b>Amp</b>	Ampicillan
<b>BRT</b>	Bioreductive Trigger
<b>CB1954</b>	5-aziridin-1-yl-2,4- dinitrobenzamide
<b>DMEM</b>	Dulbeccos Modified Eagle Medium
<b>DMSO</b>	Dimethylsulfoxide
<b>DNBM</b>	Dinitrobenzamide Mustard
<b>DTZ</b>	Dimetridazole
<b>FCS</b>	Fetal Calf Serum
<b>FMISO</b>	F-Misonidazole
<b>FUR</b>	Furazolidone
<b>GDEPT</b>	Gene Directed Enzyme Prodrug Therapy
<b>HEPES</b>	4-(2-hydroxyethyl)-1-piperazineethanesulfonic acid
<b>IC<sub>50</sub></b>	Half Maximal Inhibitory Concentration
<b>Kan</b>	Kanamycin
<b>LB</b>	Lauria Broth
<b>MISO</b>	Misonidazole
<b>MTZ</b>	Metronidazole
<b>NB2N</b>	<i>N</i> -Benznidazole
<b>NCS</b>	Niclosamide
<b>NFN</b>	Nitrofurantoin
<b>NFX</b>	Nifurtimox
<b>NFZ</b>	Nitrofurazone
<b>NTR</b>	Nitroreductase
<b>NQO1</b>	NAD(P)H: quinone oxidoreductase 1
<b>OD</b>	Optical Density (at given $\lambda$ )
<b>ORN</b>	Ornidazole
<b>PCR</b>	Polymerase Chain Reaction
<b>RNZ</b>	Ronidazole

<b>TIN</b>	Tinidazole
<b>WT</b>	Wild Type

## **Preface**

At the time that this project started, previous work in the Ackerley lab had focused on developing a nitroreductase-based strategy for GDEPT, utilising the ability of nitroreductase enzymes to activate nitro-quenched compounds. In this scenario, it was proposed that a single nitroreductase enzyme would be capable of reducing a PET imaging agent, for confirmation of localisation of the nitroreductase containing vector, a prodrug, capable of eliminating the target tumour cell population, and a nil bystander antibiotic, a safety mechanism for the ablation of the vector delivery system post treatment. My initial work was focused on identifying nil bystander antibiotic/ nitroreductase combinations that might enable vector ablation. However, this rapidly evolved into the main focus of this thesis; exploring the potential for use of nil bystander antibiotics/ nitroreductases for targeted cell ablation in developmental biology. Acknowledging this progression, the Introduction will first examine cancer therapy as a means of introducing key enzymes, strategies and compounds, but will then move onto other applications of the ability of nitroreductases to activate nitro-quenched molecules.

## **1. Introduction**

### **1.1 Current cancer treatments**

Due the multi-factorial nature of cancer, it is a difficult disease to treat in each individual. Cancer tumours are, essentially, an uncontrolled growth of cells due to the inability to regulate tissue growth (Croce, 2008). The rapid proliferation of solid tumours causes blood vessels to be forced apart, to have impaired function due to cellular mutations, or to be produced at a high enough rate resulting in the inability to maintain homeostatic regulation of tissue and blood pressure formation (Brown and Giaccia, 1998) resulting in a poorly organised vascular architecture (Padera *et al*, 2004).

In the early 20<sup>th</sup> century, radiation therapy in conjunction with surgery was the only means of treating cancer, and was the predominant treatment as late as the 1960s

(DeVita and Chu 2008). The possibility of the treatment of cancers by administration of chemicals was hypothesised as early as the late 1800s (DeVita and Chu 2008), but it was not until the mid 1900s that the broad range of chemicals that might affect the disease was narrowed. An accidental spill of sulphur mustards on troops led to the observation that bone marrow and lymph nodes were significantly depleted in those exposed (DeVita and Chu 2008). This observation led to research into the chemistry and potential therapeutic effects of mustards. Rodents were used as animal models with transplantable tumours to test for these hypothesised effects, and methods were developed to screen chemicals (DeVita and Chu 2008). Marked regression of these tumours, and subsequently tumours in human patients, were observed (DeVita and Chu 2008). Modern day cancer treatments still combine these three strategies; the actions of chemotherapeutic agents, with radiation therapy, and surgery. More recently however lead compounds used in chemotherapy have become a lot more focused and are targeted to unique characteristics of cancer cells.

## **1.2 Hypoxia targeted prodrugs**

A lot of contemporary research has focused on the use of prodrugs to target unique characteristics of cancer, as a means of improving the therapeutic index of the drug administered.

Prodrugs are drugs that are administered to cells in forms that are harmless, or have relatively minimal detrimental effects, until conversion to their activate forms. Once a prodrug has become activated it is cytotoxic to its surrounding environment through various mechanisms including DNA cross-linking, chromosomal aberrations, and inhibition of DNA synthesis ultimately resulting in apoptosis. The activation of prodrugs can be induced by a number of physiological conditions, including changes in temperature, pH, and salt concentration. Hypoxic conditions, which are uniquely characteristic of solid tumours, have also been exploited to induce the activation of prodrugs.

Hypoxia is a common feature of a large proportion of human tumours (Patterson *et al*, 2007). It is typically more severe in cancerous tumors than in healthy tissues, thus providing a basis for tumor selectivity (Brown and Giaccia, 1998).

A by-product of the highly unorganised nature of the tumour vasculature network is the inadequate oxygenation of all tumour cells. This unique anatomy makes current models of cancer treatment inadequate. Hypoxia can compromise outcomes of surgery by increasing tumor metastasis (Patterson *et al*, 2007). Moreover, radiation therapy relies on molecular oxygen to aid in DNA damage induction via ROS (Brown and Wilson, 2004), thus due to their hypoxic nature, cancer cells are much less sensitive to the effects of radiation therapy. There is also a correlation between hypoxic regions, and the distance from the vasculature, which makes it difficult to target the origin of the tumour for circulating drugs (Dachs *et al*, 2009). Many drugs have been designed with the knowledge that cancer is a rapidly proliferating disease, but hypoxic regions tend to show a decreased rate of cellular growth leaving them resistant to many antiproliferative chemotherapy agents (Kennedy *et al*, 1997).

These problems are being overcome by a new generation of prodrugs, which are selectively activated in hypoxic cells to release or activate a toxic substrate capable of killing surrounding oxygenated tumour cells. Some useful compound groups include N-oxides, quinones, and nitroaromatics (Denny, 2000).

The usual mechanism of action of hypoxia activated prodrugs, is that the prodrug acts as a substrate for an endogenous one electron reductase, thereby introducing an electron and forming a free radical. In oxic cells there are little to no harmful effects as this one electron reduction is part of a futile cycle; the unpaired electron is quickly transferred to molecular oxygen forming superoxide, and re-establishing the initial prodrug (Brown and Wilson 2004). However, in hypoxic cells, the cytotoxic form is able to become biologically available if the concentration of oxygen is low enough that the levels of the activated prodrug are able to accumulate without being cycled back into the original non-toxic form (Figure 1.1). In the majority of cases, this cytotoxic product undergoes more reactions to form a compound which is highly toxic to surrounding cells (Brown and Wilson, 2004).

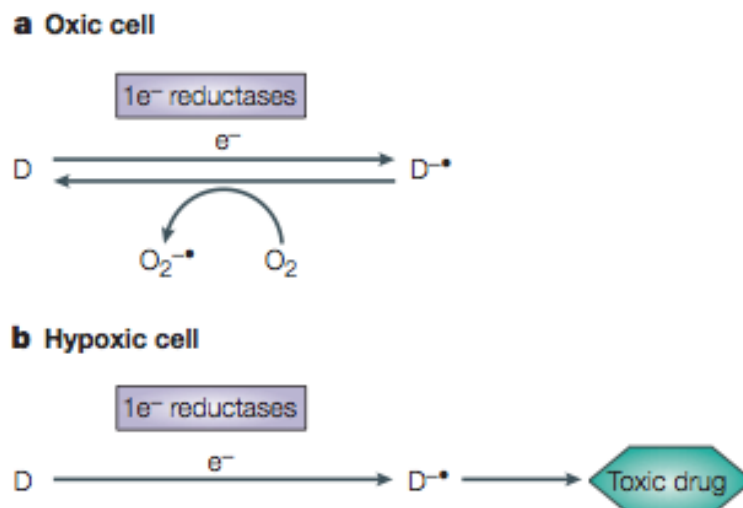


**Figure 1.1 Hypoxia prodrug mechanism of activation.** 1 electron reduction by endogenous enzymes; futile cycling back to original drug in oxic cell, superoxide metabolised to more toxic drug in hypoxic cell due to lack of oxygen to enter futile cycle. (Brown and Wilson, 2004)

*In vivo* these cytotoxic effects are masked by their inactivity towards resistant oxic cells, suggesting that to be beneficial these hypoxic selective anti tumour agents would need to be used in combination with other treatments that are effective against oxic cells, like radiotherapy (Bremmer, 1993).

### 1.2.1 Nitroaromatic hypoxia activated prodrugs

Recently, great promise has been exhibited by nitroaromatic hypoxia targeting prodrugs, which are molecules of direct relevance to this research. In hypoxic human cells, these prodrugs are reduced in a stepwise manner of one electron at a time, up to six, until the end metabolite is generated (Denny, 2000). In oxic cells however, the nitro radical anion produced in the first step of this reaction pathway can be scavenged by molecular oxygen, leaving the prodrug inactive under non-hypoxic conditions (Denny, 2000) (Figure 1.2).

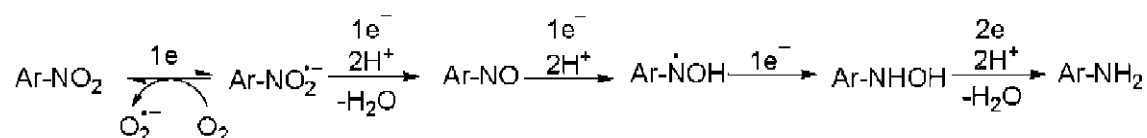


**Figure 1.2 Hypoxia activation of nitroaromatic prodrug.** Stepwise reduction reactions, 1 electron at a time, to generate a cytotoxic metabolite. The first reduction reaction can enter a futile cycle in oxic cells. (Chen and Hu 2009)



Nitroaromatic compounds for use in anti-cancer therapy were first developed from early nitroimidazole based radiosensitisers, which are selectively metabolised under hypoxic conditions (Chen and Hu 2009). These radiosensitisers were only weakly cytotoxic, but newer generation drugs based on the original structures were developed to produce a higher toxic effect in the cell (Chen and Hu 2009).

The first of the nitroaromatics discovered that was able to be reduced under hypoxic conditions was 1-(2-nitro-1-imidazolyl)-3-methoxypropanol (misonidazole). As misonidazole was shown to improve radiotherapy *in vivo*, a number of other nitroimidazole-based derivatives were then developed to give greater cytotoxicity and improved hypoxia selectivity (Chen and Hu 2009). One of these nitroimidazole-based derivatives is 1-(2-nitro-1-imidazolyl)-3-(1-aziridino)-2-propanol (RSU1069). RSU1069 is a 2-nitroimidazole with an aziridine moiety in the N1 side chain, enabling bifunctional alkylation upon reduction (Chen and Hu 2009, Deacon et al 1986) (figure 1.3). *In vitro* and *in vivo* studies have both shown that RSU1069 is more a more efficient radiosensitiser than misonidazole (Deacon et al 1986) (figure 1.3).

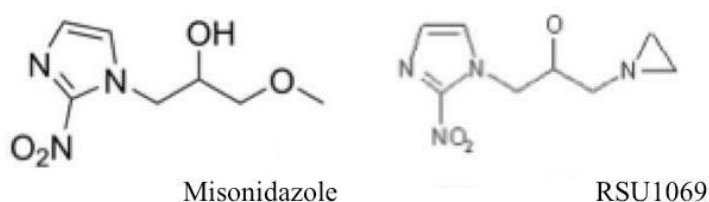


**Figure 1.3 Structures of nitroaromatic anti-cancer compounds.** Misonidazole, and RSU1069.

The dinitrobenzamide 5-aziridin-1-yl-2,4- dinitrobenzamide (CB1954) is also activated under hypoxic conditions by the endogenous 2 electron reductase, NAD(P)H oxidoreductase (DT diaphorase), although, due to the reduction of 2 electrons, the oxygen reversible intermediate is bypassed leading to poor hypoxic selectivity (Denny, 2000). This has initiated the development of a range of hypoxia-sensitive derivatives, in particular the dinitrobenzamide mustards (DNBMs). This class of compound was originally developed following investigations into the enhancement of toxicity and hypoxia selectivity of nitrophenyl prodrugs, through the addition of a nitrogen mustard functional group (Denny and Wilson, 1986). The

alkylating properties of the dormant mustard are restored following nitroreduction as shown in figure 1.4.

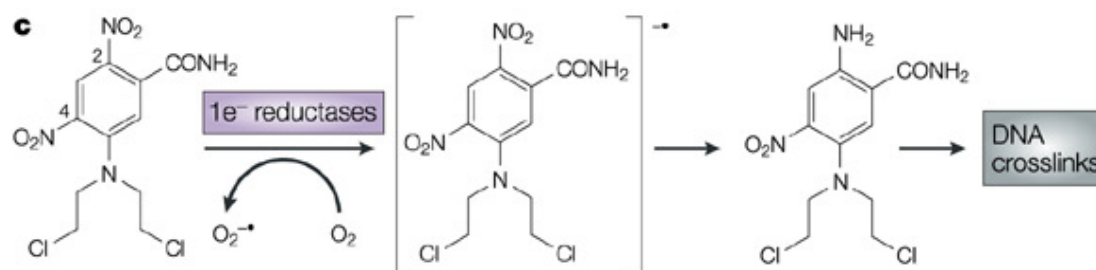


**Figure 1.4 Hypoxia activated nitroaromatic prodrug.** Reduction occurs through one-electron reductases via an oxygen-sensitive free radical intermediate to a cytotoxic metabolite which induces DNA crosslinking causing apoptosis (Brown and Wilson 2004).

### 1.3 GDEPT

Previous research into the field of enzyme and hypoxia activated prodrugs has paved the way for GDEPT, which builds on this current knowledge and provides new cutting edge technology. GDEPT has the potential to selectively eradicate tumour cells, while at the same time sparing normal tissue from damage (Greco and Dachs, 2001). It is based on the delivery of a gene that encodes an enzyme which is non-toxic in itself, but which is able to convert a prodrug into a potent cytotoxin (Greco and Dachs, 2001), leaving the transfected cells sensitised to the administered prodrug. GDEPT aims to bypass the molecular restrictions of current cancer therapies, utilising the ability of exogenous enzymes (often, but not exclusively, of bacterial origin) to activate prodrugs. This would leave targeting hypoxia unnecessary, by targeting specific molecules on the outside of tumour cells for gene delivery (Dachs *et al*, 2009), and activation of the prodrug induced by the delivered gene (figure 1.5).

A major hurdle to overcome in cancer GDEPT is the delivery of the genes to a sufficient number of tumour cells to induce regression (Rainov, 2000). Despite active research, gene transfer efficiencies in the clinic have appeared to be at a 10% maximum (Dachs *et al*, 2009). This limitation can however, be addressed by employing prodrugs with an efficient bystander effect; that is which induce the death of neighbouring non-transgenic cells as well as the transgenic cells that activate them (Dachs *et al*, 2009). A great advantage of nitroaromatic prodrugs in this context is

they can be chemically engineered to have an optimal bystander effect to maximise tumour cell kill, without impairing activation by their nitroreductase partner (Dr Adam Patterson, *personal communication*).

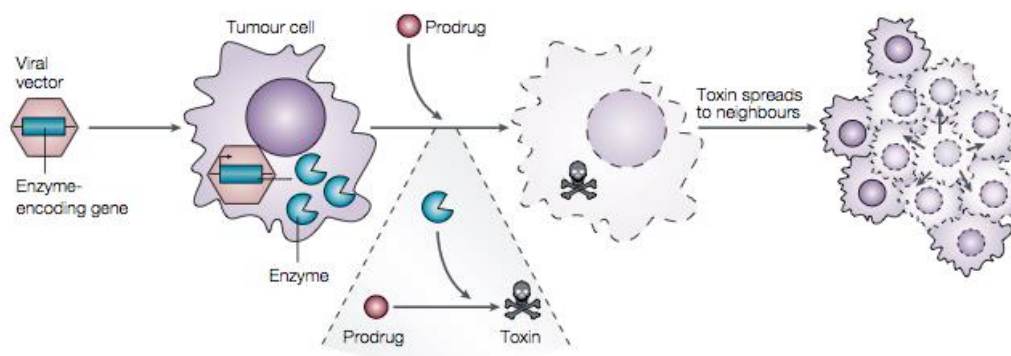


**Figure 1.5 GDEPT Overview.** Vector uptake into the cell resulting in enzyme expression in a small percentage of target cells. The bystander effect is achieved by subsequent genotoxic effect to transgenic and neighbouring cells (McCormick, 2001)

### 1.3.1 *E. coli* nitroreductase (NfsB) and 5-aziridin-1-yl-2,4-dinitrobenzamide (CB1954)

An isolated nitroreductase gene from *E. coli*, *nfsB*, expresses the NfsB\_Ec nitroreductase enzyme that has been shown to activate the prototypical nitroaromatic prodrug, 5-(aziridin-1-yl)-2,4-dinitrobenzamide (CB1954) to its toxic form.

NfsB is known to reduce a wide range of nitroaromatics, and was initially identified as a target for antibiotics (Christofferson, 2009). Its mechanism of action is dependent on FMN; NAD(P)H binds to the enzyme, and donates two electrons to the FMN cofactor, then NAD(P)<sup>+</sup> is subsequently released, enabling the substrate to bind the active site, and be reduced itself (Christofferson, 2009, Parkinson, 2000). The simultaneous 2-electron reduction of the nitro group to an electron donating hydroxylamine renders the reaction oxygen independent (Christofferson, 2009). The cytotoxin then induces DNA crosslinks which ultimately result in apoptosis. A major advantage of this prodrug-enzyme combination is that cell death isn't dependent on

active cellular replication, apoptosis can occur in cells in arrested cycle too (Christofferson, 2009).

CB1954 isn't a natural substrate for NfsB\_Ec, and has low affinity for the enzyme resulting in a low yield of cytotoxic drug (Christofferson, 2009). Regardless, the NfsB\_Ec-CB1954 combination has been evaluated in Phase I/II trials in combination and further nitroreductase / prodrug combinations are continually being explored.

There is vast potential for the discovery of other nitroreductases that may confer higher activity than NfsB\_Ec, enabling more efficient prodrug activation.

A number of novel candidates, from *E. coli* as well as other bacteria, have been identified as having nitroaromatic reducing capabilities. Many of these have not yet been screened for activity with anti-tumour prodrugs. However, some that have are a series of enzymes related to the *Bacillus amyloliquefaciens* nitroreductase *ywrO*, which shares amino acid similarities to mammalian NQO1 (Theys *et al.*, 2006). Another more recently investigated enzyme family that offers great promise are the orthologues of a second nitroreductase of *E. coli*, *nfsA*, which has also been studied in combination with the CB1954 prodrug (Vass *et al.*, 2009; Prosser *et al.*, 2010a).

There is also the potential for the use of nitroreductases for the activation of other potentially beneficial substrates, such as nitro-quenched bystander antibiotics, like metronidazole, that can eliminate vectors post-therapy; or nitro-quenched fluorophores, with imaging potential. Both of these aspects will be discussed later in this introduction.

Based on this prior work, as well as the discovery of other enzymes with nitroreductase potential, researchers in the Ackerley lab have generated a large collection of nitroreductase candidates and have screened this for activity with various nitroaromatic prodrugs (Prosser *et al.*, 2010a,b; Prosser *et al.* 2013).

## 1.4 The 58-membered nitroreductase library

The two main families and best studied of the nitroreductase enzymes are *nfsA* and *nfsB*. They are named for nitrofurantoin sensitivity, having originally been discovered on the basis of mutations in the *E. coli* genes being found to confer resistance to the antibiotic nitrofurantoin (Bryant *et al.*, 1981; Whiteway *et al.*, 1998). The characteristics that distinguish these two major families are that the *nfsA* family (type I) nitroreductases which are dependent on NADPH to reduce their substrates, and the *nfsB* family (type II) can use either NADH or NADPH for reduction (Zenno *et al.*, 1996)

*nfsA* is induced via oxidative stress as part of the soxRS regulon (Paterson, 2002). Its homolog in *Bacillus subtilis* has also been shown to be induced under oxidative stress, as well as heat shock (Streker *et al.*, 2005). There are 20 homologs of *E. coli nfsA* within the nitroreductase library (Table 1.1).

*nfsB* is a monomeric flavin mononucleotide (FMN) containing flavoprotein (Zenno *et al.*, 1996) The *nfsB* family is capable of utilising both NADH and NADPH as cofactors to efficiently reduce a number of nitro aromatic substrates (Zenno *et al.*, 1996). There are 12 homologs of *E. coli nfsB* in the core library (Table 1.1).

The remaining 26 nitroreductase enzymes come from 11 different families; *wrbA*, *yieF*, *azoR*, *mdaB*, *ywrO*, *ydjA*, *nemA*, NQO1, *kefF*, *ycaK*, and *yedI* (Prosser *et al.*, 2013). Verified nitroreductase activity has previously been observed for one or more members of the *yieF*, *azoR*, *mdaB*, *ywrO*, *nemA* and NQO1 families, but not for the remainder (Theys *et al.*, 2006; Barak *et al.*, 2006, Prosser *et al.*, 2013).

**Table 1.1 Complete 58 nitroreductase library**

#	Gene	Organism	Family	% ID/Sim
1	NfsA_Ec	<i>Escherichia coli</i>	NfsA	100/100
2	NfsA_St	<i>Salmonella enterica</i>	NfsA	87/95
3	NfsA_Ck	<i>Citrobacter koseri</i>	NfsA	86/92
4	NfsA_Kp	<i>Klebsiella pneumoniae</i>	NfsA	83/92
5	NfsA_Es	<i>Enterobacter sakazakii</i>	NfsA	82/94
6	NfsA_Ecaro	<i>Erwinia carotovora</i>	NfsA	65/82
7	NfsA_Vf	<i>Vibrio fischeri</i>	NfsA	52/68

8	NfsA_Vv	<i>Vibrio vulnificus</i>	NfsA	51/65
9	Frp1_Vh	<i>Vibrio harveyi</i>	NfsA	51/65
10	Frp2_Vh	<i>Vibrio harveyi</i>	NfsA	51/65
11	NfrA_Bs	<i>Bacillus subtilis</i>	NfsA	39/62
12	NfsA_Lw	<i>Listeria welshimeri</i>	NfsA	41/60
13	NfsA_Li	<i>Listeria innocua</i>	NfsA	39/60
14	NfsA_Bco	<i>Bacillus coagulans</i>	NfsA	38/60
15	NfsA_Np	<i>Nostoc punctiforme</i>	NfsA	38/59
16	NfsA_Bth	<i>Bacillus thuringiensis</i>	NfsA	35/58
17	NfsA_Lsak	<i>Lactobacillus sakei</i>	NfsA	40/57
18	NfsA_Pp	<i>Pseudomonas putida</i>	NfsA	35/57
19	YcnD_Bs	<i>Bacillus subtilis</i>	NfsA	35/56
20	NfsA_Ms	<i>Mycobacterium smegmatis</i>	NfsA	36/54
21	NfsB_Ec	<i>Escherichia coli</i>	NfsB	100/100
22	NfsB_Ck	<i>Citrobacter koseri</i>	NfsB	88/95
23	NfsB_St	<i>Salmonella enterica</i>	NfsB	88/91
24	NfsB_Kp	<i>Klebsiella pneumoniae</i>	NfsB	84/93
25	NfsB_Vv	<i>Vibrio vulnificus</i>	NfsB	61/75
26	NfsB_Pp	<i>Pseudomonas putida</i>	NfsB	52/71
27	NfsB_Es	<i>Enterobacter sakazakii</i>	NfsB	46/66
28	FraseI_Vf	<i>Vibrio fischeri</i>	NfsB	34/53
29	NfsB_Vh	<i>Vibrio harveyi</i>	NfsB	30/48
30	YfkO_Bs	<i>Bacillus subtilis</i>	NfsB	29/46
31	YdgI_Bs	<i>Bacillus subtilis</i>	NfsB	25/47
32	NfsB_Pa	<i>Pseudomonas aeruginosa</i>	NfsB	24/42
33	AzoR_Ec	<i>Escherichia coli</i>	AzoR	100/100
34	AzoR_St	<i>Salmonella enterica</i>	AzoR	87/95
35	AzoR_Vv	<i>Vibrio vulnificus</i>	AzoR	56/73
36	AzoR_Pp	<i>Pseudomonas putida</i>	AzoR	48/66
37	NemA_Ec	<i>Escherichia coli</i>	NemA	100/100
38	NemA_St	<i>Salmonella enterica</i>	NemA	92/96
39	NemA_Kp	<i>Klebsiella pneumoniae</i>	NemA	86/92
40	NemA_Vv	<i>Vibrio vulnificus</i>	NemA	47/65
41	YwrO_Bs	<i>Bacillus subtilis</i>	YwrO	70/82
42	YwrO_Li	<i>Listeria innocua</i>	YwrO	42/57
43	YwrO_Vf	<i>Vibrio fischeri</i>	YwrO	47/62
44	YieF_Ec	<i>Escherichia coli</i>	YieF	100/100
45	YieF_Pa	<i>Pseudomonas aeruginosa</i>	YieF	45/60
46	MdaB_Ec	<i>Escherichia coli</i>	MdaB	100/100
47	MdaB_Ps	<i>Pseudomonas syringae</i>	MdaB	60/74
48	WrbA_Ec	<i>Escherichia coli</i>	WrbA	100/100
49	WrbA_Ps	<i>Pseudomonas syringae</i>	WrbA	39/55
50	YdjA_Ec	<i>Escherichia coli</i>	YdjA	100/100
51	YdjA_Kp	<i>Klebsiella pneumoniae</i>	YdjA	79/89
52	NQO1_Pp	<i>Pseudomonas putida</i>	NQO1	37/56

53	NQO1_Pa	<i>Pseudomonas aeruginosa</i>	NQO1	41/54
54	YcdI_Ec	<i>Escherichia coli</i>	YcdI	100/100
55	YcdI_Kp	<i>Klebsiella pneumoniae</i>	YcdI	76/85
56	YcaK_Ec	<i>Escherichia coli</i>	YcaK	100/100
57	YcaK_Pa	<i>Pseudomonas aeruginosa</i>	YcaK	27/48
58	KefF_Ec	<i>Escherichia coli</i>	KefF	100/100

\* Frp1\_Vh and Frp2\_Vh are versions of Frp cloned from slightly different strains of *Vibrio harveyi*

## 1.5 Nil bystander antibiotics

The ability to safely eliminate the vector from patients is an essential feature for a complete GDEPT system, as pathogenic bacterium - such as *Clostridium* - are commonly used vectors in solid tumour targeting. Due to their pathogenic nature, the FDA require that there be a way to eliminate these vectors from the patient post treatment.

The Ackerley lab been able to show that many nitroreductases that activate anti-cancer prodrugs have the additional ability to reduce a range of nil bystander nitroaromatic antibiotics, and that this may be able to provide a potential safety mechanism for eliminating biological vectors from patients post-therapy or in case of an adverse event.

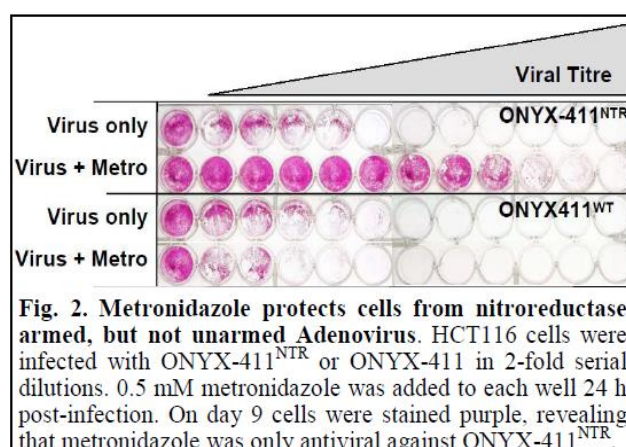


**Figure 1.6 Dr Adam Patterson, University of Auckland, unpublished work.** Metronidazole is capable of suppressing the replication of the ONYX-411 adenovirus while carrying a nitroreductase, but not the wildtype ONYX-411 adenovirus.

Dr Patterson's lab in Auckland have shown that two of the 16 candidate nil bystander antibiotics that were tested in this thesis, metronidazole and tinidazole, are widely activated by orthologues of NfsA (Ec) and NfsB (Ec), and that this activity has potential for eliminating gene therapy vectors from the host. It is intuitive how bacterial vectors might be sensitive to antibiotics; indeed, metronidazole is already the antibiotic of choice for eliminating *Clostridium* from patients (Basu, 2010). However, Dr Patterson's group have also been able to show that metronidazole has the ability to suppress the replication of the ONYX-411 adenovirus when labelled with a nitroreductase, but not the wildtype ONYX-411 adenovirus (Figure. 1.6). This observation that nitroreductases in conjunction with nil-bystander antibiotics are also able to be utilised to eliminate viral vectors was a key factor motivating this research, suggesting that we might be able to interrogate the 58 nitroreductase core library to recover multi-functional nitroreductases for use in an all encompassing GDEPT system.

## 1.6 Masked fluorophores

A library of nitro-quenched masked fluorophores has also been developed by the Auckland Cancer Society Research Centre. These compounds don't show fluorescence until they are activated, which can be achieved through the reduction mechanisms of nitroreductases. There are two distinct categories of masked fluorophore; nitro-switch or bioreductive trigger (BRT) as depicted in figure 1.7 (Horvat 2012).

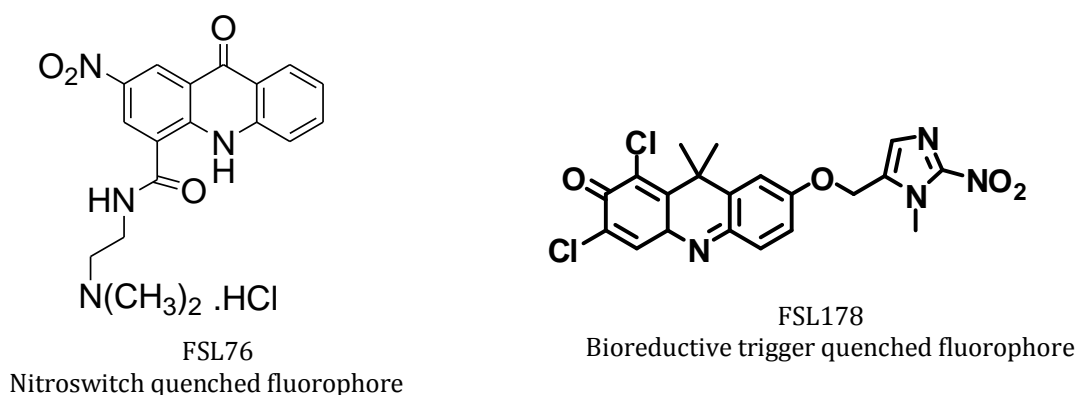


**Figure 1.7 FSL76 and FSL178.** Examples of the two different kinds of quenched fluorophore; Nitroswitch and bioreductive trigger.



Nitro-switch fluorophores are reduced at the nitro group, causing a change in electronic charge that directly activates fluorescence (Horvat 2012).

BRT molecules are made up of three distinct parts; a trigger, a linker and an effector (figure 1.8). The trigger is the substrate for the activating enzyme, the linker is broken during this metabolic process, resulting in either the effector becoming activated or released (Siim, *et al.*, 1997). In the case of the masked fluorophores, release of the effector moiety generates a fluorescent signal.



**Figure 1.8 Bioreductive trigger molecule components.** Make up and position of fragments in a bioreductive trigger molecule (Siim, *et al.*, 1997).

Currently in the Ackerley lab, both types of masked fluorophores are being utilised in the discovery and evaluation of novel nitroreductases.

### 1.7 Regenerative and developmental biological studies

Developmental biology looks to understand which cellular mechanisms are involved in which processes of development. The study of cell specific regeneration enables insights into the differentiation of specific cell types and regenerative potential of individual stem cell populations. Conditional targeted ablation is a powerful tool that can be used to study precise stages of development, and the ability to temporally and spatially control tissue damage and remove a specific cell population has wide applications for regeneration studies. Previous technology for use in regenerative studies has not been regulated on such a targeted scale, with studies focusing on more complex scenarios, such as whole limb regeneration, which involves various cell and tissue types. The ability to utilise nitroreductases in temporally and spatially targeted cell ablation will be beneficial to the study of many degenerative diseases that stem from the loss of individual cell types (Kaya *et al.*, 2012)

A wide range of genes have important roles during both embryogenesis and adulthood, knockout of these genes can cause a lethal phenotype in the embryo, making it difficult to generate animal models to study the function of the gene in later stages of development, or its role in adulthood (Davison *et al.*, 2007). Another obstacle is that many phenotypes caused by gene knockout may be due to systemic effects in the whole organism rather than a specific tissue, making them hard to analyse (Davison *et al.*, 2007). Due to this, many studies have attempted to develop genetic switches to allow the silencing of genes temporally and spatially. Essential factors for such a targeted cell ablation system in developmental and regenerative studies are the ability of the mechanism to not interfere with other genetic components, and the reversibility of the silencing. Early attempts to develop this type of switch employed the use of single transgenes with promoters that could be induced by heavy metals, heat shock, interferon or steroids. Pleiotropic effects and high basal activity in the absence of induction rendered these systems somewhat ineffective. Instead, binary transgenic systems, in which gene expression is controlled by the interaction of two components - an effector transgene, the product of which acts on a target transgene - are often used for these studies, but require complex genetic manipulations to achieve. Physical surgery and laser-mediated ablation methods are also commonplace, although they are labour-intensive, time-consuming, and not as reproducible as a genetic approach, which limits their use in large scale screening experiments.

All of these processes have been developed to conditionally target ablation, but none have been able to meet four key criteria simultaneously; to be spatially controllable and strictly confined to the target cell population, to be temporally inducible, to be germline transmissible and, to be reversible (Curudo *et al.*, 2007). The implementation of a fluorescent protein/ nitroreductase fusion protein system to ablate target cell populations could vastly improve this technology.

A handful of studies, primarily using *Xenopus* and zebrafish as model organisms, have found success in using nitroreductase genes to promote targeted cell ablation in distinct cell populations for application in these fields.

### 1.7.1 Case studies utilising nitroreductase ablation technology

A handful of studies have shown that the fluorescent protein/ nitroreductase fusion technique is capable of ablating target cell populations in a way that is spatially controllable and strictly confined to the target cell population, temporally inducible, germline transmissible and reversible (Curado and Stainier 2008)

Many of these initial studies have targeted the ablation and subsequent regeneration of islet  $\beta$  cells in an effort to study the inducibility and endogenous regeneration of  $\beta$  cells in type 1 diabetics to recover glucose homeostasis (Curado *et al.*, 2007).

One of these studies (Curado *et al.*, 2007) achieved this via a CFP/ nitroreductase fusion protein linked to the insulin promoter. The promoter drives the expression of CFP and a nitroreductase (NfsB\_Ec). The expression of the CFP allows reporting on the cell population, as fluorescence is only visible in the cell population under the control of the promoter which is also expressing NfsB\_Ec. The addition of a bystander antibiotic, metronidazole, to the system destroys the cell population, as metronidazole is reduced to its cytotoxic form in the presence of NfsB\_Ec. Figure 1.9 from Curado *et al* (2007) shows the promoter construct used in this study, and also visualisation of the zebrafish before (B) and after (C) the addition of metronidazole to the organism's environment.

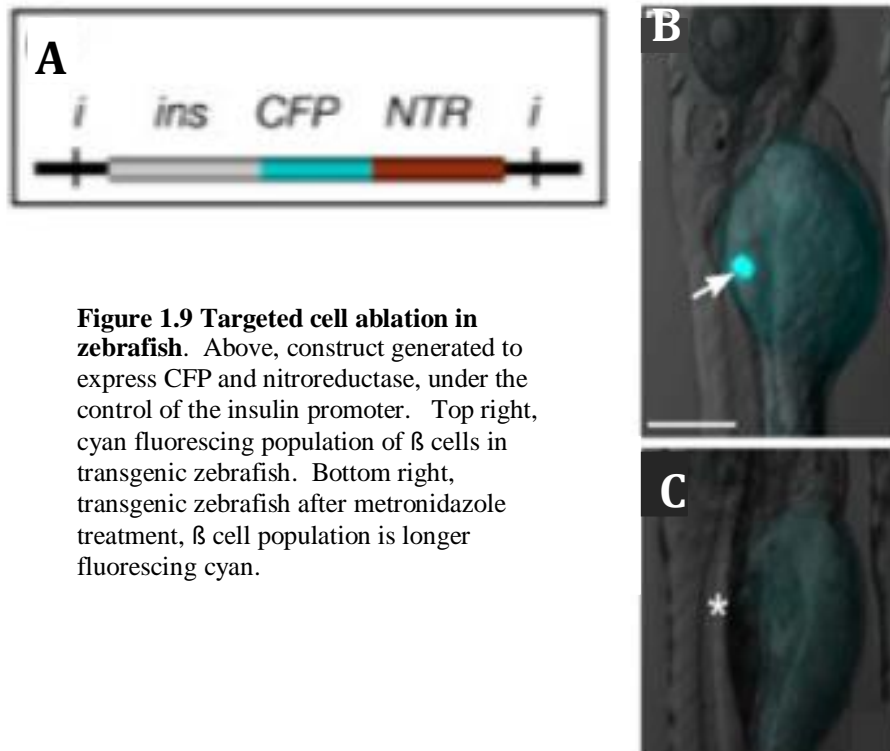


**Figure 1.9 Targeted cell ablation in zebrafish.** Above, construct generated to express CFP and nitroreductase, under the control of the insulin promoter. Top right, cyan fluorescing population of  $\beta$  cells in transgenic zebrafish. Bottom right, transgenic zebrafish after metronidazole treatment,  $\beta$  cell population is longer fluorescing cyan.

Kaya *et al*, 2012 explored demyelination and remyelination in *Xenopus* utilising a GFP: nitroreductase system under the control of the myelin basic protein, which codes for mature oligodendrocytes. Oligodendrocytes create myelin sheaths, which form a layer around the axon of a neuron that is essential for the proper functioning of the nervous system. Demyelination is implicated in many degenerative diseases. This study used live imaging to show that the removal of metronidazole from the organism's environment resulted in the complete regeneration of the target cell population (Figure 1.10).

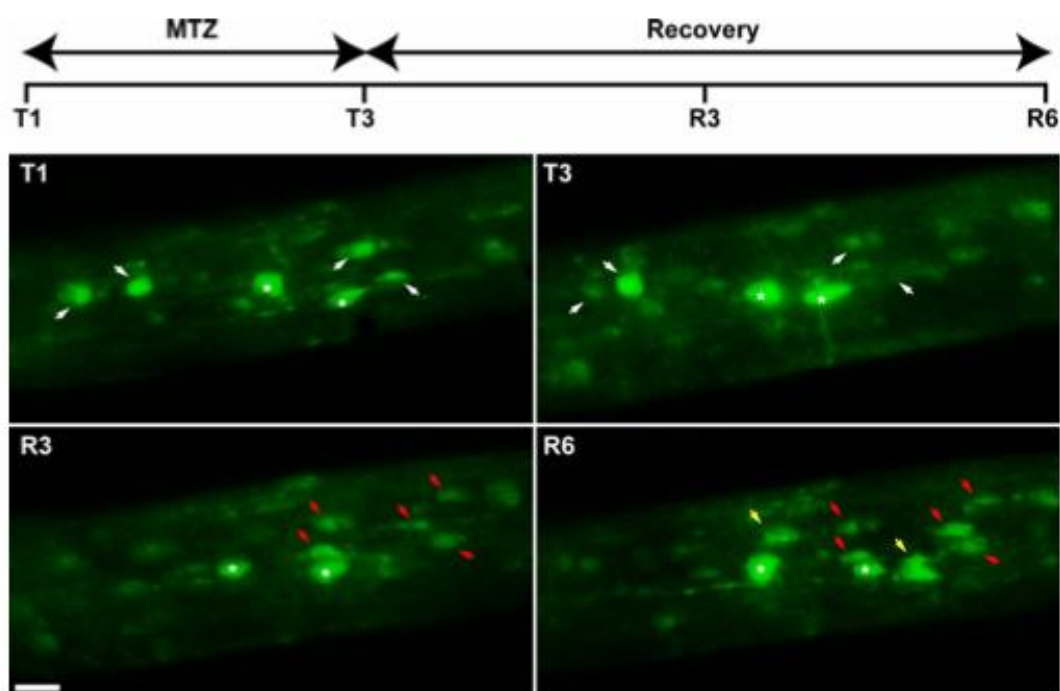


**Figure 1.10 Live imaging of oligodendrocyte depletion and reappearance following metronidazole treatment and cessation.** Successive observation of the optic nerve of the same transgenic tadpole by two-photon microscopy. Transgenic tadpoles were treated for 3d with metronidazole (10 mM) (T1, T3), then returned to normal water for 6d. Observations were before treatment (T1), after 3d in the presence of metronidazole (T3) and during recovery at 3d and 6d in normal water (R3, R6). (Kaya *et al.*, 2012)

### 1.7.2 Limitations of the NfsB\_Ec/ metronidazole system

One clear limitation of this system, is that the nitroreductase currently being used in these studies, NfsB\_Ec, is insufficiently active with metronidazole to give clean targeted cell ablation without high background toxicity. Although not mentioned in the papers that employ this ablation system, the toxicity of metronidazole to non-transgenic zebrafish (at the doses required for complete ablation of NfsB\_Ec expressing cells) is very high, such that relatively few fish from the original cohort are able to survive a multi-day experiment (Dr J.S. Mumm, Georgia Regents University, *personal communication*).

### 1.7.3 Combining this technology with masked fluorophores

Work by Singleton *et al* (2007) was the first to show that, as well as being capable of activating a wide range of drugs and antibiotics, nitroreductases are also capable of directly activating fluorescent reporter molecules. Although fluorescent proteins used

in the fluorescent protein/ nitroreductase system are successful reporters, this realisation illustrates that fluorescent protein tags are not in fact necessary for such studies. A single nitroreductase has the potential to activate both a nil bystander antibiotic, and a masked fluorophore simultaneously.

#### 1.7.4 Dual reporter/ ablation system exploiting the characteristics of nitroreductases

Exploiting the ability of nitroreductases to activate both nil bystander antibiotics and masked fluorophores simultaneously, and building on the base technology developed by Curado *et al*, we propose a two-way opposing activation system, in which one nitroreductase will be able to activate a specific antibiotic and fluorophore, while being inactive with a different antibiotic and fluorophore which is able to be activated by another nitroreductase (figure 1.11). This will allow the temporal and spatial reporting and targeted ablation of two distinct cell populations at once, giving efficient imaging of the two different populations of cells simultaneously, and the ablation of one or even both at specific stages of development as desired.

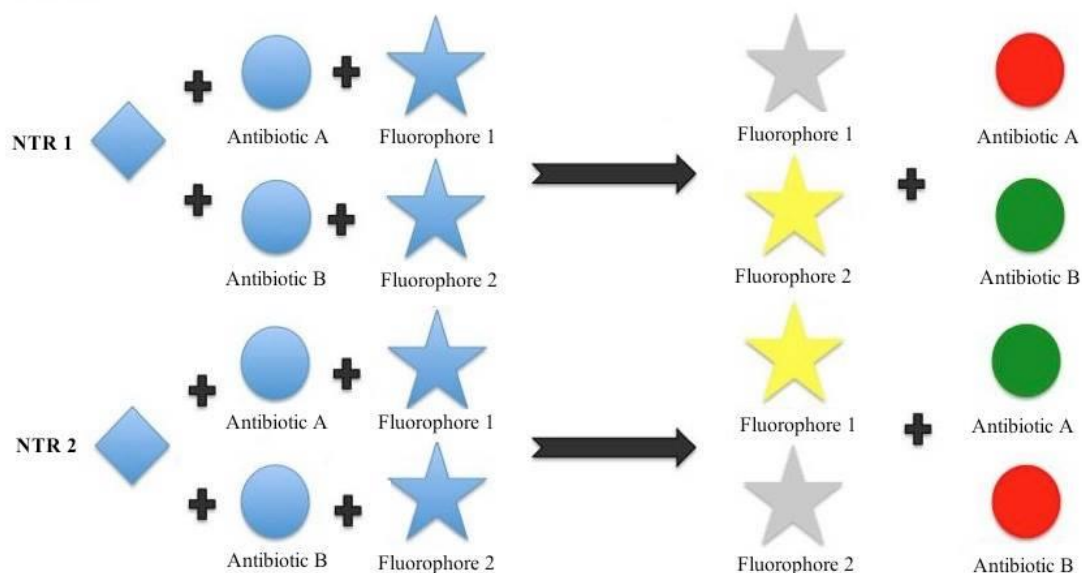


**Figure 1.11 Nitroreductases with opposing specificities for both masked fluorophores and nil-bystander antibiotics.** Nitroreductase 1 has activity with antibiotic B and fluorophore 2, but not antibiotic A or fluorophore1, while nitroreductase 2 has the opposing activation profile; activity with antibiotic A and fluorophores 1, but not antibiotic B or masked fluorophore 2.

## 1.8 Aims

This research project has various evolving aims. Firstly, to identify a nitroreductase which has a better activation profile with metronidazole than NfsB\_Ec. Following this, the full nitroreductase library will be screened with a number of nil bystander antibiotic candidates for the identification of other nitroreductase/nil bystander antibiotic combinations with potential applications in GDEPT and targeted cell ablation. Building on these initial ideas, a reporter system that eliminates the need for a bicistronic protein (currently employed in developmental and regenerative biological studies) utilising a single nitroreductase capable of activating both a masked fluorophore and a nil bystander antibiotic will be explored. The final aim is to bring all of these ideas together in a multiplex scenario, where nitroreductases with opposing activation profiles will each be capable of activating one masked fluorophore/ nil bystander antibiotic combination. This would enable spatial and temporal reporting on cell populations, and the ability to induce targeted cell death, on either one or more of these cell populations simultaneously or subsequently.

Initial screening of the 58 nitroreductase core library with metronidazole identified nitroreductases with a higher efficacy with metronidazole than NfsB\_Ec that could be utilised in developmental and regenerative biology studies. Screening of the 58 nitroreductase core library against 16 chosen nil bystander antibiotics enabled identification of which nitroreductases have the highest activity a given nil bystander antibiotic; results that could have applications both in GDEPT, and developmental and regenerative biological studies. This screening also allowed the identification of nitroreductase / nil bystander antibiotic pairs for use in a dual targeted cell ablation system. The initial screening was undertaken in bacterial cells, with promising nitroreductases then being transfected into human cell lines for confirmation of activity in mammalian cells.

During the initial screening process, it was noticed that one of the nil bystander antibiotics that was being tested, niclosamide, acted in a completely different manner to all other nil bystander antibiotics. Instead of causing the nitroreductase it was active with to cause cell death, it appeared to have a protective effect on the cell, as cells expressing an empty plasmid had complete cell death. We proposed that this be

used as a method to screen large number of nitroreductases as a high throughput method of novel nitroreductase discovery. This will be discussed in chapter 3.

The second results chapter explored the ability of nitroreductases to activate a range of masked fluorophores developed by Auckland Cancer Society Research Centre available in the lab. Nitroreductases and masked fluorophores with opposing activation profiles were identified and combined with nitroreductases and nil bystander antibiotics for the development of a dual nitroreductase combined reporter/ablation system. Again, these experiments were initially carried out in bacterial cells, with the best candidates for this system carried over for testing in human cell lines.

Although bacterial systems are extraordinarily useful for screening purposes, some nitroreductases have been shown to be unstable when transfected into human cell lines, and not behave in the same manner as observed at the bacterial level. It was due to this that it was extremely important to do testing in human cell lines as the proposed technologies would be able to be used in a mammal environment; both for effectively eliminating a vector from a patient post GDEPT therapy, and for use in developmental and regenerative biological studies.



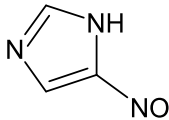
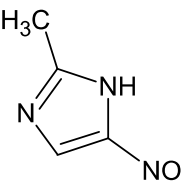
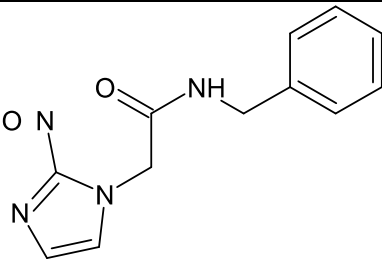
## 2. Materials and Methods

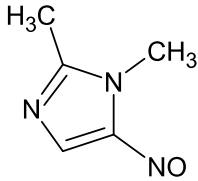
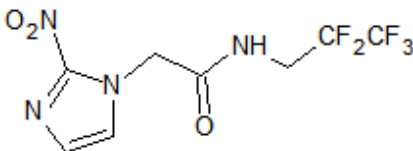
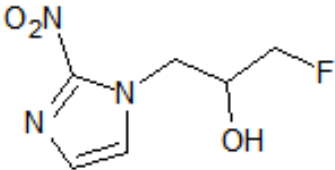
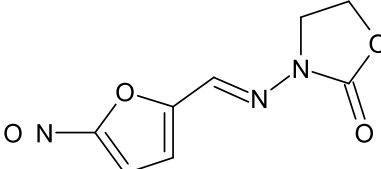
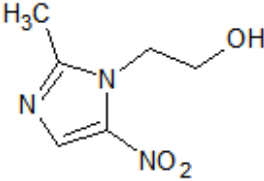
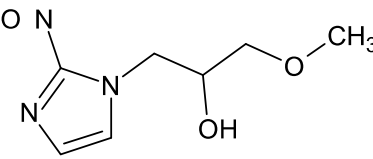
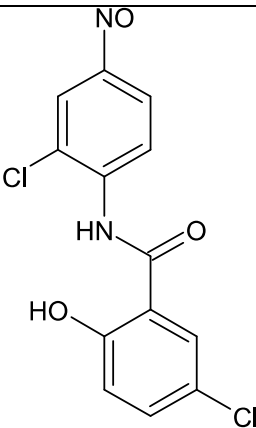
### 2.1 Chemicals

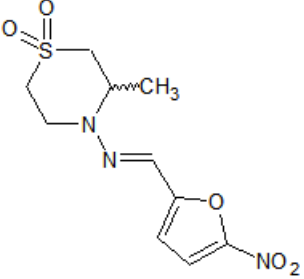
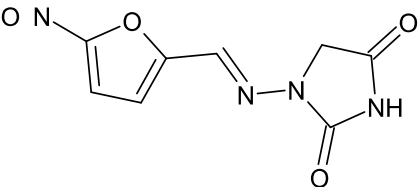
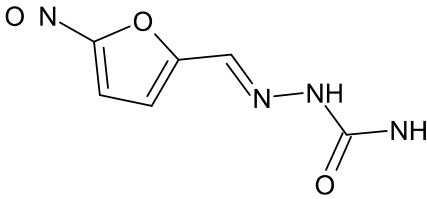
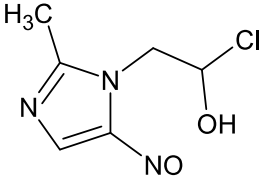
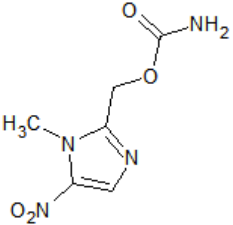
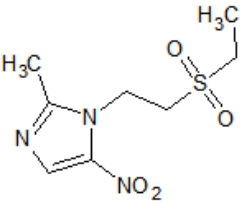
#### 2.1.1 Nil bystander antibiotics

Stock solutions of all nil bystander candidate compounds (Table 2.1) were made to 200 mM in anhydrous dimethyl sulfoxide (Sigma-Aldrich, St. Louis, MO, USA) and stored at -80 °C. The only exception to this was Niclosamide, which was made to a stock solution concentration of 5 mM. All nil bystander candidates were purchased from Sigma-Aldrich (Sigma-Aldrich, St. Louis, MO, USA) with the exception of EF5, Misonidazole and F-Misonidazole (generous gifts from Dr Jeff Smaill, ACSRC) and Nifurtimox (a generous gift from Bayer Healthcare Mo, NJ, U.S).

**Table 2.1 Nil bystander antibiotics**

Nil Bystander Antibiotic	Structure
4-NI	
5-Methyl-NI	
Benznidazole	

Dimetridazole	
EF5	
F-Misonidazole	
Furazalodine	
Metronidazole	
Misonidazole	
Niclosamide	

Nifurtimox	
Nitrofurantoin	
Nitrofurazone	
Ornidazole	
Ronidazole	
Tinidazole	

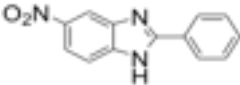
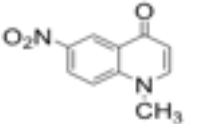
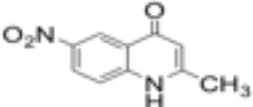
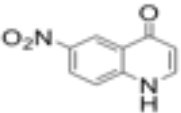
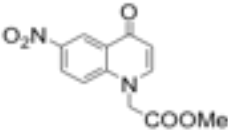
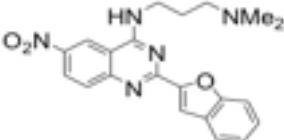
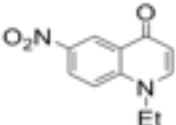
### 2.1.2 Masked fluorophores

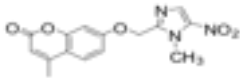
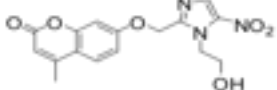
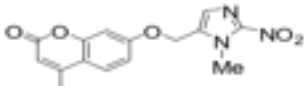
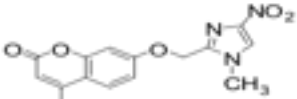
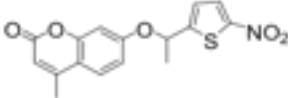
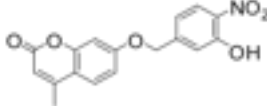
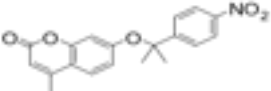
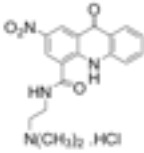
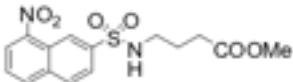
The masked fluorophores used in this study were developed by Dr Jeff Smail from an existing collection of chemicals that had been synthesized by various researchers at the ASCRC over the past fifty years. Initial work carried out by Dr Horvat (Horvat, 2012) identified NTR activated fluorophores that were further evaluated in this study.

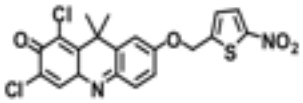
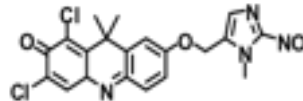
These are shown in Table 2.2. Compound stock solutions (10 mM) were prepared in anhydrous dimethyl sulphoxide (Sigma-Aldrich, St. Louis, MO, USA) and stored at -80 °C.

**Table 2.2 Masked fluorophores**

All masked fluorophores that were used in this study. The colour of the left hand column denotes the fluorescence emission of the masked fluorophore once it has been activated.

FSL Number	Structure	Excitation Maxima (nm)	Emission Maxima (nm)	Compound Type
25		325	425	Nitroswitch quenched fluorophore
41		350	455	Nitroswitch quenched fluorophore
48		355	460	Nitroswitch quenched fluorophore
59		350	455	Nitroswitch quenched fluorophore
61		355	460	Nitroswitch quenched fluorophore
95		350	475	Nitroswitch quenched fluorophore
111		355	460	Nitroswitch quenched fluorophore

162		355	460	Bioreductive trigger quenched fluorophore
163		355	460	Bioreductive trigger quenched fluorophore
169		355	460	Bioreductive trigger quenched fluorophore
170		355	460	Bioreductive trigger quenched fluorophore
171		355	460	Bioreductive trigger quenched fluorophore
175		355	460	Bioreductive trigger quenched fluorophore
176		355	460	Bioreductive trigger quenched fluorophore
76		405	585	Nitroswitch quenched fluorophore
150		355	535	Nitroswitch quenched fluorophore

177		645	660	Bioreductive trigger quenched fluorophore
178		645	660	Bioreductive trigger quenched fluorophore

## 2.2 Enzymes

Restriction Endonucleases and Phusion™ High Fidelity Polymerase were purchased from New England Biolabs (NEB; Ipswich, MA, USA). Bioline Red *Taq* Polymerase Mastermix was purchased from Bioline (London, UK). T4 DNA ligase was purchased from Fermentas (Burlington, Canada). Advantage 2 Polymerase was purchased from Clontech (Mountain View, CA, US).

## 2.3 Bacterial strains and plasmids

**Table 2.3 Bacterial Strains**

Strain	Characteristics	Source
<b>W3110</b>	<i>E. coli</i> K12: F- $\lambda$ -IN(rrnD-rrnE)1 rph1	Ackerley Lab Stock
<b>DH5<math>\alpha</math></b>	supEhh DlacU169 ( $\theta$ 80lacZ DM5) hsd R17	Invitrogen
<b>ADA510</b>	F- lac-6(del) $\lambda\phi$ (sfiA::lacZ)	(Shapiro & Baneyx, 2002)
<b>SOS-R2</b>	ADA510 $\Delta nfsA$ $\Delta nfsB$ $\Delta uvrB$ $\Delta tolC$	(Prosser et al, 2013)
<b>W3110-6KO 7NT</b>	W3110 $\Delta nfsA$ $\Delta nfsB$ $\Delta yieF$ $\Delta ycaK$ $\Delta mdaB$ $\Delta azoR$ W3110-7KO $\Delta nemA$ $\Delta tolC$	(Horvat, 2012) Dr Janine Copp

**Table 2.4 Plasmids**

Plasmid	Characteristics	Source
<b>pUCX</b>	<i>ampR</i> . <i>E. coli</i> expression vector. <i>tac</i> promoter, <i>lac</i> operator, pET28a (+) RBS	(Prosser et al., 2010a)
<b>pUC19</b>	<i>ampR</i> . Cloning plasmid, pMB1 origin of replication	Invitrogen

## 2.4 Mammalian cell lines and plasmids

**Table 2.5 Mammalian cell lines**

Cell Line	Characteristics	Source
<b>HEK293</b>	Human embryonic kidney, adherent	ATCC (American Type Culture Collection, Manassas, VA, USA)
<b>HCT-116</b>	Colorectal carcinoma, adherent	ATCC (American Type Culture Collection, Manassas, VA, USA)
<b>HCT-116 GW NfsB_Vh</b>	HCT-116 F279V5 <i>nfsB</i> Vh	Dr Horvat
<b>HEK293 GW NfsA_Ec</b>	HEK293 F279V5 <i>nfsA</i> Ec	This study
<b>HEK293 GW NfsB_Ec</b>	HEK293 F279V5 <i>nfsB</i> Ec	This study
<b>HEK293 GW NfsB_Vv</b>	HEK293 F279V5 <i>nfsB</i> Vv	This study
<b>HEK293 GW NfsA_Pp</b>	HEK293 F279V5 <i>nfsA</i> Pp	This study

**Table 2.6 Plasmids**

Plasmid	Characteristics	Source
<b>F279V5</b>	Puromycin resistance	Dr Adam Patterson, ACSRC
<b>pDONR221</b>	<i>kanR</i>	Invitrogen

## 2.5 Oligonucleotide primers

**Table 2.7 Oligonucleotide Primers**

Primer	Sequence (5'→3')
<b>NTR specific primer</b>	
NfsA_Ec_Fw	GGCATATGACGCCAACCATTGAAC
NfsA_Ec_Rv	GGGTCGACTTAGCGCGTCGCCCAACCCTG
NfsA_St_Fw	GGGGCATATGAGTCCGACCATTGAA
NfsA_St_Rv	GGGGTCGACTTAGCGCGTCGCCAGCC
NfsA_Ck_Fw	GGGGCATATGACTCCAACCATTGATT
NfsA_Ck_Rv	GGGGGTCGACTTAGCGCGTCGCCCAA
NfsA_Kp_Fw	GGGGCATATGACCCGACCATTGAG
NfsA_Kp_Rv	GGGGTCGACTCAGCGCGTTGCCACC
NfsA_Ecaro_Fw	GGGGCATATGATACCAACTATTGATTGCTACA
NfsA_Ecaro_Rv	GGGGCTCGAGCTAGCGTATCGCCCATCCTTGTTG
NfsA_Es_Fw	CCCCCATATGACGCCAACGATTGAGCTGC
NfsA_Es_Rv	GGGGCTCGAGTTAGCGTGTGCCCAGCCCTG
NfsA_Vf_Fw	CCCCCATATGAACCCTGTTATCGATAC
NfsA_Vf_Rv	CCCGTCGACTCACTTAATAGCTAGGC
NfsA_Vv_Fw	GGGGCATATGAACGCTGTTATTGAC

NfsA_Vv_Rv	GGGGTCGACTTACTTTGTCGCCAAGCC
Frp_Vh_Fw	GGGCATATGAACAATACGATTGAAA
Frp_Vh_Rv	GGGGTCGACTTAGCGTTTTGCTAGCC
NfrA_Bs_Fw	GGGGCATATGAATAACACAATCGAAACC
NfrA_Bs_Rv	GGGGGTCGACTTAGTTTTTATTAAAGCCCT
NfsA_Li_Lw_Fw	GGGGCATATGAATCAGGCGATAGATGCCATTTT
NfsA_Li_Lw_Rv	GGGGGTCGACTTATTTTTTGATTTAAATGTTGC
NfsA_Bc_Fw	GGGGCATATGAATACTATCATTGAAACGATTCTC
NfsA_Bc_Rv	GGGGGTCGACTTACTTTTTATCAAACCCTTGCGCT
NfsA_NP_Fw	GGCATATGCCTTTACAGATGGAA
NfsA_NP_Rv	GGGTCGACTTACAGTAGCTTGAA
NfsA_Bth_Fw	GGGGCATATGAATGAAATGATACATAAAATGGAG
NfsA_Bth_Rv	GGGGGTCGACTCATTTCTTATTTAATCCTCTCTCAT
NfsA_Lsak_Fw	GGGGCATATGTCTGATTTAATCGCACAAATGCAAC
NfsA_Lsak_Rv	GGGGGTCGACTTATGCTAATGTAAACCCCTGTTTCTT
NfsA_Pp_Fw	CCCCCATATGAGCCTTCAAGACGAAG
NfsA_Pp_Rv	CTAGGTCGACTCAGCGCAGGCCGAAAC
YcnD_Bs_Fw	CCCCCATATGAATGAAGTGATTAAATC
YcnD_Bs_Rv	CCCCGTCGACTTATTTTTCAACTTTAAATC
NfsA_Ms_Fw	GGGGCATATGACGGTCATCGCGCGCTACGCAGACGTCGAT
NfsA_Ms_Rv	GGGGCTCGAGTCAGCGGATTCCCAGGCCCAACCGCTCG
NfsB_Ec_Fw	GGGCATATGGATATCATTTCTG
NfsB_Ec_Rv	GGGGAATTCTTACACTTCGGTTAAG
NfsB_Ck_Fw	CCCCCATATGGATATCGTTTCTGTGCGC
NfsB_Ck_Rv	CCCGTCGACTCAGACTTCCGTCAGGGTG
NfsB_St_Fw	GGGGCATATGGATATCGTTTCTGTG
NfsB_St_Rv	GGGGGTCGACTTAGACTTCCGTCAGTG
NfsB_Kp_Fw	GGGGCATATGGATATCGTATCGGTC
NfsB_Kp_Rv	GGGGCTCGAGTTAAATCTCGGTAATGGT
NfsB_Vv_Fw	GGGGCATATGACTATTGTTCAAGCT
NfsB_Vv_Rv	GGGGTCGACTTAGATTTTCGGTAAAAACAG
NfsB_Pp_Fw	GGGGCATATGGATACCGTATCGCTG
NfsB_Pp_Rv	GGGGCTCGAGTCAGAGGAAGGTGAACACTT
NfsB_Es_Fw	CCCCCATATGAACCTTAATGAGATCATTCGC
NfsB_Es_Rv	CCCGTCGACTCAGAGCTGCGTGATCAC
FraseI_Vf_Fw	GGGGCATATGACGCATCCAATTATTCA
FraseI_Vf_Rv	GGGGGTCGACCTAAAGAATGGTAATTAC
NfsB_Vh_Fw	CCCCCATATGTCTCATCAAATCATTACAGAC
NfsB_Vh_Rv	CCCCTCGAGTTAAAGAGTAGTAATTACGTC
YfkO_Bs_Fw	GGGGCATATGGCAGATCTAAAGACACA
YfkO_Bs_Rv	CTAGGTCGACTTAAACCCACTTCACAACAT
YdgI_Bs_Fw	GGGGCATATGATCAAAACAAACGATTTTATGG
YdgI_Bs_Rv	GGGGGTCGACTTATTTCCATTCTGCAATTG
YdgI_Pa_Fw	GGGGCATATGCATATCGAAGACGCC



YdgI_Pa_Rv	GGGGGTCGACTCAGAAGCGGTCGCGAATGA
AzoR_Ec_Fw	GGGGGCATATGAGCAAGGTATTAGTTCTT
AzoR_Ec_Rv	GGGGGTCGACTTATGCAGAAACAATGCTGT
AzoR_St_Fw	CCCGCATATGAGCAAGGTATTAGTTCTT
AzoR_St_Rv	CCCGTCGACTTAAGCGGCCACGAC
AzoR_Vv_Fw	CCCGCATATGTCTCGTTTACTAGTATT
AzoR_Vv_Rv	CCCGGTCGACTTAAGCTGTTAGCGCTGCAAG
AzoR_Pp_Fw	GGGGCATATGTCCCGCGTACTGATCATC
AzoR_Pp_Rv	GGGGCTCGAGTCAGGCCACCGCTGCCAGCTT
NemA_Ec_Fw	CTAGGGATCCATGTCATCTGAAAACTG
NemA_Ec_Rv	CTAGGTCGACTTACAACGTCGGGTAATC
NemA_St_Fw	CCCGGATCCATGTCATCAGCAAACTG
NemA_St_Rv	CCCGGTCGACTTACAGAGTAGGGTAGTC
NemA_Kp_Fw	CCCCATATGTCGGAAGCAA
NemA_Kp_Rv	CCCCTCGAGTTACAGAGTCGGGTAA
NemA_Vv_Fw	CCCCATATGAGCAAACCTGTTTGAA
NemA_Vv_Rv	CCCGTCGACTCACACATGCAAAGCGGT
YwrO_Bs_Fw	AAATTTGGATCCATGAAAATATTGGTTTTGGC
YwrO_Bs_Rv	CCCGTCGACTTAAACAAAAGGCTGCTG
YwrO_Li_Fw	CCCCCATATGAAAACATTAGTTATTAT
YwrO_Li_Rv	CCCGTCGACCTAATTTAACGTTTTAATA
YwrO_Vf_Fw	AAATTTGGATCCATGACAAGCCCGGCT
YwrO_Vf_Rv	CCCGTCGACTTATTCCTTAATAAATTTATC
YieF_Ec_Fw	GGGGCATATGTCTGAAAAATTGCAGGTG
YieF_Ec_Rv	GGGGGTCGACTTAGATCTTAACCTCGCTG
YieF_Pa_Fw	GGGGCATATGAGCGACGACATCAAG
YieF_Pa_Rv	GGGGGTCGACTCAACCGCGCAGGCGGCGCA
MdaB_Ec_Fw	GGGCATATGAGCAACATCCTG
MdaB_Ec_Rv	GGGGTCGACTTAACCAAAAATTTC
MdaB_Ps_Fw	GGGGCATATGAAAAAAGTATTGTTCTCAAC
MdaB_Ps_Rv	CTAGCTCGAGTTACTGCGCACCAAACACTT
WrbA_Ec_Fw	GGGCATATGGCTAAAGTTCTGGTG
WrbA_Ec_Rv	GGGGTCGACTTAGCCGTTAAGTTT
WrbA_Ps_Fw	GGGGCATATGAGCAAACCTTACATTCTGG
WrbA_Ps_Rv	CTAGGTCGACTCAGCTGCGTGTTGTGTC
YdjA_Ec_Fw	CTAGCATATGGATGCACTCGAACTATTG
YdjA_Ec_Rv	CTAGGTCGACTCAGAAATAAGTTACAAACGG
YdjA_Kp_Fw	CCCCCATATGGATGCTCTCGATCTACTGC
YdjA_Kp_Rv	CCCCGTCGACTCAGAATCGCGTCACAAACG
YdjA_Pp_Fw	GGGGCATATGCTTGTGAATGTACTG
YdjA_Pp_Rv	GGGGGTCGACTCACGTCAGCGGGTACAACG
YdjA_Pa_Fw	GGGGCATATGAACGTAAGTATCGTC
YdjA_Pa_Rv	GGGGGTCGACTCAGCGCGCCAGCGGCTGGA
YcdI_Ec_Fw	CTAGCATATGAACGAAGCCGTTAGCC

YcdI_Ec_Rv	CTAGGTCGACTTACAACAGCCCGCAGG
YcdI_Kp_Fw	GGGGCATATGAACGACGCGATAAACCA
YcdI_Kp_Rv	CTAGCTCGAGTTATGCCAGGCAGGCT
YcaK_Ec_Fw	GGGGCATATGCAGTCTGAACGTATT
YcaK_Ec_Rv	GGGGGTCGACTTATAGTGCATCTACCATAT
0853_Pa_Fw	GGGGCATATGGTTGAAACCGCCAAGACC
0853_Pa_Rv	GGGGGTCGACCTAGACCTGGCTGCCGAGCT
KefF_Ec_Fw	GGGGCATATGATTCTTATAATTTATGCG
KefF_Ec_Rv	GCCTGAGTCGACGTATGGCTATCCATGATGGG
<b>Miscellaneous primers</b>	
pMMB_Fw	GGCTCGTATAATGTGTGG
pMMB_Rv	GACCGCTTCTGCGTTCTGAT
M13_Fw	GTAAAACGACGGCCAG
M13_Rv	CAGGAAACAGCTATGAC
<b>Gateway Primers</b>	
NfsA_Bth_Gateway_Fw	GGGGACAAGTTTGTACAAAAAAGCAGGCTT CGAAGGAGATAGAACCATGGGCAATGAAAT GATACATAAAAT
NfsA_Bth_Gateway_Rv	GGGGACCACTTTGTACAAGAAAGCTGGGTC CTATTTCTTATTTAATCCTCTTT
NfsA_Ecaro_Gateway_Fw	GGGGACAAGTTTGTACAAAAAAGCAGGCTT CGAAGGAGATAGAACCATGGGCATACCAAC TATTGATTTGCT
NfsA_Ecaro_Gateway_Rv	GGGGACCACTTTGTACAAGAAAGCTGGGTC CTAGCGTATCGCCCATCCTTGTT
NfsA_Es_Gateway_Fw	GGGGACAAGTTTGTACAAAAAAGCAGGCTT CGAAGGAGATAGAACCATGGGCACGCCAAC GATTGAGCTGCT
NfsA_Es_Gateway_Rv	GGGGACCACTTTGTACAAGAAAGCTGGGTC CTAGCGTGTCGCCAGCCCTGCT
NfsA_Li_Gateway_Fw	GGGGACAAGTTTGTACAAAAAAGCAGGCTT CGAAGGAGATAGAACCATGGGCAATCAGGC GATAGATGCCAT
NfsA_Li_Gateway_Rv	GGGGACCACTTTGTACAAGAAAGCTGGGTC CTATTTTTGATTTAAATGTTGCT
NfsB_Vh_Gateway_Fw	GGGGACAAGTTTGTACAAAAAAGCAGGCTT CGAAGGAGATAGAACCATGGGCTCTCATCA AATCATTACAGA
NfsB_Vh_Gateway_Rv	GGGGACCACTTTGTACAAGAAAGCTGGGTC CTAAAGAGTAGTAATTACGTCAT
NfsB_Vv_Gateway_Fw	GGGGACAAGTTTGTACAAAAAAGCAGGCTT CGAAGGAGATAGAACCATGGGCACTATTGT TCAAGCTGCCCCA
NfsB_Vv_Gateway_Rv	GGGGACCACTTTGTACAAGAAAGCTGGGTC

	CTAGATTTTCGGTAAAAACAGTCT
O199_Gateway_Fw	GGGGACAAGTTTGTACAAAAAAGCAGGCTTCG AAGGAGATAGAACCATGGGCCCTTTACAGATG GAATTGGT
O199_Gateway_Rv	GGGGACCACTTTGTACAAGAAAGCTGGGTC CTACAGTAGCTTGAAGCCAAGAT
YdgI_Gateway_Fw	GGGGACAAGTTTGTACAAAAAAGCAGGCTT CGAAGGAGATAGAACCATGGGCATCAAAAC AAACGATTTTATG
YdgI_Gateway_Rv	GGGGACCACTTTGTACAAGAAAGCTGGGTCC TATTTCCATTCTGCAATTTTATC

All primers used in this study were synthesised by Invitrogen (Carlsbad, CA, USA) or Integrated DNA Technologies (IDT; Coralville, IA, USA) and supplied lyophilized. For long-term storage, primers were resuspended in 1x TE, pH 8.0 (10 mM Tris-Cl pH 8.0, 0.1 mM EDTA) to a final concentration of 100  $\mu$ M and stored at -20 °C. For working stocks, aliquots were diluted in autoclaved, 0.22  $\mu$ m filter-sterilized distilled and deionised (ddH<sub>2</sub>O) water to a 10  $\mu$ M final concentration.

## 2.6 Growth and maintenance of bacteria

### 2.6.1 Media

All media listed below was made up to required volumes with ddH<sub>2</sub>O then autoclaved at 121 °C for 30 minutes. Media was stored at room temperature unless supplemented with antibiotics or another heat sensitive chemical in which case it was stored at 4 °C.

#### 2.6.1.1 Liquid media

##### **Luria-Bertani (LB) Broth**

1% Bacterial Peptone

0.5% Yeast Extract

1% NaCl

##### **SOC**

0.5% Yeast Extract

2% Tryptone  
 10 mM NaCl  
 2.5 mM KCl  
 10 mM MgCl<sub>2</sub>  
 10 mM MgSO<sub>4</sub>  
 20 mM Glucose

### 2.6.1.2 Solid media

Solid media was made by adding agar to LB at a final concentration of 1.5%, then autoclaving. Supplements, when required, were added post-autoclaving once the media had cooled to < 50 °C. Approximately 15 mL of medium was then poured into 90 mm x 15 mm Petri dishes and left to solidify. These were stored at 4 °C until use.

**Table 2.8 Growth media supplements and antibiotics**

	Final Concentration	Solvent
<b>Ampicillin</b>	100 mg mL <sup>-1</sup>	ddH <sub>2</sub> O
<b>Kanamycin</b>	100 mg mL <sup>-1</sup>	ddH <sub>2</sub> O
<b>IPTG</b>	100 mg mL <sup>-1</sup>	ddH <sub>2</sub> O
<b>Luria Broth</b>	20%	ddH <sub>2</sub> O
<b>Glucose*</b>	20%	ddH <sub>2</sub> O
<b>Glycerol</b>	80%	ddH <sub>2</sub> O

\* Sterilised through a 0.22 µm filter

### 2.6.2 Growth of bacterial strains

For standard growth of *E. coli* strains in liquid media, LB media (plus supplements if required) was inoculated and incubated at 37 °C with shaking at 200 revolutions per minute (rpm) unless otherwise stated. Solid media was incubated at 37 °C static and plates stored at 4 °C for up to a month. If long term storage of a strain was required liquid cultures of bacteria were mixed at a 1:1 ratio with 80% glycerol and stored at -80 °C.

## 2.7 Growth and maintenance of mammalian cell lines

### 2.7.1 Media

Dulbecco's Modified Eagle Medium (DMEM) was purchased from Invitrogen (Carlsbad, CA, USA) and supplemented with 2% 4-(2-Hydroxyethyl)piperazine-1-ethanesulfonic acid sodium salt (HEPES), 10% Fetal Calf Serum (FCS) and 2% Penicillin/Streptomycin. Puromycin was also added to a final concentration of 2  $\mu$ M in media when required for selection and maintenance of nitroreductase transfected cell lines. All media was filter sterilised through a 0.22  $\mu$ M filter into 50 mL aliquots and stored at 4 °C, and warmed to 37 °C before use.

### 2.7.2 Antibiotics

**Table 2.9 Antibiotics used in the growth of mammalian cell lines**

Antibiotic	Stock Concentration	Solvent
Puromycin	10 mM	ddH <sub>2</sub> O
Penicillin/ Streptomycin	10 mM	ddH <sub>2</sub> O

### 2.7.3 Growth of mammalian cells

To initiate growth of a mammalian cell line, a cryotube containing frozen cells was thawed and added to a T25 flask containing 15 mL of pre-warmed media. The flask was incubated overnight at 37 °C 5% CO<sub>2</sub>. The media was then removed and replaced with fresh media. Cells were left to grow until they reached approximately 80% confluency, at which point they were harvested using the standard trypsin/EDTA protocol (see 2.7.3.1), diluted and seeded into a new flask.

Cell lines requiring long term storage were grown in a T75 flask until confluency was reached then harvested using the standard trypsin/EDTA protocol (2.7.3.1). The cell number was calculated and the cells were resuspended in Fetal Calf Serum containing 10% DMSO to give a final concentration of 5x10<sup>6</sup> cells per mL. For storage 1 mL aliquots of cells were placed into cryotubes and frozen by reducing the temperature by one degree per minute. When a temperature of -80 °C was reached the cryotubes were placed in liquid nitrogen for long-term storage.

### 2.7.3.1 Harvesting cells

When cells reached approximately 80% confluency, media was aspirated and cells washed in 1x PBS. Sufficient 0.25% Trypsin/EDTA was added to cover the cell surface of the well or flask and incubated at 37 °C for five minutes. Cells were removed from the culture dish surface using 1x PBS and transferred to a 15 mL or 50 mL sterile centrifuge tube as appropriate. Cells were then centrifuged at 1250 rpm for 5 minutes to pellet the cells. The supernatant was discarded and cells re-suspended in 1 mL pre-warmed culture media. If exact numbers of cells were required, 10 µL of cell suspension was removed and put in a clean 1.5 mL microfuge tube and mixed with 10 µL of Trypan blue. Cells were then counted using a hemocytometer (Improved Neubauer, Hausser, Horsham, PA) and seeded into fresh media at the desired density.

## 2.8 Standard molecular biology protocols

### 2.8.1 Chemically competent cells

*E. coli* from glycerol stocks were inoculated in 3 mL LB + 10 mM MgCl<sub>2</sub> and incubated overnight at 37 °C, 200 rpm. Overnight cultures were diluted 50-fold into 50 mL LB + 10 mM MgCl<sub>2</sub>, and incubated at 37 °C, 200 rpm until the OD<sub>600</sub> was between 0.3 and 0.5. When the OD<sub>600</sub> was in this range, the cells were transferred to ice for 10 minutes. The cells were then centrifuged at 4 °C, 4000 rpm for 15 minutes, then re-suspended in 40 mL TFB I (table 2.1) and left on ice for 2 h. The cells were then centrifuged again at 4 °C, 4000 rpm for 15 minutes, and re-suspended in 4 mL TFB II (table 2.1). Cells were then transferred to sterile microcentrifuge tubes in 100 µL aliquots and stored at -80 °C.

**Table 2.10 Recipes for chemically competent cell buffers**

<b>TFB I*</b>	<b>Final Concentration</b>
Potassium Acetate	30 mM
MnCl <sub>2</sub>	50 mM
CaCl <sub>2</sub>	10 mM
Glycerol	15%
<b>TFB II*</b>	<b>Final Concentration</b>

MOPS pH 7.0	10 mM
CaCl <sub>2</sub>	75 mM
KCl	10 mM
Glycerol	15%

\* Sterilised through a 0.22 µm filter and stored at 4 °C

### 2.8.2 Transformation protocol

Competent cells were defrosted on ice from -80 °C storage, 50 – 100 µL were used for each transformation reaction. Between 1-3 µL of DNA at a concentration of 20-200 ng/µL was added, the resulting mixture was kept on ice for 3 minutes. The cells were then heat shocked at 42 °C for 90 s and put immediately back on ice for 45-60 minutes. Cells were plated on LB + (selection compound) + agar plates and incubated overnight in a static 37 °C incubator.

### 2.8.3 Electrocompetent cells

A single colony was used to inoculate 3 mL of LB and grown overnight at 37 °C 200 rpm. Subsequently 100 µL of the overnight culture was used to inoculate 10 mL of fresh LB and the new culture grown at 37 °C 200 rpm to an OD<sub>600</sub> of 0.4- 0.6 . The cells were then pelleted by centrifugation at 4000 rpm for 10 minutes at 4 °C and the supernatant removed. The cells were then re-suspended in 500 µL of ice-cold 10% glycerol and transferred to a 1.5 mL sterile microcentrifuge tube. Cells were then centrifuged at 13,000 rpm for 30 seconds, the supernatant removed and cells re-suspended in 500 µL of ice cold 10% glycerol. This was repeated 2x with a final re-suspension of the cells in 30 µL of ice cold 10% glycerol. Cells were then immediately used for electroporation or stored for 2-4 weeks at -80 °C.

### 2.8.4 Electroporation protocol

Electrocompetent cells were transferred to a 0.2 mm electroporation cuvette and 5-8 µL of DNA was added. The cells were then electroporated (2.5 kV, 25 µF, 100 Ω)

using a Gene Pulser Xcell™ electroporation machine (BioRad, Hercules, CS, USA) and 900 µL of SOC was added to the cuvette, mixed with the cells and the cell mixture transferred to a 1.5 mL sterile microcentrifuge tube. Cells were then allowed to recover for 90 min at 37 °C, 200 rpm. Half of the cell suspension was then plated on LB agar plates with the appropriate antibiotic and the plates incubated at 37 °C overnight. The remaining cell suspension was left at room temperature overnight and plated onto agar plates the next day.

### **2.8.5 Colony screening**

Colonies that grew from transformation or electroporation were screened for the correct gene/plasmid insert by PCR using gene specific or plasmid specific primers, with a small (just visible) “smudge” of cells obtained by dipping a pipette tip into a colony used as template. Colonies shown to have the correct insert were grown overnight in LB plus antibiotic. For storage an aliquot of this overnight culture was mixed with glycerol (final concentration 40%) and stored at -80 °C.

### **2.8.6 DNA quantification**

DNA concentration and purity was measured for purified PCR and plasmid products using a NanoDrop ND-1000 spectrophotometer (ThermoScientific, WA, MA, USA).

### **2.8.7 Polymerase chain reaction (PCR)**

For most PCR reactions Bioline Biomix Red™ (London, UK) *Taq* polymerase or Phusion™ high fidelity polymerase was used; the former for the generation of general PCR products, and the latter for products to be used in cloning.

### **2.8.8 PCR components**

#### **Table 2.11 PCR components**



Component	Volume
<b>Bioline Biomix Red<sup>TM</sup></b>	
Biomix red	10 µL
Primer 1(100 µM)	1 µL
Primer 2 (100 µM)	1 µL
Template DNA	1 µL
ddH <sub>2</sub> O	7 µL
<b>Phusion<sup>TM</sup></b>	
5x Phusion HF Buffer	4 µL
dNTPs	0.4 µL
Primer 1(100 µM)	1 µL
Primer 2 (100 µM)	1 µL
Phusion Polymerase	0.2 µL
Template DNA	1 µL
ddH <sub>2</sub> O	12.4 µL

### 2.8.9 PCR parameters

PCR reactions were run using cycle parameters as presented in Table 2.12. Annealing temperature was generally 5 °C lower than the lowest T<sub>m</sub> of the pair of primers used in the reaction.

**Table 2.12 PCR parameters**

Bioline Biomix Red <sup>TM</sup>	
95 °C 5 min	
95 °C 30 s	30 cycles
52-60 °C °C 30 s	
72 °C 1 min/kb	
Hold at 16 °C	
Phusion <sup>TM</sup>	
98 °C 1 min	

98 °C 15 s	30 cycles
52 -60 °C °C 30 s	
72 °C 30 s/kb	
72 °C 5 min	
Hold at 16 °C	

---

### 2.8.10 Agarose gel electrophoresis

To analyse the size of PCR products and other DNA samples, an aliquot of the sample was run on a 1% agarose gel (1% agarose dissolved in 1xTAE buffer) containing ethidium bromide ( $1 \mu\text{g mL}^{-1}$ ) and submerged in 1xTAE buffer. The gel was run at 120-140 V for 30-40 minutes and then the DNA bands viewed under ultra-violet (UV) light.

### 2.8.11 Restriction digests

Restriction digests were set up as described in Table 2.13 to a final volume of 50  $\mu\text{L}$ . They were incubated at 37 °C from 3 h to overnight depending on the restriction enzymes being used and the amount of DNA present in the reaction. After the desired amount of time the restriction digests were heat inactivated at the appropriate temperature and time as recommended by the manufacturer. The restriction buffer that gives optimal restriction enzyme activity was chosen according to the NEB website

([http://www.neb.com/nebecomm/tech\\_reference/restriction\\_enzymes/buffer\\_activity\\_restriction\\_enzymes.asp](http://www.neb.com/nebecomm/tech_reference/restriction_enzymes/buffer_activity_restriction_enzymes.asp) accessed 20.09.2013).

**Table 2.13 Restriction digest parameters**

Component	Volume
Restriction buffer 10x	5 $\mu\text{L}$
Bovine Serum Albumin (BSA $2\text{mg mL}^{-1}$ )	2.5 $\mu\text{L}$
Restriction enzyme 1	1-1.5 $\mu\text{L}$

Restriction enzyme 2	1-1.5 $\mu$ L
DNA	As applicable
ddH <sub>2</sub> O	To make up to 50 $\mu$ L final volume

---

### **2.8.12 Sequencing**

All sequencing was carried out by Macrogen Inc. (Seoul, Korea).

### **2.8.13 Miniprep protocol**

In a 15 mL Falcon tube 3 mL of LB plus antibiotic was inoculated with a single colony and grown overnight at 37 °C 200 rpm. The following day plasmid DNA was extracted from the cells using the Geneaid high-speed plasmid mini kit (Taiwan, ROC) following manufacturer's instructions.

### **2.8.14 Midiprep protocol**

In a 250 mL conical flask 50 mL of LB plus antibiotic was inoculated with a single colony and grown overnight at 37 °C 200 rpm. The following day plasmid DNA was extracted from the cells using the Geneaid high-speed plasmid midi kit (Taiwan, ROC) following manufacturer's instructions.

### **2.8.15 SDS PAGE protocol**

To carry out SDS PAGE 12% polyacrylamide gels were cast as follows; 5 mL of 12% separating gel (Section 2.8.15.1) was added to the gel cast, covered by 100% isopropanol and left to set (at least 30 minutes). Once set the isopropanol was poured off and sufficient 4% stacking gel (Section 2.8.15.1) was poured in to cover the wells of a multi-well comb (roughly about 2 mL). This was left to set.

Protein samples for SDS PAGE were prepared by adding an appropriate volume of 3x SDS loading buffer (Section 2.8.15.1) and then boiling at 95 °C for five minutes. The samples were then loaded into the wells of the gel and the gel run on a Bio-Rad

Protean II apparatus (Hercules, CA, USA) in 1x SDS Run Buffer at 150 V for 1 hour. Gels were then removed from the plates and stained by submerging the gel in Coomassie blue stain (Section 2.8.15.1) and rocking for 30 minutes. The gel was then washed in tap water to remove excess stain and then destained using destain solution (Section 2.8.15.1) to give the desired contrast between protein bands and the surrounding gel.

### **2.8.15.1 Recipes for SDS PAGE gels and buffers**

#### **12% Separating Gel (Per 10 mL)**

3.75 mL 1 M Tris-Cl (pH 8.8)  
0.05 mL 20 % SDS  
2.92 mL 40% Acrylamide Solution  
1.6 mL 2% Bis-acrylamide Solution  
2.83 mL ddH<sub>2</sub>O  
100 µL 10% ammonium persulphate (APS)\*  
6 µL Tetramethylethylenediamine (TEMED)\*

#### **4% Stacking Gel (Per 3 mL)**

375 µL 1 M Tris-Cl (pH 6.8)  
15 µL 20% SDS  
300 µL 40% Bis/Acrylamide Mix  
2.3 mL ddH<sub>2</sub>O  
30 µL 10% APS\*  
5 µL TEMED\*

#### **3 x SDS Loading Buffer**

150 mM Tris-Cl (pH 6.8)  
6% SDS  
0.3% Bromophenol Blue  
30% Glycerol

300 mM  $\beta$ -Mercaptoethanol

**10 x SDS Run Buffer (per Litre)**

144 g Glycine

30.3 g Tris

10 g SDS

**Coomassie Blue Stain (per Litre)**

2.5 g/L Coomassie Brilliant Blue

450 mL 100% Ethanol

100 mL 100% Acetic Acid

450 mL ddH<sub>2</sub>O

**Destain (per Litre)**

400 mL 100% Methanol

100 mL 100% Acetic Acid

500 mL ddH<sub>2</sub>O

**\*Added immediately prior to pouring gel.**

## **2.9 Bacterial cell protocols**

### **2.9.1 SOS assay**

Cultures of SOSR-2 pUCX:nitroreductase cultures were inoculated from glycerol stocks and grown overnight (~16 hours) in 96 well plates containing 200  $\mu$ L LB + amp (100  $\mu$ g mL<sup>-1</sup>) + 0.4% glucose. The internal wells of the plate were each inoculated with a single nitroreductase from the 58 nitroreductase library (Table 1.1), plus an empty plasmid control, and plates were incubated overnight at 30 °C, 200 rpm. The following day, 15  $\mu$ L of overnight culture was added to 200  $\mu$ L of assay media (LB + amp 100  $\mu$ g mL<sup>-1</sup>, 0.05 mM IPTG, 0.2% glucose) in a new 96 well plate and incubated at 30 °C, 200 rpm for 3 hours. Day cultures were then split into 100  $\mu$ L into new 96 well plates in duplicate, containing either 100  $\mu$ L challenge media (assay media + prodrug, 2%

DMSO) or 100  $\mu$ L control media (assay media + 2% DMSO). The plates were then incubated for a further 3 – 4 hours at 30 °C 200 rpm. Plates were then removed from the incubator and a 20  $\mu$ L cell aliquot was added to 130  $\mu$ L of ZOB buffer in a fresh 96 well plate to allow measurement of  $\beta$ -galactosidase activity. This plate was then incubated at 37 °C until sufficient yellow colouration was observed. At this point, the reaction was halted by addition of 50  $\mu$ L of 1 M  $\text{Na}_2\text{CO}_3$ . The unchallenged and challenged plates had their absorbance recorded at 600 nm while the plates that were used for  $\beta$ -galactosidase assay had their absorbance readings at 420 nm and 550 nm on the plate reader (Enspire 2300 Multiplate Reader, PerkinElmer, Waltham, MA, USA). From these readings Miller units were calculated by the Miller equation [Miller units =  $(\text{OD}_{420} - [1.75 \times \text{OD}_{550}]) / (\text{OD}_{600} \times t \times v)$ ].

**Table 2.14 Recipes for SOS assay buffers**

<b>1 M Sodium Phosphate Buffer pH 7*</b>	<b>Final Concentration</b>
$\text{Na}_2\text{HPO}_4$	0.577 M
$\text{NaH}_2\text{PO}_4$	0.423 M
<b>Z Buffer*</b>	<b>Final Concentration</b>
$\text{Na}_2\text{HPO}_4$	0.074 M
$\text{NaH}_2\text{PO}_4$	0.126 M
$\text{MgSO}_4$	2 mM
CTAB	399 $\text{mg.L}^{-1}$
Sodium Deoxycholate	199.5 $\text{mg.L}^{-1}$
$\beta$ -Mercaptoethanol**	0.174 M
<b>T Base***</b>	<b>Final Concentration</b>
$\text{K}_2\text{HPO}_4$	0.08 M
$\text{KH}_2\text{PO}_4$	0.044 M
$(\text{NH}_4)_2\text{SO}_4$	15.1 mM
Tri Sodium Citrate	1 $\text{g.L}^{-1}$
ONPG	8 $\text{mg.mL}^{-1}$

\*Combined (650 mL 1 M Sodium Phosphate Buffer pH 7, 300 mL Z Buffer) and stored at 4 °C

\*\*  $\beta$ -mercaptoethanol added just prior to use

\*\*\* Stored at -20 °C

**NB.** 1 M Sodium Phosphate Buffer pH 7, Z Buffer, and T Base combined make up the ZOB buffer used in the SOS assay. ZOB buffer sufficient for one 96 well plate (13 mL) was comprised of 9 mL 1 M Sodium Phosphate Buffer pH 7, 3.9mL Z Buffer, and 100  $\mu$ L T Base).

## 2.9.2 Growth inhibition assay

Bacterial cultures were grown overnight from glycerol stocks as previously described in section 2.9.1. The following day, 15  $\mu\text{L}$  of overnight culture was added to 200  $\mu\text{L}$  of assay media (LB + amp 100  $\mu\text{g mL}^{-1}$ , 0.05 mM IPTG, 0.2% glucose) in new 96 well plates and incubated at 30  $^{\circ}\text{C}$ , 200 rpm for 3.5 h. Day cultures were then split into 100  $\mu\text{L}$  into new 96 well plates in duplicate, containing either 100  $\mu\text{L}$  challenge media (assay media + nil bystander (concentration stated in results), 2 % DMSO) or 100  $\mu\text{L}$  control media (assay media + 2 % DMSO), the plates then had their absorbance recorded at 600 nm, and were then incubated for a further 4 h, 30  $^{\circ}\text{C}$ , 200 rpm, then the absorbance was again recorded at 600 nm from the plate reader (Enspire 2300 Multiplate Reader, PerkinElmer, Waltham, MA, USA). From these readings the percentage decrease in cell growth was deduced by comparing T4-T0 OD<sub>600</sub> data of NTRs with compounds to the unchallenged plates.

### **2.9.3 IC<sub>50</sub> analysis**

Bacterial cultures were grown overnight from glycerol stocks as previously described in section 2.9.1. The following day, 50  $\mu\text{L}$  of overnight culture was added to 1 mL of assay media (LB + amp 100 $\mu\text{g mL}^{-1}$ , 0.05 mM IPTG, 0.2% glucose) in 15 mL falcon tubes and incubated at 30  $^{\circ}\text{C}$ , 200 rpm for 2.5 h. Day cultures were then splint into new 96 well plates in duplicate, containing 40  $\mu\text{L}$  of challenge media (assay media + nil bystander (concentration stated in results), , 2% DMSO) in a gradient concentration across 7 wells. and an eighth unchallenged well. The plates then had their absorbance recorded at 600 nm, and were incubated for a further 4 h, 30  $^{\circ}\text{C}$ , 200 rpm, then the absorbance was again recorded at 600 nm from the plate reader (Enspire 2300 Multiplate Reader, PerkinElmer, Waltham, MA, USA). From these readings the IC<sub>50</sub> was obtained using the statistical analysis software Prism<sup>®</sup>.

### **2.9.4 Fluorescence assay**

Bacterial cultures were grown overnight from glycerol stocks as previously described in section 2.9.1. The following day, 15  $\mu\text{L}$  of overnight culture was added to 200  $\mu\text{L}$  of assay media (LB + amp 100 $\mu\text{g mL}^{-1}$ , 0.05 mM IPTG, 0.2 % glucose) in new 96 well plates and incubated at 30  $^{\circ}\text{C}$ , 200 rpm for 3.5 h. Day cultures were then split into 100  $\mu\text{L}$  into new 96 well plates in duplicate, containing either 100  $\mu\text{L}$  challenge

media (assay media + fluorophore (concentration stated in results), , 2 % DMSO) or 100  $\mu$ L control media (assay media + 2% DMSO), and incubated for 3-4 h 30 °C, 200 rpm. The absorbance was then read at three different excitation/ emission settings dependent on the masked fluorophore present; red fluorescence (ex 645/ em 660), green fluorescence (ex 405/ em 585), blue fluorescence (ex 355/ em 460) on the plate reader (Enspire 2300 Multiplate Reader, PerkinElmer, Waltham, MA, USA). The fluorescence level of the empty plasmid control strain, pUCX, was deducted from each nitroreductase: fluorophore fluorescence level to account for background fluorescence.

### **2.9.5 Combined growth inhibition and fluorescence assays**

Bacterial cultures were grown overnight from glycerol stocks as previously described in section 2.9.1. The following day, 15  $\mu$ L of overnight culture was added to 200  $\mu$ L of assay media (LB + amp 100 $\mu$ g mL<sup>-1</sup>, 0.05 mM IPTG, 0.2% glucose) in new 96 well plates and incubated at 30 °C, 200 rpm for 3.5 h. Day cultures were then split into 100  $\mu$ L into new 96 well plates in duplicate, containing either 100  $\mu$ L challenge media (assay media + fluorophore (concentration stated in results), + nil bystander antibiotic (concentration stated in results), + 2% DMSO) or 100  $\mu$ L control media (assay media + 2% DMSO). The plates then had their absorbance recorded at 600 nm and were incubated for 3-4 h 30 °C, 200 rpm. The absorbance at 600 nm was then read again to evaluate growth inhibition, and also at three different excitation/ emission settings; red fluorescence ex 645/ em 660), green fluorescence (ex 405/ em 585), blue fluorescence on the plate reader (Enspire 2300 Multiplate Reader, PerkinElmer, Waltham, MA, USA). The fluorescence level of the empty plasmid, pUCX, was deducted from each nitroreductase: fluorophore fluorescence level to account for background fluorescence.

### **2.9.6 Bacterial confocal microscopy**

Cultures were set up and challenged with either masked fluorophore(s) – as for the fluorescence assay above (Section 2.9.5) - or a combination of masked fluorophore(s) and a nil bystander antibiotic (concentrations stated in results), - as for combined growth inhibition and fluorescence assay above (Section 2.9.5). A 5  $\mu$ L of culture



was collected and mixed with 5  $\mu\text{L}$  of 4% paraformaldehyde. The mixture was then placed in the centre of a microscope slide and covered with a cover slip. Slides were observed and photographed under the confocal microscope (Olympus FV1000) on the same day as they were made.

### **2.9.7 Validation of liquid media protocol with potential to be used for novel nitroreductase discovery**

Bacterial cultures from glycerols were grown overnight in a 15 mL falcon 3 mL LB + antibiotic. The following day 50  $\mu\text{L}$  of overnight culture was added to 3mL LB + 100  $\mu\text{g mL}^{-1}$  amp + 2.5  $\mu\text{M}$  niclosamide. The  $\text{OD}_{600}$  was measured at 0 h, 2 h, 4 h, 8 h.

### **2.9.8 Validation of solid media protocol with potential to be used for novel nitroreductase discovery**

Bacterial cultures from glycerols were grown overnight in a 15 mL falcon 3 mL LB + antibiotic. The following day the cells were pelleted by centrifugation at 1250 rpm. The pellet was washed and resuspended in 1 mL of 1 x PBS. The culture was diluted  $1 \times 10^6$  fold in 1 x PBS 100  $\mu\text{L}$  of the dilution plated on solid media plates containing of 100  $\mu\text{g mL}^{-1}$  amp, 0.05 mM IPTG, 10  $\mu\text{M}$  metronidazole, and 2.5  $\mu\text{M}$  niclosamide. After a 48 h growth period, colonies were picked and PCR screened to determine using Bioline Biomix Red<sup>TM</sup> as per components and parameters outlined in 2.8.8 and 2.8.9, as well as undergoing fluorescence screening as per 2.9.4 with masked fluorophore FSL41 (concentration stated in results),.

## **2.10 Mammalian cell protocols**

### **2.10.1 Construction of mammalian nitroreductase stable expression cell lines**

For experimental analysis of bacterial NTR activity in mammalian cells, mammalian cell lines stably expressing bacterial nitroreductases were generated in HEK293 cell lines (Table 2.5).

### 2.10.2 Creating Gateway® constructs

The Gateway primers as listed in Table 2.6 were used to amplify the NTR gene using the standard PCR method as described in Section 2.8.9. PCR reactions were then analysed by gel electrophoresis to check for a product of the correct size for the target NTR. The PCR reactions were then DNA purified using the Zymo DNA Clean and Concentrate™ Kit (Zymo Research, Irvine, CA, USA).

### 2.10.3 BP recombination

The Gateway entry clone was then created through a BP recombination step using the pDONR221 (purchased from Invitrogen, Carlsbad, CA). The BP clonase II kit was also purchased from Invitrogen (Carlsbad, CA). The components of Table 2.12 were added to a 1.5 mL microfuge tube and then incubated at 25 °C for at least twelve hours. After incubation 1 µL of Proteinase K was added to each reaction tube and incubated at 37 °C for 10 minutes. Each BP reaction was then transformed into DH5α competent cells. Transformations were then plated on LB + kanamycin plates and incubated overnight at 37 °C.

**Table 2.15 BP recombination reaction components**

Component	Sample	Positive Control	Negative Control
PCR product (20- 50 fmol)	1-7 µL	-	-
pDONR221 vector (150 ng/µl)	1 µL	1 µL	1 µL
pEXP7-tet positive control (50 ng/µl)	-	2 µL	-
TE Buffer, pH 8.0	Up to 8 µL	5 µL	7 µL

### 2.10.4 Analysing entry clones

Five colonies were picked from the plates from the BP recombination step and cultured overnight in 3 mL LB + kanamycin. Plasmid DNA was then isolated from

the overnight cultures using the miniprep protocol described in section (2.8.13). Restriction enzyme NheI was used to cut the plasmid to confirm the presence and correct orientation of the insert. Entry clones that showed the correct restriction pattern were then sequenced to confirm the correct insert was present.

### 2.10.5 LR recombination

The next step was to carry out the LR recombination step. The LR clonase II enzyme mix, proteinase K solution and pENTR-gus were all purchased from Invitrogen (Carlsbad, CA). The destination vector used in these experiments was F279/V5 which was created by Dr Adam Patterson at the ACSRC (Prosser *et al.*, 2013). The components of the reaction as listed in Table 2.13 were added to 1.5 mL microfuge tubes and reactions then incubated at 25 °C for 12 hours.

After incubation 1 µL of Proteinase K solution was added to each reaction and incubated at 37 °C for 10 minutes. Samples were either stored at -20 °C or 4 µL of each LR recombination was transformed into DH5α competent cells. Expression clones were selected for by plating on LB + ampicillin plates.

**Table 2.16 LR recombination reaction components**

Component	Sample	Positive Control
Entry clone (50- 150 ng/reaction)	1-7 µL	-
Destination Vector (150 ng/µL)	1 µL	1
pENTR-gus (50 ng/µL)	-	2
TE Buffer, pH 8.0	Up to 8 µL	5

### 2.10.6 Confirming the identity of F279/ V5 destination clones

This was done through a restriction digest using the restriction enzyme HindIII and analyzing the result by gel electrophoresis. Confirmed expression clones were sequenced and then a midiprep of the construct carried out using the Geneaid high-speed plasmid midi kit (Taiwan, ROC). These constructs were then used to transfect cell lines of interest.

### 2.10.7 Stable Transfection Cell Lines

### **2.10.7.1 Lipofectamine<sup>TM</sup> 2000 reagent protocol**

250,000 HEK WT cells were seeded into a tissue culture treated 6 well plate containing 2 mL DMEM (life technologies) media with 5% Fetal Calf Serum (FCS), 2% Penicillin/ Streptomycin, and 2% HEPES. Plates were then incubated at 37 °C 5% CO<sub>2</sub> for 24 hours.

For each transfection 4 µg of DNA from the F279/ V5 constructs was diluted in 500 µl of serum free media and mixed thoroughly in a sterile microcentrifuge tube. In a separate sterile microcentrifuge tube, 8 µL of the transfection reagent was added to 492 µL of serum free media. These separate sterile microcentrifuge tubes were incubated at room temperature for 5 minutes and then combined and incubated at room temperature for a further 20 minutes.

After incubation the transfection mixture was added to the well containing the cells and mixed in gently. Cells were put back in the 37 °C 5% CO<sub>2</sub> incubator. Cell populations were then sub-cultured at least 3 times, with increasing concentrations of puromycin, to a final concentration of 2 µM.

### **2.10.7.2 Making stocks of stable cell lines**

Cells from a 6 well plate that had almost grown to confluence after transfection were harvested and seeded into T75 cell culture flasks. Cells were left to grow at 37 °C 5% CO<sub>2</sub> until 90% confluence was reached, and then harvested following the Trypsin/EDTA method. The cells were centrifuged at 1250 rpm for 5 minutes to pellet. The supernatant was discarded and the pellet was then resuspended in PBS. Cells counted, and 5 million were added to 1 mL FCS and 10% DMSO in cryotubes. The 1 mL aliquots were then frozen down at a rate of -1 °C per minute. Once samples had reached -80 °C they were transferred into liquid nitrogen for long-term storage.

### **2.10.8 MTS assay**

The viability of mammalian NTR expression cell lines post incubation with nil

bystander antibiotics was assessed using a standard MTS assay (ref a MTS assay paper). Cells were seeded (10,000 per well in 100  $\mu$ L of media) into a tissue culture treated 96 well plate. For each strain sufficient wells were seeded so that cell viability could be monitored in triplicate at 0, 5, 10, 30, 40 and 80  $\mu$ M of nil bystander (unless otherwise stated) and following both 24 and 48 hours exposure to antibiotic.

Plates were incubated at 37 °C 5% CO<sub>2</sub> overnight. Media was then aspirated from each well and replaced with 100  $\mu$ L of phenol free media supplemented with appropriate concentration of nil bystander antibiotic.. Plates were returned to the incubator. After 24 hours one experimental plate set was removed from the incubator. To each well 30  $\mu$ L of MTS reagent (CellTitre 96 Aqueous One Solution Cell Proliferation Assay - Promega, Madison, WI, USA) was added. Plates were returned to the incubator for an hour. Plates were read on a plate reader at 590 nm (Enspire 2300 Multiplate Reader, PerkinElmer, Waltham, MA, USA). At 48 hours the remaining plates were removed and steps from the 24 hour time period repeated.

#### **2.10.9 Confocal microscopy in mammalian cells**

5x10<sup>6</sup> cells were seeded into 35 mm Fluorodish Cell Culture Dishes (World Precision Instruments Inc., Sarasota, FL) in 1 mL phenol free media and incubated at 37 °C 5% CO<sub>2</sub> overnight. Masked fluorophore was added to a final concentration of 50  $\mu$ M and the cells incubated for a further hour. Fluorescent cells were then visualized in the culture dishes using an Olympus FV1000 confocal microscope.

#### **2.10.10 Microscopy of challenged mammalian cells**

2.5x10<sup>4</sup> cells were seeded into T25 cell culture flasks in 5 mL DMEM media and incubated at 37 °C 5% CO<sub>2</sub> overnight. Nil bystander antibiotic was added to a final concentration of 5  $\mu$ M and the cells incubated for a 48 hour period. Cells were then visualized on an Olympus IX51 Microscope.

#### **2.10.11 Confocal microscopy of challenged mammalian cells treated with masked fluorophores**

$5 \times 10^6$  cells were seeded into 35 mm Fluorodish Cell Culture Dishes (World Precision Instruments Inc., Sarasota, FL) in 2 mL phenol free media and incubated at 37 °C 5% CO<sup>2</sup> overnight. Nil bystander antibiotic was added to a final concentration of 150 µM and the cells incubated for a further two hours. After one hour masked fluorophore was added to a final concentration of 25 µM and the cells incubated for a further hour. Cells were then visualized in the culture dishes using an Olympus FV1000 confocal microscope.

### 3. Nil Bystander Antibiotics

#### 3.1 Introduction

This chapter outlines the results from screening of the 58 nitroreductase core library with the 16 chosen nil bystander antibiotics. The 58 nitroreductase core library was developed in the Ackerley lab and is a very valuable resource, as it encompasses a large variety of nitroreductases. The library is weighted heavily toward the two major characterised nitroreductase families; NfsA and NfsB. The 16 nil bystander antibiotics were chosen based on availability in the lab, as well as either known nil-bystander prodrug activity or structural features consistent with such activity. All of the experiments undertaken in this thesis were based on the results observed in the growth inhibition screening assays (protocol 2.9.2).

The initial motivation for this work was to investigate the ability of nitroreductases to reduce a range of nitro-quenched nil-bystander antibiotics, to provide a potential safety mechanism for eliminating biological vectors from GDEPT patients post-therapy, or if PET imaging were to indicate undesirable vector localisation. This is a very desirable feature, as pathogenic microorganisms are the most commonly used vectors in solid tumour targeting. Due to their pathogenic origins the FDA requires that there be a way to eliminate these vectors from the patient. While bacteria such as *Clostridium* species are already sensitive to antibiotics such as metronidazole (and indeed, in the clinic are typically cleared with this antibiotic), heightened sensitivity is a very desirable feature. Moreover, whereas viruses are not generally sensitive to antibiotics, recent work by our collaborator Dr Adam Patterson has suggested that nitroreductase-mediated activation of potent nil-bystander prodrug antibiotics may provide a mechanism to clear viral vectors (Figure 1.6).

Contemporary use of nitroreductases has also explored the possibility of their use in developmental biology. Curado *et al.* (2007) engineered a system whereby a promoter drives the expression of a nitroreductase; in this case NfsB\_Ec. When the nil bystander antibiotic metronidazole is added, it is converted to its cytotoxic form, inducing DNA damage in the cells in which the nitroreductase is present, resulting in cell death. The promoter is also fused (as a bicistronic construct) to a reporter gene

such as GFP, which enables visualisation of the cells expressing the nitroreductase prior to the addition of metronidazole and the confirmation of nitroreductase activation after addition as the fluorescence ceases, indicating the cells with GFP and nitroreductase are no longer intact and expressing.

Previous experiments undertaken in the Ackerley lab however have suggested that NfsB\_Ec has relatively low activity with metronidazole compared to other nitroreductases in our collection. As mentioned in section 1.9.?, NfsB\_Ec, is insufficiently active with metronidazole to give clean targeted cell ablation without high background toxicity, thus, identification of superior nitroreductases for activation of metronidazole and/or superior nitroreductase/ nil bystander antibiotic combinations would be highly advantageous in this context. Achieving one or both outcomes was the initial goal of the research described in this thesis.

A more ambitious research goal was to expand on a uni-dimensional GFP: nitroreductase ablation system to identify pairs of nil bystander antibiotics/ nitroreductase s with opposing activation profiles. The idea behind this was the possibility of using these in a multiplexed scenario, to specifically target two distinct cell populations and observe the effects of ablation of each; either simultaneously or independently (as per Figure 1.11).

Thus, the research described in the first part of this chapter begins with initial screening in *E. coli* of the 58 nitroreductase core library against the 16 nil bystander antibiotics and the creation of a heat-map based on activation profiles observed in growth inhibition screens - allowing rapid identification of nitroreductases with high activation of nil bystander antibiotics, and also pairs of nitroreductases that exhibit opposing activation profiles with different nil-bystander antibiotics. This initial screen was followed up by a more detailed and more quantitative IC<sub>50</sub> analysis of nitroreductase / nil bystander combinations that appeared to have potential for use in the dual ablation system.

The second part of this chapter explored the translation of results observed in bacterial cells into human cell lines. The ability of the nitroreductases to be active in



eukaryotic cells is essential for their continued use in developmental and regenerative biology, and in GDEPT. Previous studies from the Ackerley lab have indicated that not all bacterial nitroreductases are tolerated in transgenic human cells, with approximately 50% of candidates unable to form stably transfected cell lines (Prosser *et al.*, 2013). Thus, it was essential to test that results observed in bacterial assays were predictive of the phenotypes that would be observed in nitroreductase transfected eukaryotic cell lines.

During the initial screening in bacterial cells one of the candidate nil bystander antibiotics that was examined, niclosamide, appeared to have the opposite activation profile with the nitroreductase library than had been expected, i.e. was toxic to wild type *E. coli* but not to bacteria expressing active nitroreductases. The final section of this chapter explores this anomaly, and the potential of niclosamide to be exploited as a novel nitroreductase screening method.

### **3.1.1 Nil bystander antibiotics**

The nil bystander antibiotic candidates that were tested in this study are summarised in table 2.1. As confirmation that a particular molecule does indeed exhibit a negligible bystander effect is a complex and time-consuming task (requiring 3D mixed cell cultures, e.g. Wilson *et al*, 2002), for this study candidate molecules were chosen based on historical significance, availability in the laboratory, and/or structural similarity to molecules that were already in use in the lab. Below, I will briefly discuss the grounds for inclusion of the nil bystander antibiotics.

These compounds should be non-toxic in their original state. However, the reduction of their nitro group leads to the production of short-lived cytotoxic intermediates. The toxicity of the intermediates is due to their interaction with deoxyribonucleic acid and possibly with other macromolecules (Muller, 1983). Metronidazole is one of the most well-studied of the nil bystander antibiotics used in this research. It has been implemented medically for over 45 years (Löfmark *et al*, 2010) and is capable of wiping out anaerobic bacterial populations. Metronidazole's mechanism of action is not fully elucidated; it is readily taken up by obligate anaerobic organisms and is subsequently reduced by low-redox potential electron-transport proteins to an active,

cytotoxic intermediate product. The reduced product of metronidazole causes DNA strand breaks, thereby inhibiting DNA synthesis and bacterial cell growth (<http://www.drugbank.ca/drugs/DB00916>, accessed 20.08.2013).

Tinidazole is also a well-studied antibiotic. It has antiprotozoal properties, and its nitro group is reduced upon activation, generating a series of free nitro radicals. Toxicity is achieved via depletion of sulfhydryl groups and DNA strand breaks, with multiple hits having an additive effect, ultimately leading to cell death (<http://www.drugbank.ca/drugs/DB00911> accessed 20.08.2013). It was originally used in the treatment of several protozoal infections (Sawyer *et al.*, 1976) but as with all of these molecules the potential to damage DNA upon activation gives it generic cell ablation capabilities.

Another advantage of metronidazole and tinidazole is that they have been shown to be capable of targeted ablation of individual bacteria or virus infected cells without localised tissue damage, and that they are able to be activated by two common nitroreductases NfsA\_Ec and NfsB\_Ec (Prosser *et al.*, 2010b). Researchers at the Auckland Cancer Society Research Centre (ACSRC) have also been able to show that metronidazole has the ability to suppress the replication of the ONYX-411 adenovirus in cultured human cell lines when it is labelled with *nfsB\_Ec*, but not the wildtype ONYX-411 adenovirus (Figure. 1.6). This revelation has made these two nil bystander antibiotics the most focused on throughout this thesis.

Misonidazole and F-misonidazole are both nitroimidazole radiosensitisers. They induce the formation of free radicals and deplete thiols, consequently sensitising hypoxic cells to the cytotoxic effects of ionizing radiation induced by single strand breaks in DNA resulting in the inhibition of DNA synthesis (<http://www.cancer.gov/drugdictionary?cdrid=39504> accessed 20.08.2013, <http://www.cancer.gov/drugdictionary?cdrid=458064> accessed 20.08.2013). F-misonidazole has the added potential to be labelled with the radionuclide  $^{18}\text{F}$  to enable PET imaging of hypoxia (<http://imaging.cancer.gov/programsandresources/fmiso-documentation> accessed 02.09.2013).

EF5 is a fluorinated derivative of the 2-nitroimidazole etanidazol. Reduction of EF5 is carried out by a diverse group of enzymes in the cytoplasm, microsomes and mitochondria. Tissue hypoxia detection via EF5 has been seen in several cancers, including squamous cell carcinoma of the cervix and the head and neck, and in sarcoma (Komar *et al.*, 2008).

Dimetridazole, ornidazole, and ronidazole have antiprotozoal and antibacterial properties, and are most commonly used in the agricultural sector to prevent bacterial infections, cure protozoan infections, and for the treatment of swine dysentery respectively (Moreno & Docampo, 1985). Ornidazole has also been explored as a treatment for Crohn's disease and is commonly used as an antimicrobial agent in patients undergoing gastrointestinal surgeries (Steib *et al.*, 1993).

Furazolidone is a broad-spectrum nitrofurantoin with antiprotozoal and antibacterial properties. It has been used in both human and veterinary medicine. It works by binding bacterial DNA which leads to the gradual inhibition of monoamine oxidase (<http://www.drugbank.ca/drugs/DB00614> accessed 20.08.2013).

Niclosamide is a taeniocide, a substance used to eradicate tapeworms, which is used for the treatment of most tapeworm infections (<http://www.drugbank.ca/drugs/DB06803> accessed 20.08.2013). More recently it has been explored for potential use in cancer treatment (Sack *et al.*, 2011, Osada *et al.*, 2011).

Nifurtimox is a nitrofurantoin derivative with antiprotozoal characteristics. It is reduced by cytosol enzymes or flavin-containing microsomal enzymes to a highly reactive nitro anion free radical. These derivatives alkylate macromolecules such as nucleic acids and proteins, resulting in the disruption of their structure and function. (<http://www.cancer.gov/clinicaltrials/search/view?cdrid=586650&version=HealthProfessional> accessed 20.08.2013) Along with *N*-benznidazole, nifurtimox is commonly used for the treatment of Chagas disease (Castro and Diaz de Toranzo 1988).

Nitrofurantoin is a broad spectrum antibacterial that is active against some gram-positive and gram-negative organisms. It is commonly used for treating urinary tract infections, but is of particular interest due to its high stability to the development of bacterial resistance, a property thought to be due to its multiplicity of mechanisms of action. (<http://www.drugbank.ca/drugs/DB00698> accessed 20.08.2013).

Nitrofurazone is a topical anti-infective agent effective against gram-negative and gram-positive bacteria. It is most commonly used for superficial wounds, burns, ulcers, and skin infections, although it has also been administered orally in the treatment of trypanosomiasis (<http://www.drugbank.ca/drugs/DB00336> accessed 20.08.2013).

2-Methyl-5-Nitroimidazole and 4-Nitroimidazole are generic imidazole derivatives, which are routinely used in the treatment of many systemic fungal infections (Gunay *et al.*, 1999, Benkli *et al.*, 2003)

### **3.1.2 Nitroreductase library**

The core nitroreductase library in the Ackerley lab was constructed by various past and present lab members in the *E.coli* SOS-R2 strain (table 2.3). Preliminary nitroreductases were chosen from the NCBI database through BLAST homology searches using each of the *E. coli* enzymes as well as human NQO1 and YwrO as query sequences. The library was categorised into separate families based around these key members. Nitroreductases were chosen from a range of bacterial species based on availability in the Ackerley laboratory; this included both Gram-positive and Gram-negative strains, with the only other criteria for selection being sharing at least 25% amino acid identity with the key family member. Nitroreductase enzymes that were identified were subsequently cloned into the plasmid pUCX (Figure 3.1).

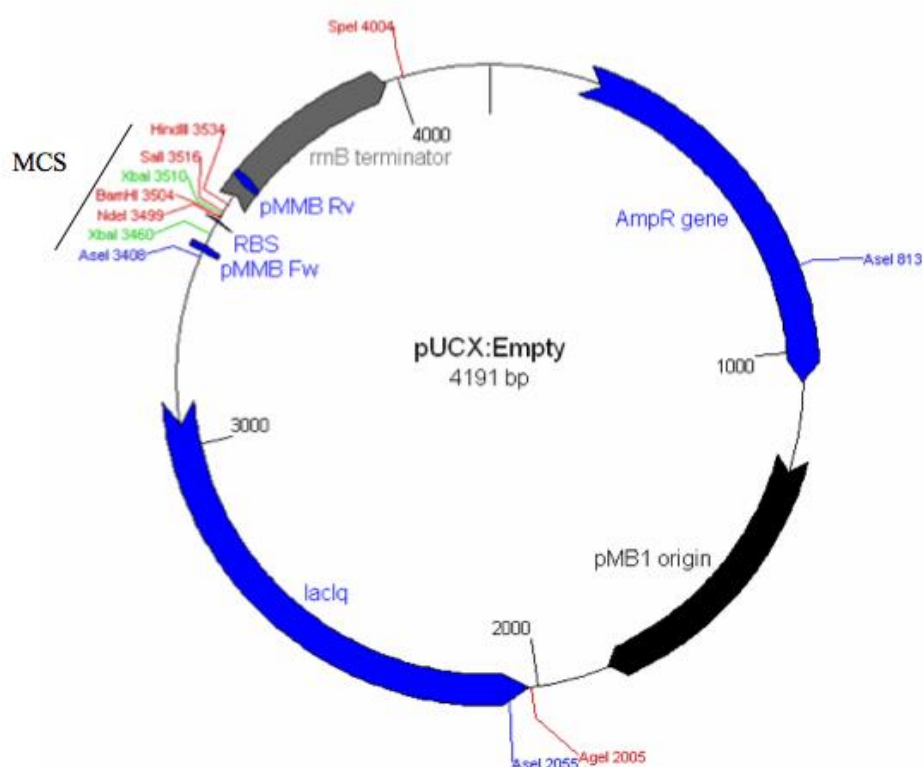


**Figure 3.1 Map of pUCX expression plasmid.** This plasmid was created by Dr Gareth Prosser by combining parts of commercially available plasmids pMMB and pUC19 to give a plasmid that exhibited improved expression of nitroreductases inserted into the multiple cloning site (MCS) (Prosser *et al.*, 2010). The empty plasmid was used as a control in library screening.

The library was specifically designed to identify nitroreductases which were capable of reduction of nitro-quenched prodrugs. A core library of 58 nitroreductases (table 3.1) was established to test activity with the prodrugs CB1954 and PR104A (Prosser *et al.*, 2013). It was discovered that nitroreductases that are members of the NfsA or NfsB families were consistently the most active (19 of the 20 most active enzymes) with each prodrug (Prosser *et al.*, 2013). This general trend has also been seen across a wide range of other nitro-aromatic substrates (Dr David Ackerley, *personal communication*).

### 3.1.3 Aims

The key aims of the research described in this chapter were to: i) Measure the activation profiles of the 16 different nil bystander antibiotics with members of the 58 nitroreductase core library, identifying nitroreductases with higher activation of metronidazole (and other promising prodrugs) than NfsB\_Ec, and identifying pairs of

nil bystander antibiotics/ nitroreductases which show opposing activation profiles; ii) Translate the results observed in bacterial cells into human cell lines for proof of principle of use in eukaryotic models; and (iii) Explore the potential of niclosamide to be used in a functional screening system for the discovery of new nitroreductases.

## **3.2 Results**

### **3.2.1 Identification of nitroreductases with a superior activation profile with metronidazole than NfsB\_Ec**

As noted above, contemporary studies in mammalian models in developmental and regenerative biology are exploring the use of nitroreductases paired with nil bystander antibiotics for temporally and spatially controlled targeted cell ablation. These studies have focused on the combination of metronidazole and to date have exclusively used the nitroreductase NfsB\_Ec. However, in previous pilot screens of a subset of the 58 nitroreductase library in the Ackerley lab, NfsB\_Ec didn't register as a nitroreductase with good efficacy for metronidazole. In order to more rigorously quantify the relative activity of the different nitroreductases in the 58 nitroreductase library, this library was screened with metronidazole by growth inhibition assay (Section 2.9.2). Growth inhibition assays allow the evaluation of the potency of a compound in given cell population. For example, higher levels of cell death at a particular concentration of indicate higher reduction efficiency by the nitroreductase present, subsequently causing a higher growth inhibition in these populations than in populations which the nitroreductases ability to activate metronidazole is less efficient. Growth inhibition assays are relatively high throughput and reproducible, giving reliable data on which to base further experiments. The results of the metronidazole growth inhibition screening are illustrated in Figure 3.2.

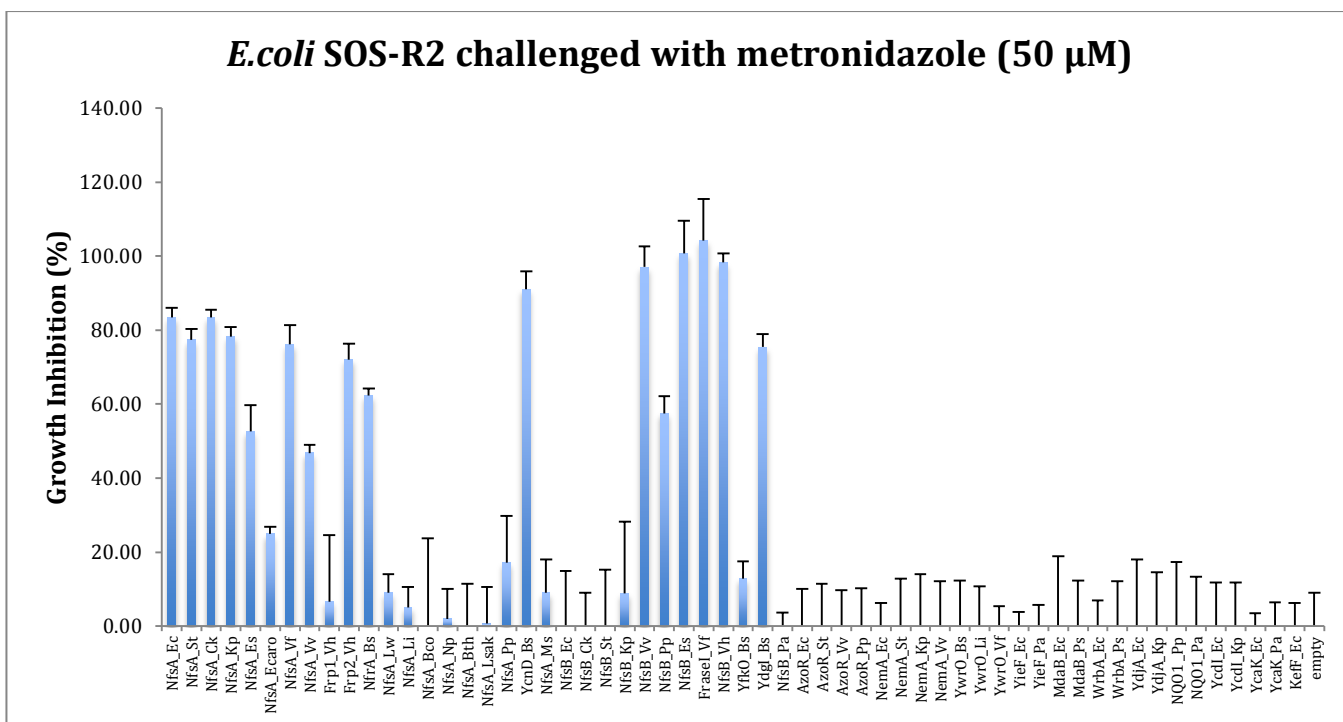


**Figure 3.2 Metabolism of metronidazole by members of the 58 nitroreductase over-expression library as measured by growth inhibition assay.** Turbidity (OD<sub>600</sub>) of nitroreductase over-expressing *E. coli* cultures was recorded directly before and after 4 h incubation with 50 µM metronidazole. Growth Inhibition is expressed as the percentage decrease in OD<sub>600</sub> of challenged cells relative to unchallenged control cells for each strain post-incubation. Data are the average of 5 independent assays and the error bars indicate  $\pm 1$  standard deviation. The bars corresponding to the NfsA and NfsB family members are as marked, and the arrow indicates NfsB\_Ec. The empty plasmid control is indicated by “Empty”, at the far right of the graph.

As can be seen in figure 3.2, the initial screening in bacterial cells showed that many other nitroreductases were capable of activating metronidazole at far lower concentrations. The nitroreductase with the highest activation profiles with metronidazole were from the NfsB family; NfsB\_Vh, NfsB\_Vv, NfsB\_Es, and the NfsB like FraseI\_Vf. More quantitative IC<sub>50</sub> assays were carried out with *E. coli* strains over-expressing these nitroreductases as well as NfsB\_Ec, NfsA\_Ec and pUCX empty plasmid control (figure 3.3).

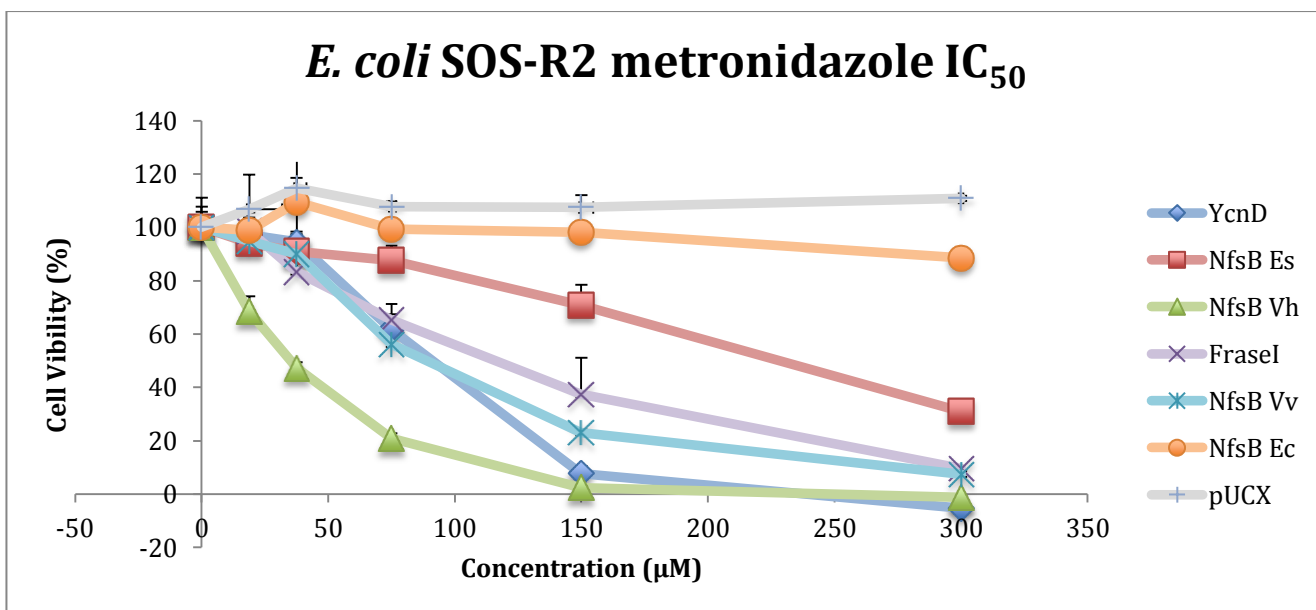


**Figure 3.3 Metabolism of metronidazole by 6 nitroreductase enzymes from the 58 nitroreductase enzyme over-expression library over a range of concentrations as measured by IC<sub>50</sub> analysis.** Turbidity (OD<sub>600</sub>) of nitroreductase over-expressing *E. coli* cultures was recorded directly before and after 4 h incubation with 5 different metronidazole concentrations (18.75 µM, 37.5 µM, 75 µM, 150 µM 300 µM). Cell viability is expressed as the percentage decrease in OD<sub>600</sub> of challenged cells relative to unchallenged control cells for each strain post-incubation. Data are the average of 3 independent assays and the error bars indicate  $\pm 1$  standard deviation.

**Table 3.1 IC<sub>50</sub> results of 6 nitroreductase enzymes from the 58 nitroreductase enzyme over-expression library**

This table shows the IC<sub>50</sub> values shown graphically in figure 3.3 as calculated by the statistical analysis software Prism<sup>®</sup>.

Nitroreductase	IC <sub>50</sub> Value (µM)
YcnD	76.62
NfsB Es	431.2
NfsB Vh	47.48
FraseI	169.2
NfsB Vv	90.12
NfsB Ec	928.1

From the results, we can conclude that all of the nitroreductases identified in the initial full-library screen as having substantially greater activity with metronidazole than NfsB\_Ec were confirmed by the IC<sub>50</sub> analysis. NfsB\_Vh showed the best activity. We have previously observed that nitroreductase activity seen in bacterial cells isn't always translated into human cell lines. Fortunately, as part of a different study NfsB\_Vh had previously been transfected into the human colon carcinoma cell line HCT-116 by Dr Horvat, so this stably transfected cell line was able to be used in initial experiments for metronidazole activity in human cell lines.



Cells were seeded into T25 and treated with 5  $\mu$ M drug - this drug concentration was based on previous MTS assays carried out by Dr Horvat, which indicated that after a 48 h period 5  $\mu$ M metronidazole was an optimal concentration to induce complete cell death in human cell lines sensitive to metronidazole.

These experiments in HCT-116 NfsB\_Vh showed that a low concentration of metronidazole was capable of inducing cell death in these cell lines as can be seen in figure 3.4. A HEK293: NfsB\_Ec cell line was generated as per described in section 3.2.5. to compare the effect of metronidazole on human cells when NfsB\_Ec was present. As can be seen in figure 3.5, metronidazole appears to have no effect on human cell lines containing the nitroreductase NfsB\_Ec. This demonstrates that NfsB\_Vh is far superior at activating metronidazole than NfsB\_Ec in human cells, suggesting that it would be an ideal candidate for further experimental work in eukaryotic model organisms.

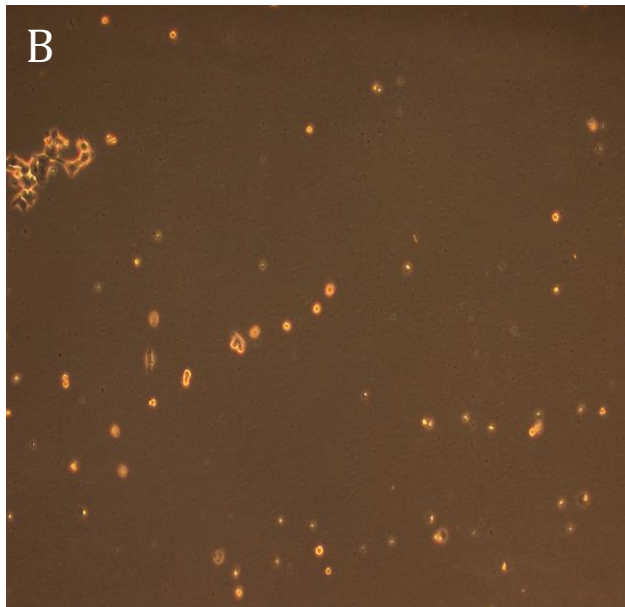
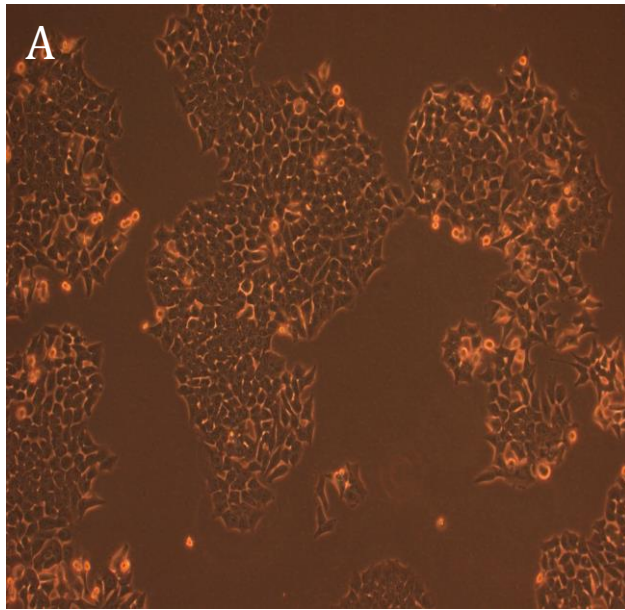


**Figure 3.4 Metronidazole challenged HCT-116: NfsB Vh cells.** Cells were seeded at a density of 250,000 into T25 flasks and left to grow overnight to approximately 80% confluency. 5 $\mu$ M metronidazole was added to the cells and they were left for 48 h. Bright field images of the cell population were taken at 0 h and 48 h with an Olympus IX51 microscope using the 20x lens. **A.** HCT-116: NfsB Vh cells (0 h) **B.** HCT-116 NfsB Vh cells challenged with 5 $\mu$ M metronidazole 48 h. After 48 hours in the presence of a low concentration of metronidazole, the cells look unhealthy as the cell morphology has changed and population has decreased dramatically compared to when the population had not been in the presence of metronidazole.

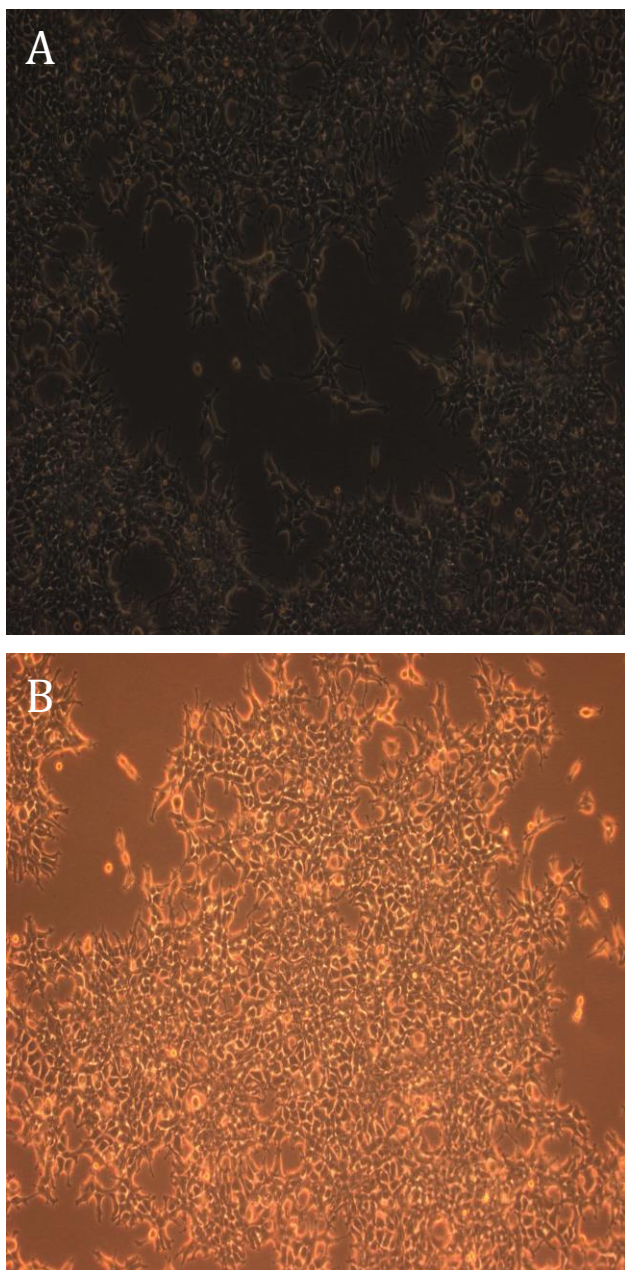


**Figure 3.5 Metronidazole challenged HEK293: NfsB\_Ec cells.** Cells were seeded at a density of 250,000 into T25 flasks and left to grow overnight to approximately 80% confluency. 5μM metronidazole was added to the cells and they were left for 48 h. Bright field images of the cell population were taken at 0 h and 48 h with an Olympus IX51 microscope using the 20x lens. **A.** HEK293: NfsB\_Ec (0 h) **B.** HEK293: NfsB\_Ec cells challenged with 5μM metronidazole 48 h. After 48 hours in the presence of a low concentration of metronidazole, the cells look healthy as the cell morphology is unchanged and cell population appears to have increased compared to 0 h, suggesting at concentrations this low, NfsB\_Ec is incapable of activating metronidazole in human cell line HEK293.

### 3.2.2 Growth inhibition assays

As an alternative approach to identifying a nitroreductase with higher activity with metronidazole than NfsB\_Ec, we explored the possibility of employing a different nil bystander antibiotic for use in the ablation of specific cell types in developmental biology model organisms. Growth inhibition assays as detailed in 2.9.2 were carried out on the 58 nitroreductase core library with all 16 of the nil bystander antibiotics as listed in table 3.1. Each assay was carried out at least 5 times to guarantee statistical

significance, as these results were to provide the basis of all further experimental research in this thesis.

The percentage of cell death for each nil bystander antibiotic/ nitroreductase combination was determined by calculating the percentage of cell death after 4 hours of challenge with the nil bystander antibiotic compared to unchallenged control cells for each strain after 4 hours. Graphs of each of these nil bystander antibiotic/ 58 nitroreductase library screens were generated by averaging the percentage of cell death observed and adding error bars ( $\pm$  1 standard deviation).

To provide an easily interpreted summary of which nil bystander antibiotic/ nitroreductase combinations were active or not active, arbitrary cut off points were set to denote high activity, some activity, or no activity. These points were 75-100% growth inhibition, 30-74% growth inhibition and 0-29% growth inhibition respectively. The numerical data from the screening was collated into a table colour-coded heat-map to denote these percentage cutoffs – green high activity, orange some activity, or red no activity. The results of this screening can be seen below in the heat-map (figure 3.6).

	2M5NI	4NI	DTZ	EF5	FMISO	FUR	MTZ	MISO	NB2NI	NCS	NFX	NFN	NFZ	ORN	TIN	RNZ
NfsA_Ec	17.42	72.63	14.99	57.24	79.51	83.18	83.45	85.63	107.11	24.84	80.14	84.76	91.08	81.70	93.17	108.47
NfsA_St	28.65	70.98	19.67	105.40	100.16	82.00	77.37	79.03	106.71	29.08	77.69	88.22	93.04	78.66	72.39	99.39
NfsA_Ck	45.64	71.02	5.37	67.59	90.63	76.90	83.44	79.25	101.20	37.46	78.91	57.85	88.85	83.47	93.44	96.22
NfsA_Kp	26.46	53.43	-2.22	32.16	38.20	86.54	78.20	76.29	98.33	84.33	74.03	64.35	93.65	79.22	81.99	86.21
NfsA_Es	36.06	58.01	3.43	84.75	87.16	85.75	52.61	86.73	104.87	110.09	47.33	55.28	94.90	39.99	19.95	73.10
NfsA_Ecaro	31.20	40.29	9.82	91.47	88.50	89.83	24.94	82.56	104.93	102.18	74.10	77.85	97.16	56.68	71.82	67.59
NfsA_Vf	52.01	69.22	45.55	31.44	76.37	81.82	76.13	95.35	111.16	2.12	72.98	76.98	77.74	85.68	94.49	103.91
NfsA_Vv	61.24	66.20	0.00	20.93	66.59	90.09	46.83	90.77	108.13	0.00	73.73	58.75	95.48	85.98	86.54	98.44
Frp1_Vh	0.00	14.72	18.18	68.32	71.88	57.63	6.67	57.91	86.33	103.36	35.02	66.31	36.24	50.06	56.81	90.71
Frp2_Vh	65.64	64.71	41.12	39.16	79.05	86.46	72.07	85.04	103.95	37.33	62.46	87.71	99.01	84.02	92.78	104.35
NfrA_Bs	41.43	74.51	19.26	31.14	65.85	94.99	62.31	93.82	102.28	46.74	83.98	83.54	103.29	98.23	93.81	103.85
NfsA_Lw	29.81	32.81	0.00	57.84	46.26	89.72	8.99	84.97	96.86	106.23	73.23	70.90	101.81	43.56	52.60	64.64
NfsA_Li	7.79	11.96	23.15	22.87	34.90	72.62	5.08	80.04	87.90	98.14	51.40	65.43	71.39	71.15	89.10	85.18
NfsA_Bco	3.23	61.14	0.00	45.33	85.82	82.90	0.00	69.47	91.81	107.48	84.92	69.92	79.31	2.16	9.44	75.52
NfsA_Np	12.22	9.73	0.00	76.81	76.80	71.92	1.99	75.29	72.21	108.90	56.92	72.86	71.13	24.65	28.30	30.83
NfsA_Bth	6.11	70.15	0.00	47.65	75.18	47.70	0.00	88.37	96.68	56.94	72.31	33.88	97.04	18.71	0.00	96.02
NfsA_Lsak	4.91	17.27	7.06	41.51	55.67	82.78	0.64	51.17	52.18	108.67	63.87	69.49	87.75	0.72	18.41	27.28
NfsA_Pp	22.73	14.66	6.65	59.23	78.30	75.63	17.11	83.06	100.75	39.04	81.82	77.86	80.60	75.38	87.64	77.85
YcnD_Bs	30.83	94.85	98.04	13.85	95.83	54.33	91.08	110.13	43.03	7.49	61.45	37.76	93.60	97.68	54.59	108.52
NfsA_Ms	2.90	63.59	6.18	11.53	24.10	75.41	8.98	32.51	37.50	108.30	47.74	69.54	48.93	11.80	17.51	26.55
NfsB_Ec	0.00	13.61	10.67	3.00	4.30	62.98	0.00	14.79	445.01	24.73	65.46	75.98	55.55	10.02	19.36	63.58
NfsB_Ck	0.00	17.16	3.59	2.23	5.99	89.31	0.00	24.06	42.30	24.63	63.88	70.12	54.69	11.86	13.95	102.25
NfsB_St	10.86	14.56	32.82	0.99	3.22	82.32	0.00	10.84	15.47	26.57	75.08	58.06	54.20	25.82	36.84	115.15
NfsB_Kp	5.96	14.58	11.95	0.00	1.65	78.40	8.90	53.14	53.97	14.07	69.33	62.29	44.73	58.98	58.78	107.59
NfsB_Vv	12.41	30.05	74.31	0.00	5.85	93.42	97.07	85.90	8.36	0.00	73.49	65.81	67.77	77.53	28.77	119.35
NfsB_Pp	0.00	47.60	35.74	0.00	30.01	89.63	57.56	44.44	40.62	70.57	77.62	55.55	79.08	18.91	7.84	110.65
NfsB_Es	0.00	0.37	87.01	0.94	0.03	77.37	100.79	69.23	43.40	22.75	62.88	55.87	66.69	85.53	87.19	108.15
FraseI_Vf	170.52	6.57	99.16	0.33	15.37	89.67	104.22	80.84	54.29	22.84	67.91	60.57	34.94	86.34	100.54	104.16
NfsB_Vh	0.00	4.80	97.66	7.17	11.57	71.97	98.26	65.68	15.45	57.01	72.47	49.96	56.84	93.24	70.08	113.15
YfkO_Bs	0.00	1.96	33.02	14.26	12.45	79.12	12.85	67.76	70.40	26.55	86.15	60.56	99.23	24.44	49.75	107.74
Ydgl_Bs	0.00	15.91	36.74	0.78	11.06	84.04	75.45	94.03	27.38	95.10	65.60	71.91	63.97	95.11	105.66	107.91
NfsB_Pa	0.00	0.00	6.71	0.00	0.00	82.82	0.00	0.00	20.90	106.37	57.26	52.52	58.25	8.71	0.00	99.22
AzoR_Ec	0.00	0.00	6.26	0.00	0.00	74.53	0.00	6.58	10.04	9.87	47.08	26.22	45.76	0.00	9.79	24.42

AzoR_St	0.00	0.00	8.20	0.00	0.00	80.74	0.00	7.83	17.47	7.64	67.29	35.40	50.54	3.59	0.00	43.46
AzoR_Vv	7.46	0.00	3.12	0.00	0.00	73.88	0.00	6.25	10.34	52.51	64.46	27.40	50.85	20.08	0.00	16.30
AzoR_Pp	0.00	0.00	3.30	0.00	0.00	77.79	0.00	6.43	1.41	76.48	58.33	31.07	45.25	0.00	0.00	13.60
NemA_Ec	0.00	0.00	5.62	0.00	0.00	76.80	0.00	17.88	22.74	108.44	34.62	32.14	34.26	17.29	20.55	12.16
NemA_St	0.00	0.00	0.00	0.00	0.00	54.22	0.00	11.67	16.04	111.36	7.17	29.03	15.73	4.77	3.26	0.00
NemA_Kp	0.00	0.00	3.03	0.00	0.00	55.45	0.00	26.60	0.00	112.32	13.42	32.08	42.98	10.39	3.49	0.66
NemA_Vv	0.00	0.00	6.77	0.00	0.00	78.81	0.00	13.34	28.39	115.46	35.78	28.85	61.01	11.10	5.87	13.91
YwrO_Bs	0.36	0.00	0.00	0.00	0.00	38.88	0.00	11.96	17.17	112.04	4.41	16.97	26.04	13.71	0.00	0.00
YwrO_Li	47.69	0.00	0.00	0.00	0.00	34.98	0.00	12.49	16.95	111.98	2.34	26.95	6.80	1.20	0.00	0.00
YwrO_Vf	0.00	0.00	0.00	0.00	0.00	49.54	0.00	2.49	19.34	110.22	0.00	28.26	12.50	0.00	0.00	0.00
YieF_Ec	4.33	9.60	0.00	0.00	0.00	53.97	0.00	0.00	49.43	108.27	0.00	23.11	18.26	8.94	0.00	5.74
YieF_Pa	0.00	8.55	1.56	0.00	1.46	40.90	0.00	5.13	52.73	117.58	0.00	26.88	21.23	0.00	0.00	21.08
MdaB_Ec	0.00	13.52	41.00	0.00	0.00	62.61	0.00	13.31	43.31	118.95	16.35	24.94	19.32	14.69	3.96	44.92
MdaB_Ps	0.00	0.00	0.00	0.00	0.00	43.67	0.00	4.50	18.56	116.50	14.78	7.96	62.08	0.00	0.00	0.00
WrbA_Ec	0.00	0.00	6.23	0.00	0.00	22.20	0.00	15.47	20.07	113.62	0.00	18.80	18.79	0.00	0.00	4.22
WrbA_Ps	0.00	0.33	0.00	0.00	0.00	52.74	0.00	2.33	17.06	113.16	2.07	24.06	74.30	0.00	0.00	0.00
YdjA_Ec	0.00	3.29	0.00	0.00	7.95	46.91	0.00	3.57	19.98	114.79	0.00	0.56	17.41	0.00	0.00	0.13
YdjA_Kp	0.00	0.00	0.00	0.00	8.04	30.62	0.00	0.00	15.25	115.23	0.00	12.89	11.91	0.11	0.00	0.00
NQO1_Pp	0.00	3.33	0.00	0.00	11.81	27.43	0.00	0.00	29.10	113.58	0.00	0.00	23.00	0.00	0.00	5.15
NQO1_Pa	0.00	0.00	0.00	0.00	0.00	10.80	0.00	0.00	20.44	115.86	0.00	10.66	21.71	3.54	19.63	0.00
YcdI_Ec	0.00	18.76	0.00	0.00	0.00	19.60	0.00	0.00	30.68	115.82	9.06	28.78	13.15	0.00	33.84	0.00
YcdI_Kp	0.00	0.00	0.00	0.00	0.00	46.20	0.00	0.00	46.67	108.63	0.00	7.95	7.67	0.00	0.00	0.00
YcaK_Ec	0.00	0.00	0.00	0.00	0.00	68.12	0.00	0.00	36.79	109.43	16.50	1.30	0.00	9.10	0.00	4.36
YcaK_Pa	7.03	4.48	0.00	0.00	9.42	26.37	0.00	0.00	22.42	119.87	0.00	19.60	35.02	0.00	0.00	0.00
KefF_Ec	0.00	0.00	0.00	0.00	0.00	45.28	0.00	0.00	29.58	111.13	3.63	15.82	24.81	0.38	0.00	6.06
empty	0.00	0.00	0.00	0.00	0.00	25.10	0.00	6.67	19.10	110.95	0.00	12.34	0.00	0.00	0.00	0.00

**Figure 3.6. Colour coded heat-map summarising activation profiles of nitroreductase/ nil bystander antibiotic combinations.** The heat-map was generated from growth inhibition averages from 5 independent assays. Growth inhibition is expressed as the percentage decrease in OD<sub>600</sub> of challenged cells relative to unchallenged control cells for each strain post-incubation. Turbidity (OD<sub>600</sub>) of nitroreductase over-expressing *E. coli* cultures was recorded directly before and after 4 h incubation with nil bystander antibiotic. In this heat-map, the green squares denote nitroreductase enzymes that have high activity with the given nil bystander antibiotic, orange some activity, and red no activity. These activity margins are deduced from growth inhibition assays giving either 75-100%, 30-74%, or 0-29% cell death respectively (percentages given within each cell to 2dp). (2M5NI) 2-Methyl-5-Nitroimidazole (200 µM), (4NI) 4-Nitroimidazole (25 µM), (DTZ) Dimetridazole (25 µM), EF5 (130 µM), (FMISO) F-Misonidazole (130 µM), (FUR) Furazolidone (45 µM), (MTZ) Metronidazole (50 µM), (MISO) Misonidazole (300 µM), (NB2NI) *N*-Benznidazole (40 µM), (NCS) Niclosamide (2.5 µM), (NFX) Nifurtimox (75 µM), (NFN) Nitrofurantoin (24 µM), (NFZ) Nitrofurazone (60 µM), (ORN) Ornidazole (75 µM), (TIN) Tinidazole (75 µM), (RNZ) Ronidazole (150 µM).



### 3.2.3 Identification of pairs of nitroreductases / nil bystander antibiotics with opposing activation profiles

The heat-map in figure 3.6 allows rapid identification of the nitroreductases that are most active with individual nil bystander antibiotics. It also revealed that some nitroreductase pairs have opposing activation profiles with pairs of nil bystander antibiotics. This led to the proposal of implementing a dual targeted cell ablation system; simultaneously using one nitroreductase which is capable of activating a given nil bystander antibiotic but not a second nil bystander antibiotic, in partnership with a different nitroreductase which is capable of activating the second nil bystander antibiotic, but not the first one (as per the scheme in Figure 1.11). A system such as this would, by placing each nitroreductase under control of a distinct tissue-specific promoter in the same transgenic organism, enable the targeted ablation of two completely independent cell populations with temporal and spatial discretion.

The colour coded heat-map made it possible to identify prospective pairs of nil bystander antibiotic/ nitroreductase combinations with opposing activation profiles. Examples of promising combinations are summarised in Figures 3.7-3.10.

	Tinidazole	Metronidazole
NfsA_Ecaro	97.16	24.94
NfsA_Li	89.10	5.08
NfsA_Pp	87.64	17.11
NfsB_Vv	28.77	97.07

**Figure 3.7. Identification of nitroreductase enzymes that exhibit opposing activation profiles with tinidazole and metronidazole.** Results summarised from heat-map, where green indicates high activity with that nil bystander antibiotic, while red indicates little to no activity. The numbers in each cell indicate the percentage of growth inhibition observed from the growth inhibition assays.

	F-Miso	Metronidazole
NfsA_Np	76.80	1.99
NfsA_Bth	75.18	0.00
NfsB_Vv	5.85	97.07

**Figure 3.8 Identification of nitroreductase enzymes that exhibit opposing activation profiles with F-misonidazole and metronidazole.** Results summarised from heat-map, where green indicates high activity with that nil bystander antibiotic, while red indicates little to no activity. The numbers in each cell indicate the percentage of growth inhibition observed from the growth inhibition assays.

	EF5	Dimetridazole
NfsA_Es	84.75	3.43
NfsB_Vh	7.17	97.66

**Figure 3.9 Identification of nitroreductase enzymes that exhibit opposing activation profiles with EF5 and dimetridazole.** Results summarised from heat-map, where green indicates high activity with that nil bystander antibiotic, while red indicates little to no activity. The numbers in each cell indicate the percentage of growth inhibition observed from the growth inhibition assays.

	EF5	Metronidazole
NfsA_Np	76.81	1.99
YdgI_Bs	0.78	75.45
NfsB_Vh	7.17	98.26

**Figure 3.10 Identification of nitroreductase enzymes that exhibit opposing activation profiles with EF5/ and metronidazole.** Results summarised from heat-map, where green indicates high activity with that nil bystander antibiotic, while red indicates little to no activity. The numbers in each cell indicate the percentage of growth inhibition observed from the growth inhibition assays.

IC<sub>50</sub> analysis was subsequently undertaken on some promising pairs of nil bystander antibiotic/ nitroreductase combinations with opposing activation profiles. IC<sub>50</sub> assays measure the effectiveness of a compound in inhibiting biological function, indicating the concentration of a compound required to inhibit growth by 50% and are a standard measure of drug potency. Focus was given to the nitroreductases that had opposing activities with tinidazole and metronidazole (figure 3.7) on the basis that these nil bystander antibiotics have both been well studied, are cheap and widely available, and all nitroreductases that were capable of activating tinidazole but not metronidazole were members of the NfsA family, whereas the nitroreductase that was found capable of activating metronidazole but not tinidazole was a member of the NfsB family – these two families are distinctly different and the most well studied of the nitroreductase enzymes. IC<sub>50</sub> analysis was undertaken with these nitroreductases and nil bystander antibiotics (figures 3.11-3.14).



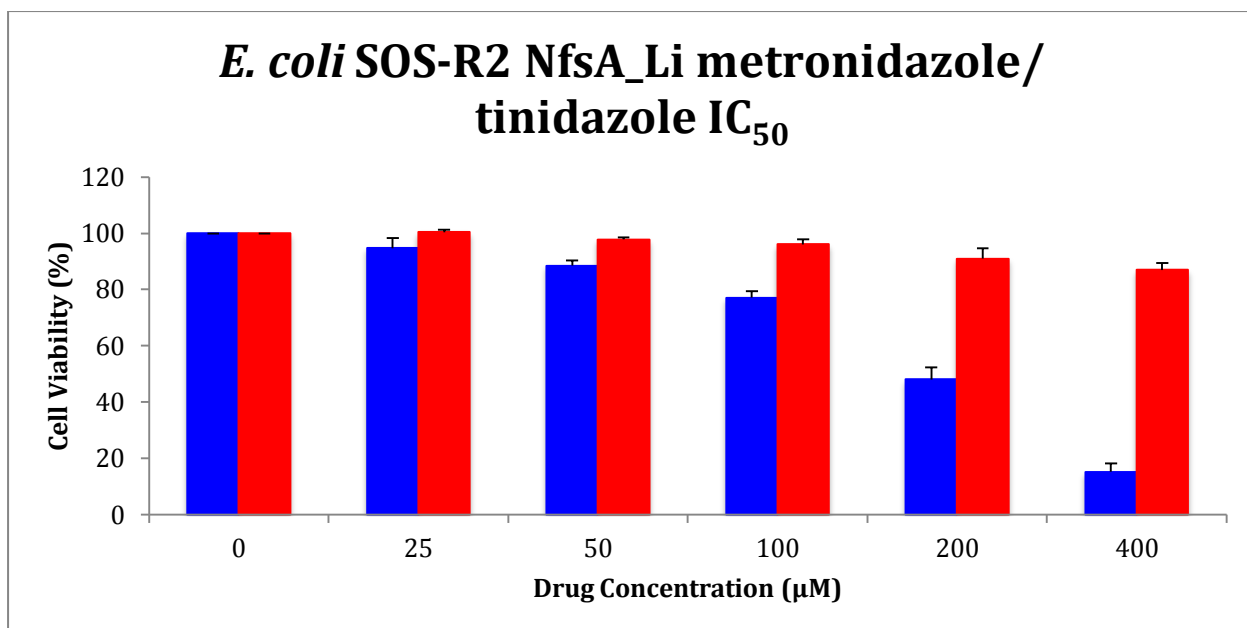


**Figure 3.11 Metabolism of metronidazole and tinidazole by *E. coli* cells over-expressing nitroreductase NfsA\_Li over a range of concentrations as measured by IC<sub>50</sub> analysis.** Turbidity (OD<sub>600</sub>) of nitroreductase over-expressing *E. coli* cultures was recorded directly before and after 4 h incubation with 5 different nil bystander antibiotic concentrations (25 µM, 50 µM, 100 µM, 200 µM 400 µM). Metronidazole is shown in blue, and tinidazole red. Cell viability is expressed as the percentage decrease in OD<sub>600</sub> of challenged cells relative to unchallenged control cells for each strain post-incubation. Data are the average of 3 independent assays and the error bars indicate  $\pm 1$  standard deviation. The IC<sub>50</sub> values of NfsA\_Li with tinidazole was 178 µM, while the IC<sub>50</sub>I value for metronidazole was unable to be extrapolated, but from the graph we can see that it is >400 µM.

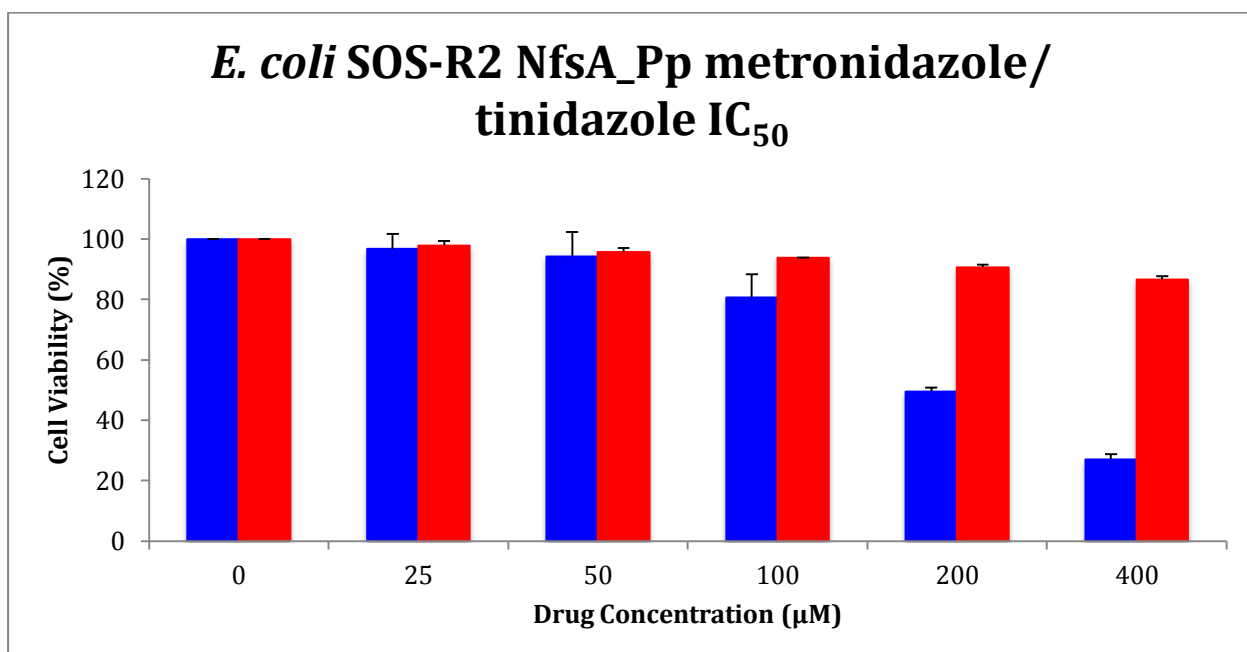


**Figure 3.12 Metabolism of metronidazole and tinidazole by *E. coli* cells over-expressing nitroreductase NfsA\_Pp over a range of concentrations as measured by IC<sub>50</sub> analysis.** Turbidity (OD<sub>600</sub>) of nitroreductase over-expressing *E. coli* cultures was recorded directly before and after 4 h incubation with 5 different nil bystander antibiotic concentrations (25 µM, 50 µM, 100 µM, 200 µM 400 µM).

400  $\mu\text{M}$ ). Metronidazole is shown in blue, and tinidazole red. Cell viability is expressed as the percentage decrease in  $\text{OD}_{600}$  of challenged cells relative to unchallenged control cells for each strain post-incubation. Data are the average of 3 independent assays and the error bars indicate  $\pm 1$  standard deviation. The  $\text{IC}_{50}$  values of NfsA\_Pp with tinidazole was 204  $\mu\text{M}$ , while the  $\text{IC}_{50}$ I value for metronidazole was unable to be extrapolated, but from the graph we can see that it is  $>400$   $\mu\text{M}$ .

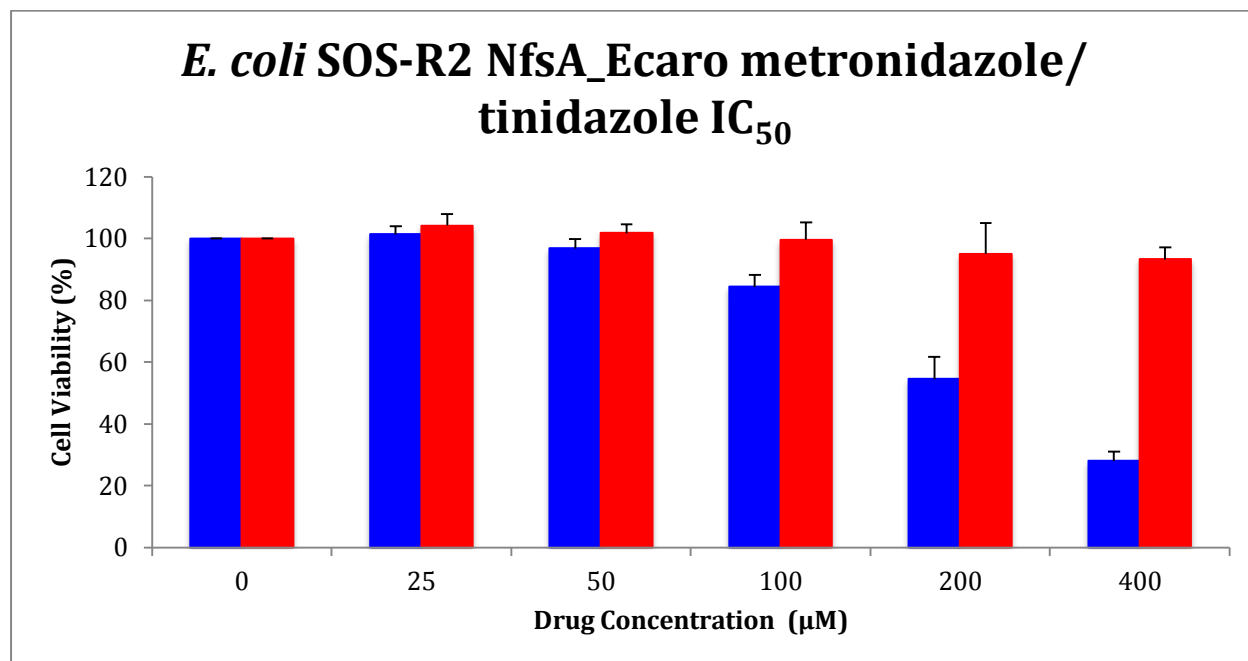


**Figure 3.13 Metabolism of metronidazole and tinidazole by *E. coli* cells over-expressing nitroreductase NfsA\_Ecaro over a range of concentrations as measured by  $\text{IC}_{50}$  analysis.**

Turbidity ( $\text{OD}_{600}$ ) of nitroreductase over-expressing *E. coli* cultures was recorded directly before and after 4 h incubation with 5 different nil bystander antibiotic concentrations (25  $\mu\text{M}$ , 50  $\mu\text{M}$ , 100  $\mu\text{M}$ , 200  $\mu\text{M}$  400  $\mu\text{M}$ ). Metronidazole is shown in blue, and tinidazole red. Cell viability is expressed as the percentage decrease in  $\text{OD}_{600}$  of challenged cells relative to unchallenged control cells for each strain post-incubation. Data are the average of 3 independent assays and the error bars indicate  $\pm 1$  standard deviation. The  $\text{IC}_{50}$  values of NfsA\_Ecaro with tinidazole was 204  $\mu\text{M}$ , while the  $\text{IC}_{50}$ I value for metronidazole was unable to be extrapolated, but from the graph we can see that it is  $>400$   $\mu\text{M}$

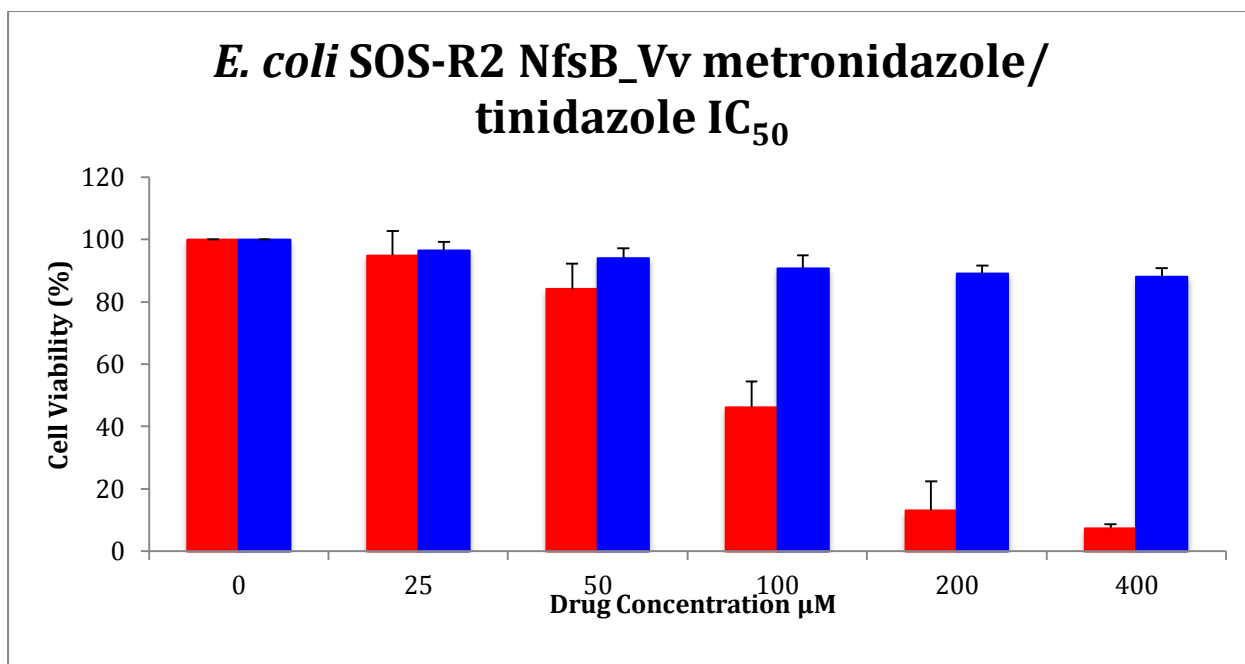


**Figure 3.14 Metabolism of metronidazole and tinidazole by *E. coli* cells over-expressing nitroreductase NfsB\_Vv over a range of concentrations as measured by IC<sub>50</sub> analysis.** Turbidity (OD<sub>600</sub>) of nitroreductase over-expressing *E. coli* cultures was recorded directly before and after 4 h incubation with 5 different nil bystander antibiotic concentrations (25 μM, 50 μM, 100 μM, 200 μM, 400 μM). Metronidazole is shown in blue, and tinidazole red. Cell viability is expressed as the percentage decrease in OD<sub>600</sub> of challenged cells relative to unchallenged control cells for each strain post-incubation. Data are the average of 3 independent assays and the error bars indicate ± 1 standard deviation. The IC<sub>50</sub> values of NfsB\_Vv with metronidazole was 99 μM, while the IC<sub>50</sub> value for tinidazole was unable to be extrapolated, but from the graph we can see that it is >400 μM

The IC<sub>50</sub> analysis showed the combination of nil bystander antibiotics metronidazole and tinidazole with the nitroreductases NfsA\_Li and NfsB\_Vv had the most potential to work as a dual ablation system. The ability of NfsB\_Vv to be a strong activator of metronidazole had previously been looked at as it was initially one of the better candidates in place of NfsB\_Ec, however NfsB\_Vh showed a much better IC<sub>50</sub> (table 3.1). Cell populations carrying the NfsB\_Vv nitroreductase, were capable of activating metronidazole leading to cell death, while cells containing the NfsA\_Li nitroreductase remained relatively unharmed. When cell populations were challenged with tinidazole, the opposite effect was observed; cell populations carrying the NfsA\_Li nitroreductase were capable of activating tinidazole leading to cell death, while cells containing the NfsB\_Vv nitroreductase remained relatively unharmed.. Although NfsA\_Pp and NfsA\_Ecaro also showed great potential to be used as tinidazole activating enzymes in partnership with metronidazole-activating NfsB\_Vv, NfsA\_Li was chosen as the best candidate as it had the least ability to activate metronidazole (Figure 3.7). It can also be seen clearly that metronidazole has the

least growth inhibition effect on cells with NfsA\_Li, as opposed to NfsA\_Pp or NfsA\_Ecaro from the IC<sub>50</sub> analysis (Figures 3.11-3.14).

### **3.2.4 Nitroreductase mediated cell ablation in human cell lines**

Previous work by others in the Ackerley lab, and at the Auckland Cancer Society Research Centre have shown that although the ability of nitroreductases to activate nil bystander antibiotics and severely inhibit growth in bacterial cells are a good indicator of what will be observed in mammalian cells, not all nitroreductases are able to be stably transfected into mammalian cells, meaning that not all results observed in bacterial cells will be able to be replicated in human cell lines

The nitroreductase with the highest efficacy with metronidazole – NfsB\_Vh – had previously been transfected into HCT-116 cells by a past Ackerley lab member, Dr Horvat, so this was the first human cell line to be used for optimisation of experiments (Figure 3.4). NfsA\_Ec and NfsB\_Ec were subsequently transfected into human cell lines, as well as promising nitroreductase combinations that had previously shown opposing activation profiles in bacterial cells. This was carried out to test whether activation profile of these nitroreductases was able also applicable in human cell lines.

Dr Horvat previously encountered a great deal of difficulty in working with HCT-116 cell lines; As such, it was decided to work instead in the human embryonic kidney cell line HEK293, as these cells are commonly used as a generic working model in various experiments in human cell lines and are much more easily manipulated and transfected than HCT-116.

NfsA\_Li and NfsB\_Vv with tinidazole and metronidazole was the top nitroreductase/nil bystander antibiotic combination identified above; these nitroreductases were therefore given the most preference to be transfected into HEK293. Time constraints and technical difficulties however hindered the generation of a stable HEK293 NfsA\_Li cell line. However, a stable HEK293: NfsA\_Pp cell line was successfully established and was used as an opposing activation profile nitroreductase - as it had a very similar activation profile to NfsA\_Li (figures 3.11; 3.12).

### 3.2.5 Gateway<sup>TM</sup> recombination system

To transfer nitroreductase genes into HEK293 cells the Gateway recombination system developed by Invitrogen Life Technologies was employed (Hartley *et al.*, 2000). The Gateway recombination system uses signal DNA sequence and enzymatic machinery of the *E. coli* bacteriophage lambda recombination system to achieve in vitro site-specific recombination (Hartley *et al.*, 2000) at unique 7bp sequences denoted as *att* sites (*attP* in the entry clone and *attB* on the target gene). Clonase<sup>TM</sup> enzyme mix mediates recombination occurring at these sites.

Two recombination reactions, LR and BP, constitute the Gateway cloning technology. The LR reaction is the *in vitro* version of the phage lambda excision reaction. Mediated by LR clonase through *attL* and *attR* sites, transfer of the target DNA fragment into a plasmid with flanking recombination sequences *attL* entry clone, to a destination vector, a plasmid containing *attR* recombination sequences. These steps generate a clone with the *attB* sites flanking the gene of interest and capable of gene expression, known as an expression clone. The BP reaction transfers the DNA fragment of the Expression clone or the *attB*-flanked PCR product to a Donor vector through *attB* and *attP* by BP clonase, creating an entry clone (Sasaki *et al.*, 2004).

For the transfection of nitroreductases into human cell lines, specific primer sets were designed to amplify chosen nitroreductases while incorporating Gateway recombination sites (table 2.7).

Recombination between *attB*-flanked PCR product of a nitroreductase gene and the vector donor pDONR221 (Invitrogen) to create an entry gene is the first step to generate nitroreductase Gateway clones. This is followed by a second recombination step where the entry clone is recombined with a destination vector to create an expression clone (figure 3.15).

Restriction digests carried out after these two recombination steps confirmed the insertion of nitroreductases into the vectors. The following human cell lines were successfully generated; HEK293: NfsA\_Ec, HEK293: NfsB\_Ec, HEK293: NfsA\_Pp,

HEK293: NfsB\_Vv.

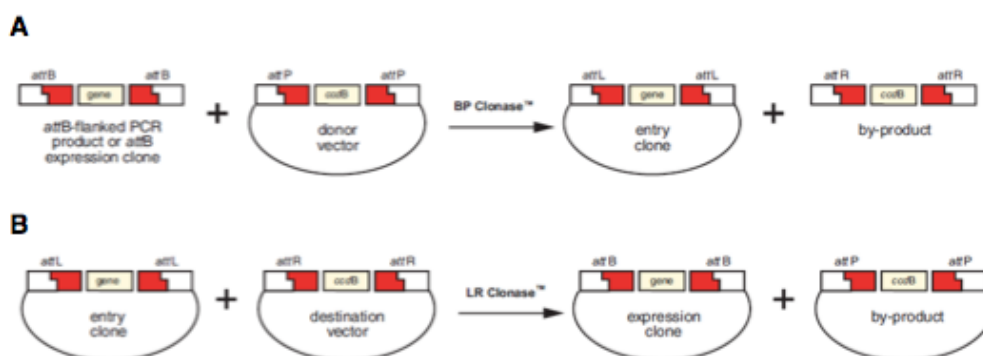


**Figure 3.15 Overview of the Gateway™ recombination system.** The recombination steps in creating expression vectors using the Gateway recombination cloning system. A) The BP recombination step, the PCR product of the gene of interest is recombined with the pDONR22 vector by recombination at the *att* sites to create an entry clone. B) The LR recombination step, the entry clone is recombined with a destination vector to create an expression strain that can then be transfected into the target cell line. Figure reproduced from the Invitrogen Gateway Technology Manual ([www.invitrogen.com/content/sfs/manuals/gatewayman.pdf](http://www.invitrogen.com/content/sfs/manuals/gatewayman.pdf) accessed 29.09.2013).

### 3.2.6 Cell ablation in human cell lines

The results observed in bacterial cells with NfsB\_Vh, NfsA\_Pp, and NfsB\_Vv were predictive of what was observed in human cells. Initially MTS assay experiments were planned which would enable the IC<sub>50</sub> values of given nil bystander antibiotics with the nitroreductases in human cell lines to be observed. However, problems with optimisation of the MTS assay meant that this work couldn't be verified in this manner. Instead another approach that would allow the visualisation of the ablation of the nitroreductase transfected cells in the presence of nil bystander antibiotics was undertaken. Cells were seeded into T25 and treated with 5 µM drug - this drug concentration was based on previous MTS assays carried out by Dr Horvat, which indicated that after a 48 h period 5 µM metronidazole was an optimal concentration to induce complete cell death in human cell lines.



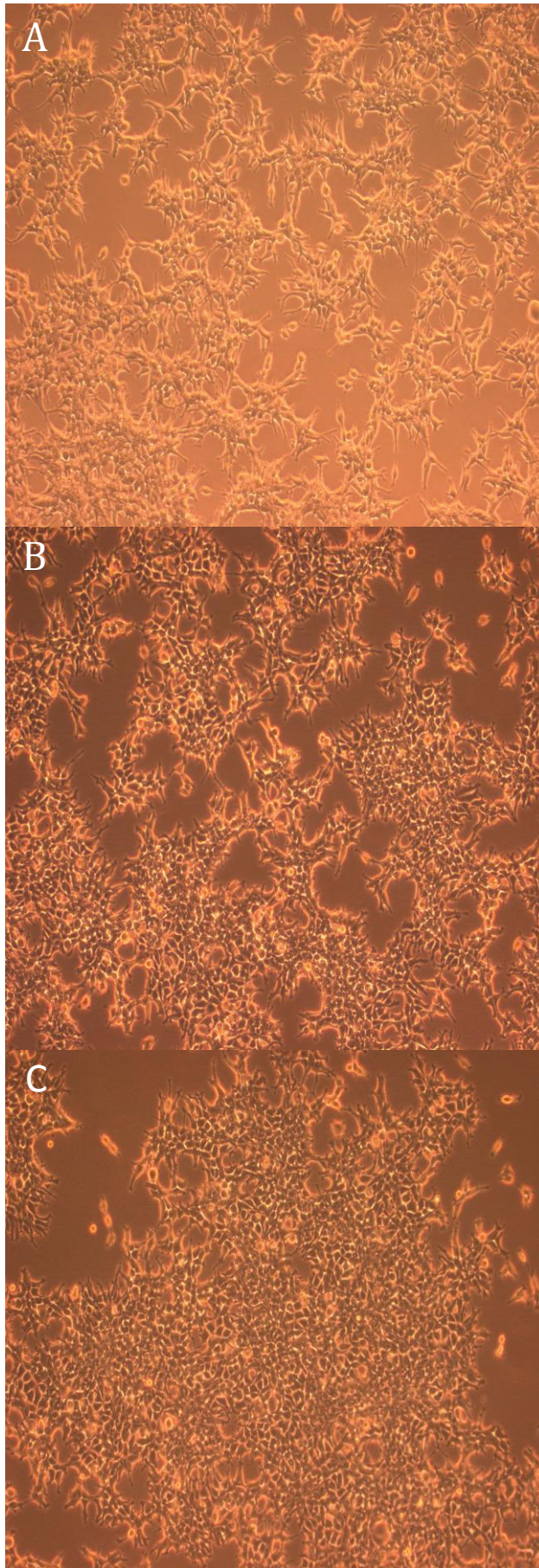


**Figure 3.16 Metronidazole and tinidazole challenged HEK293 WT cells.** Cells were seeded at a density of 250,000 into T25 flasks and left to grow overnight to approximately 80% confluency. 5 μM metronidazole or 5 μM tinidazole was added to the cells and they were left for 48 h. Bright field images of the cell populations were taken at 0 h and 48 h with an Olympus IX51 microscope using the 20x lens. **A.** Unchallenged HEK293 WT cells **B.** HEK293 WT cells challenged with 5 μM metronidazole 48 h **C.** HEK293 WT challenged with 5 μM tinidazole 48 h. After 48 hours in the presence of a low concentration of both metronidazole and tinidazole, the cells look healthy and the morphology appears unchanged from 0 h. The cell population size appears to have increased over the 48 hours, suggesting that the presence of neither metronidazole nor tinidazole has any effect on the cells.

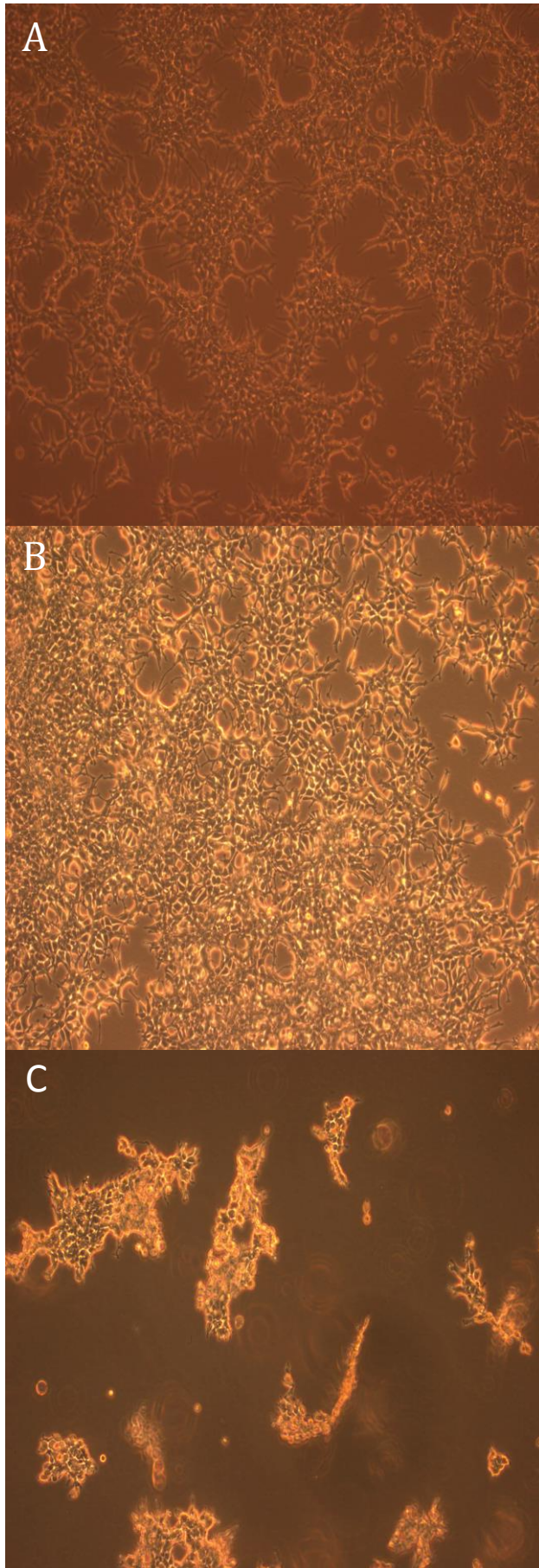


**Figure 3.17 Metronidazole and tinidazole challenged HEK293: NfsA\_Pp cells.** Cells were seeded at a density of 250,000 into T25 flasks and left to grow overnight to approximately 80% confluency. 5μM metronidazole or 5μM tinidazole was added to the cells and they were left for 48 h. Bright field images of the cell populations were taken at 0 h and 48 h with an Olympus IX51 microscope using the 20x lens. **A.** Unchallenged HEK293 NfsA\_Pp cells **B.** HEK293 NfsA\_Pp cells challenged with 5μM metronidazole 48 h **C.** HEK293 NfsA\_Pp challenged with 5μM tinidazole 48 h. After 48 hours in the presence of a low concentration of tinidazole, the cells look unhealthy as the cell morphology has changed and population has decreased dramatically compared to when the population had not been in the presence of a nil bystander antibiotic. However, the addition of metronidazole appears to have no effect on HEK293: NfsA\_Pp cell population, as the morphology appears unchanged from 0 h, and the cell population size appears to have increased over the 48 hours.



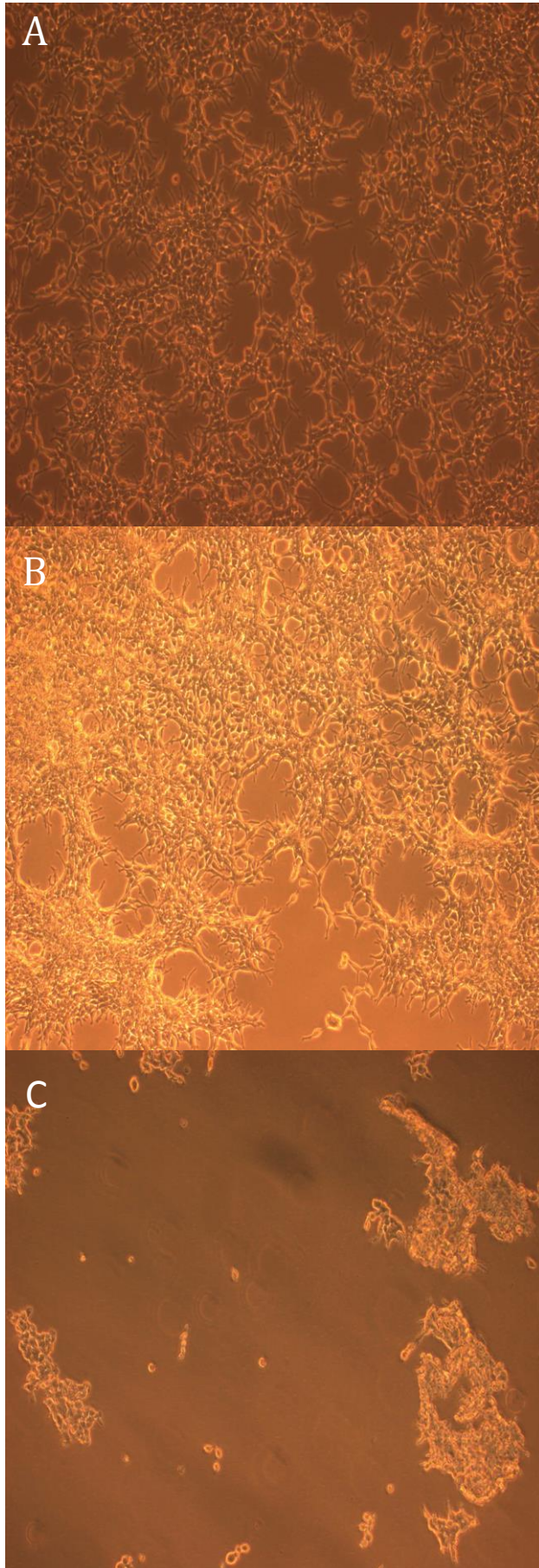


**Figure 3.18 Metronidazole and tinidazole challenged HEK293: NfsB\_Vv cells.** Cells were seeded at a density of 250,000 into T25 flasks and left to grow overnight to approximately 80% confluency. 5µM metronidazole or 5µM tinidazole was added to the cells and they were left for 48 h. Bright field images of the cell populations were taken at 0 h and 48 h with an Olympus IX51 microscope using the 20x lens. **A.** Unchallenged HEK293 NfsB\_Vv cells **B.** HEK293 NfsB\_Vv cells challenged with 5µM tinidazole 48 h **C.** HEK293 NfsA\_Pp challenged with 5µM metronidazole 48 h. After 48 hours in the presence of a low concentration of metronidazole, the cells look unhealthy as the cell morphology has changed and population has decreased dramatically compared to when the population had not been in the presence of a nil bystander antibiotic. However, the addition of tinidazole appears to have no effect on HEK293: NfsB\_Vv cell population, as the morphology appears unchanged from 0 h, and the cell population size appears to have increased over the 48 hours.

The visualisation of stably transfected human cell lines treated with antibiotics was consistent with the results that had been seen in bacterial cells. HCT-116: NfsB\_Vh showed high cell death after a 48 h incubation period with only 5  $\mu$ M metronidazole (figure 3.4), a much lower concentration than the 10mM that is currently being used in developmental and regenerative biology studies (Kaya *et al.*, 2012). The cells analysed for their potential use in a dual ablation system also conferred the results we had expected based on earlier experiments in bacterial cells. HEK WT showed no cell death or change in cell morphology after a 48 h incubation period with either metronidazole or tinidazole (figure 3.16). HEK: NfsA\_Pp showed high cell death after a 48 h incubation period with tinidazole, but no change in cell morphology after a 48 h incubation period with metronidazole (figure 3.17). HEK: NfsB\_Vv showed high cell death after a 48 h incubation period with metronidazole, but no change in cell morphology after a 48 h incubation period with tinidazole (figure 3.18).

In summary, a number of promising pairs for use in a dual ablation system have been identified in bacterial cells. Proof of principle that this concept could be utilised in eukaryotic cells has been demonstrated using cell lines HEK293: NfsA\_Pp and HEK293: NfsB\_Vv in conjunction with the nil bystander antibiotics metronidazole and tinidazole. This offers great promise that these, or other, nitroreductases and nil bystander antibiotics could be implemented for use in eukaryotic model organisms as a means of targeted cell ablation in developmental biology studies.

### **3.2.7 Niclosamide**

Niclosamide was one of the original nil bystander antibiotic candidates screened with the 58 nitroreductase library. During the initial screening process however, it was observed that while most nil bystander antibiotics had a similar activation pattern across the nitroreductases, niclosamide had the opposite activation profile, i.e. high levels of growth inhibition for the empty plasmid control, but low levels of growth inhibition for most strains expressing an active nitroreductase (Figure 3.6). The presence of active nitroreductases therefore appeared to be elucidating a protective effect on the cells, rather than a detrimental effect. This can be clearly illustrated by superimposing the activation profile of one of the other nil bystander antibiotics – in

this case Metronidazole – onto a graph depicting niclosamide’s activation profile (Figure 3.19).

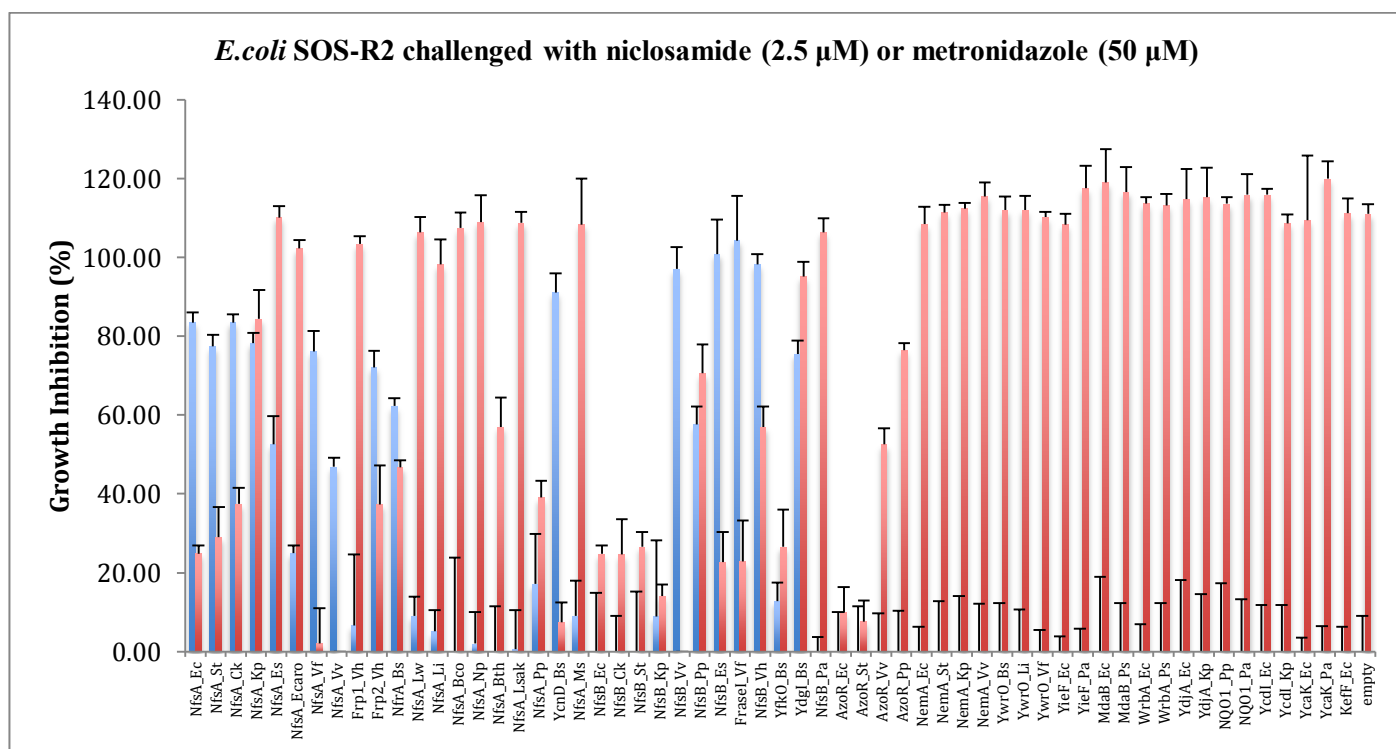


**Figure 3.19 Metabolism of metronidazole or niclosamide by members of the 58 nitroreductase over-expression library as measured by growth inhibition assay.** Turbidity ( $OD_{600}$ ) of nitroreductase over-expressing *E. coli* cultures was recorded directly before and after 4 h incubation with 50  $\mu$ M metronidazole or 2.5  $\mu$ M niclosamide. Growth Inhibition is expressed as the percentage decrease in  $OD_{600}$  of challenged cells relative to unchallenged control cells for each strain post-incubation. Data are the average of 5 independent assays and the error bars indicate  $\pm 1$  standard deviation. This graph shows the opposing activation profiles of metronidazole (blue) and niclosamide (red). Whereas with metronidazole, a lot of the NfsA and NfsB nitroreductase enzymes show high cell death, only cells expressing certain NfsA, NfsB or AzoR family members are able to grow in the presence of niclosamide, suggesting that these nitroreductases are exerting a protective effect on the cells as opposed to a detrimental effect.

### 3.2.8 Exploiting the characteristics of niclosamide

#### 3.2.8.1 Optimisation of niclosamide selection in liquid media

Although niclosamide is not useful for the original intentions of this thesis, i.e. as a nitroreductase activated prodrug, its opposing activation profile to known bystander antibiotics suggests it might have value in a range of potentially useful applications. For example, niclosamide might have utility as a high throughput positive selection agent to identify novel nitroreductases in large genetic (e.g.

metagenomic, or directed evolution) libraries. However, prior to any such applications it was necessary to better understand the concentrations of niclosamide that should be applied for effective selection.

Although not ultimately pursued, it was first sought to examine the effects of niclosamide challenge in conjunction with fluorescence screening. This was to be tested using nitro-quenched fluorophores, molecules that will be discussed in greater detail in Chapter 4. For now, the critical detail is that in order to apply these fluorophores it was necessary to shift from the *E. coli* SOS-R2 strain in which all growth inhibition assays described above had been conducted, to a different strain, *E. coli* 6KO (whereas SOS-R2 has had four endogenous nitroreductase genes knocked out, the 6KO strain has six nitroreductase gene deletions (Table 2.3); this has been found to be important for minimising background in fluorescence assays; Horvat, 2012). However, it quickly became apparent that the 6KO strain responded quite differently to niclosamide challenge than SOS-R2. Numerous experiments were conducted using the full NTR library in both strains. However, for simplicity, the remainder of this section will just describe key observations made for NfsA\_Vv expressing “nitroreductase positive” cells *versus* the pUCX empty plasmid negative control cells.

Initial experiments aiming to optimise niclosamide challenge concentrations were undertaken in liquid media as described in Section 2.9.7. The OD<sub>600</sub> readings for both NfsA\_Vv and pUCX were taken at four different time points, 0 h, 2 h, 4 h, and 8 h, across a range of niclosamide concentrations. The results that were observed in 6KO however, were not consistent with those observed in the SOS-R2 strain. Whereas the NfsA\_Vv over-expressing 6KO strain behaved as expected, showing increased OD<sub>600</sub> readings at later time points (consistent with a protective role for the over-expressed nitroreductase), the empty plasmid control also showed increased OD<sub>600</sub> readings across all time points, indicating that niclosamide was not inhibiting its growth (Figure 3.21). The same experiments were then carried out using another nitroreductase gene-deleted strain available in the lab, 7KO, with the same results (Figure 3.22). In contrast, when the experiment was repeated in SOS-R2, the empty plasmid control strain was once again growth-inhibited by niclosamide (Figure 3.23).

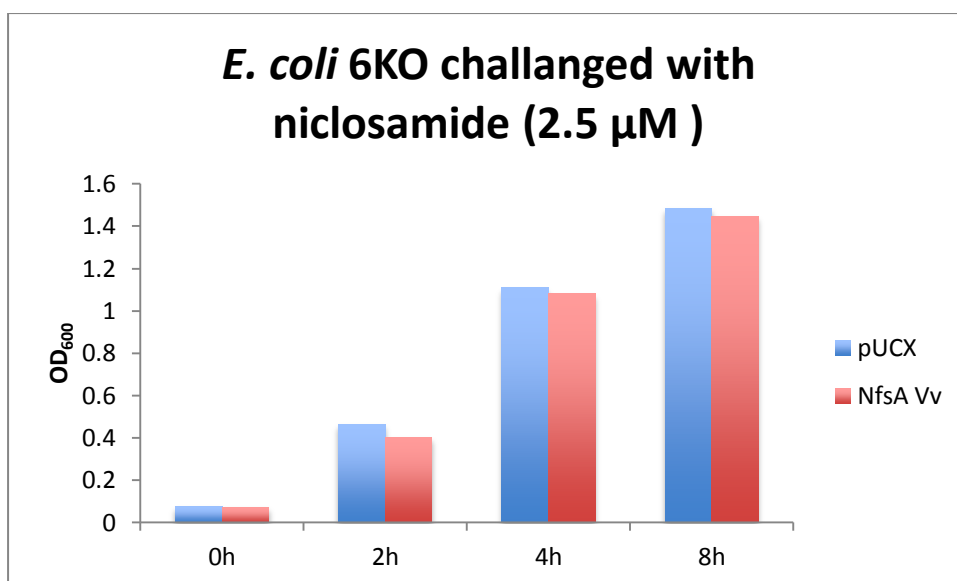


**Figure 3.20 Metabolism of niclosamide by *E. coli* 6KO overexpressing NfsA\_Vv or pUCX over an 8 h time period.** The *E. coli* 6KO strain containing either NfsA\_Vv as a positive control or pUCX as a negative control was challenged with 2.5  $\mu$ M niclosamide. OD<sub>600</sub> values were taken at four different time points 0 h, 2 h, 4 h, and 8 h. Results observed were inconsistent with those seen in growth inhibition assays when the *E. coli* SOS-R2 58 nitroreductase library was challenged with 2.5  $\mu$ M niclosamide for 4 h. It was expected that there would be growth inhibition of cells containing pUCX, but not cells expressing NfsA\_Vv. In the *E. coli* 6KO strain no growth inhibition with either NfsA\_Vv or pUCX was observed.

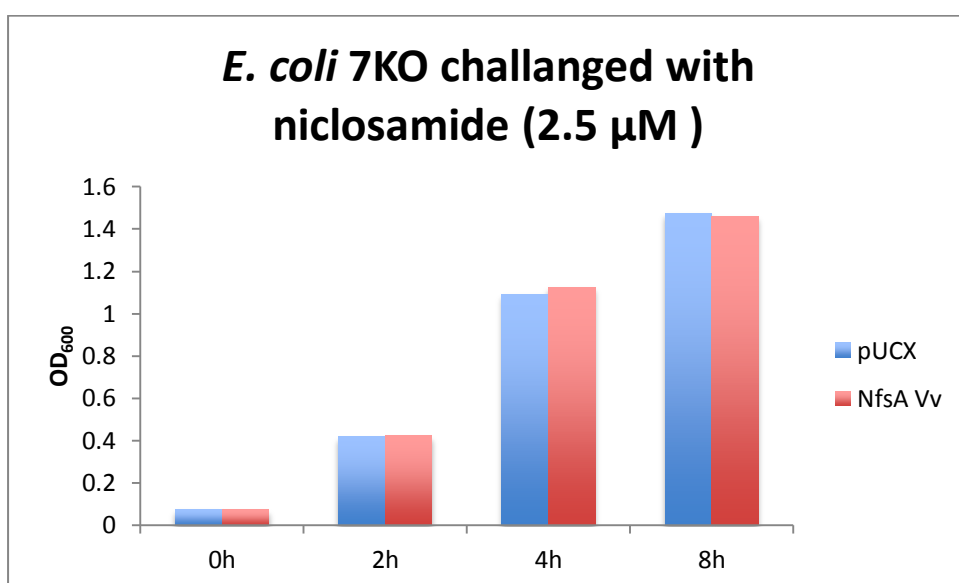


**Figure 2.21 Metabolism of niclosamide by *E. coli* 7KO overexpressing NfsA\_Vv or pUCX over an 8 h time period.** The *E. coli* 7KO strain containing either NfsA\_Vv as a positive control or pUCX as a negative control was challenged with 2.5  $\mu$ M niclosamide. OD<sub>600</sub> values were taken at four different time points 0 h, 2 h, 4 h, and 8 h. Results observed were inconsistent with those seen in growth inhibition assays when the *E. coli* SOS-R2 58 nitroreductase library was challenged with 2.5  $\mu$ M niclosamide for 4 h. It was expected that there would be growth inhibition of cells containing pUCX, but not cells expressing NfsA\_Vv. In the *E. coli* 7KO strain no growth inhibition with either NfsA\_Vv or pUCX was observed.

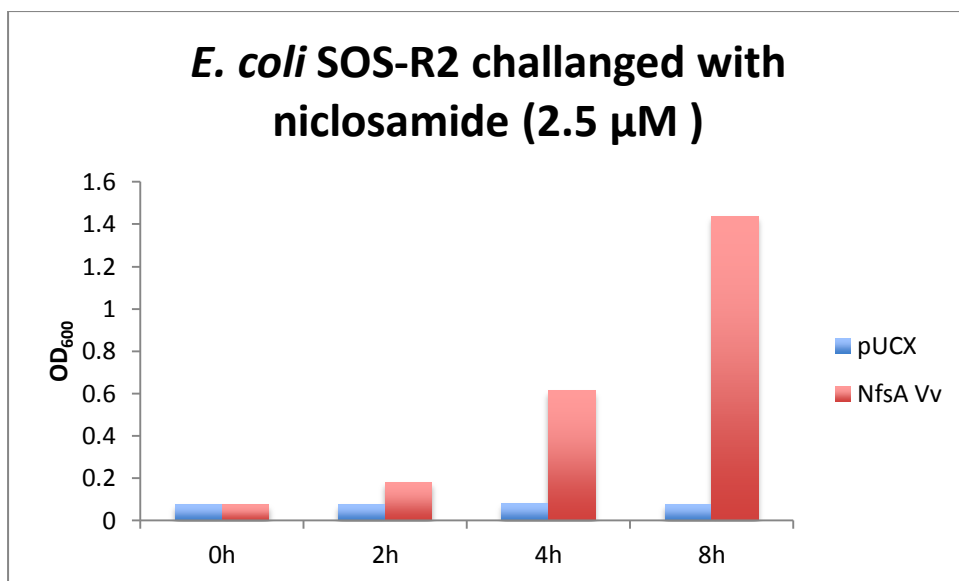


**Figure 3.22 Metabolism of niclosamide by *E. coli* SOS-R2 overexpressing NfsA\_Vv or pUCX over an 8 h time period.** The *E. coli* SOS-R2 strain containing either NfsA\_Vv as a positive control or pUCX as a negative control was challenged with 2.5 μM niclosamide. OD<sub>600</sub> values were taken at four different time points 0 h, 2 h, 4 h, and 8 h. Results observed agree with those which had been seen in growth inhibition assays when the *E. coli* SOS-R2 58 nitroreductase library was challenged with 2.5 μM niclosamide for 4 h. Growth inhibition was observed in cells containing pUCX, but not in cells containing NfsA\_Vv.

Apart from containing fewer nitroreductase gene knockouts, the only overt difference between SOS-R2 and the 6KO/ 7KO strains is that SOS-R2 also lacks a gene encoding the TolC efflux regulator. It was therefore inferred that TolC might be playing an active role in minimising the toxic effect of niclosamide on *E. coli* cells.

The role of the TolC efflux regulator is to expel a number of diverse molecules, including protein toxins and antibiotic drugs, from the cell (Thanabalu *et al*, 1998, Koronakis *et al* 2004). We hypothesised that TolC is able to cause niclosamide to be rapidly eliminated from *E. coli* cells, rendering nitroreductase-mediated protection redundant. Therefore, to utilise this anomaly observed with niclosamide in combination with a masked fluorophore screening method to confirm the presence of active nitroreductases, another member of the lab, Dr Janine Copp, developed a new strain with a *tolC* gene knockout; 7NT. 7NT otherwise has the same characteristics as 7KO (table 2.3). As previously observed in SOS-R2 cells, in the 7NT strain 2.5 μM niclosamide was found to be an effective concentration for preventing the growth of the pUCX control strain, while allowing the NfsA\_Vv expressing strain to grow freely (not shown).

### 3.2.8.2 Optimisation of niclosamide selection in solid media

The Ackerley lab has an interest in discovering new nitroreductase enzymes from metagenome libraries. These libraries provide access to the genetic material of the >99% of microbes that cannot be cultured in the lab (Vartoukian *et al.*, 2010). Functional screens of such libraries are a very powerful tool to recover enzymes from these libraries (van Rossum *et al.*, 2013). The observation made here, that a *tolC* and endogenous nitroreductase gene deleted strain of *E. coli* will be unable to grow in the presence of niclosamide unless an alternative (protective) nitroreductase gene is supplied, suggested a means for screening metagenome libraries to recover clones encoding novel nitroreductases. While working in liquid media provided some essential insights into the effect of activated niclosamide on various *E. coli* strains, it is not ideal for this kind of screening as working in liquid media may lead to a minority of nitroreductase expressing cells completely detoxifying niclosamide and thereby allowing the vast majority of non-resistant clones to proliferate. To utilise the characteristics observed in niclosamide in this context, it was preferable to demonstrate activity on solid media.

Another purpose of the niclosamide validation experiments was to establish whether the system could also be used in the future for directed evolution, selecting for loss of specific nitroreductase activities. This would be useful in gaining further combinations of nitroreductases/ nil bystander antibiotics with opposing activation profiles, or for tailoring the activity of nitroreductases already identified as showing promise in an opposing activation profile context. For example, NfsA\_Pp wasn't the first choice of nitroreductase to be used in the dual ablation system outlined in 3.2.3, and was only selected because NfsA\_Li was unable to be expressed functionally in human cell lines. Whereas both NfsA\_Li and NfsA\_Pp are highly active with tinidazole, unlike NfsA\_Li, NfsA\_Pp shows low-level activation of metronidazole. The ability to eliminate any possibility of NfsA\_Pp activating metronidazole would make the proposed dual ablation system (in combination with NfsB\_Vv) much more targeted. One strategy proposed to achieve this was to randomly mutate the gene encoding NfsA\_Pp, to express the variant gene library in SOS-R2 or 7NT cells, and then to plate that library on media containing both a high level of metronidazole and niclosamide. Only variants that have lost activity with metronidazole should be able

to grow; whereas the inclusion of niclosamide in the growth medium would ensure that at least some level of generic nitroreductase activity is retained. Surviving variants could then be tested to ensure an appropriate level of activity with tinidazole has been retained.

To test the feasibility of this idea, initial experiments were undertaken in the SOS-R2 strain with controls first tested using plates containing metronidazole only, or niclosamide only. Colonies that were able to grow in the presence of niclosamide indicate the presence of a nitroreductase, while the ability to also grow in the presence of metronidazole indicates that the nitroreductase cannot activate metronidazole. Again, as in the liquid media optimisation experiments, NfsA\_Vv was used as a positive control, as it is a well-validated nitroreductase but has only poor activity with metronidazole. Alongside NfsA\_Vv, pUCX was employed as a negative control. When NfsA\_Vv was plated on solid media containing mertronidazole or niclosamide only, colonies formed, whereas pUCX containing colonies only formed on plates containing metronidazole. These outcomes established the parameters for niclosamide selection of active nitroreductases from mixed cultures.

7NT strain cells expressing either NfsA\_Vv or pUCX were then grown in separate cultures, before being mixed at a 1:1 ratio and plated on solid media containing 10  $\mu$ M metronidazole and 2.5  $\mu$ M niclosamide. To confirm the growth of only *E. coli* colonies containing an active nitroreductase (NfsA\_Vv) PCR analysis of randomly picked colonies this plate was undertaken. The PCR colony screen confirmed that all colonies growing contained the nitroreductase insert NfsA\_Vv; none contained empty pUCX (figure 3.23).



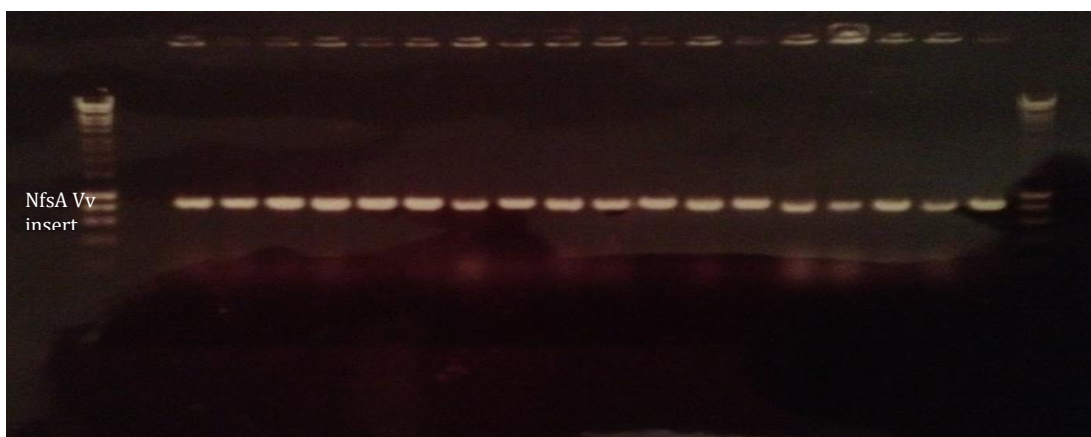


**Figure 3.23 PCR confirmation of active nitroreductase enzymes from colonies picked from mixed culture NfsA\_Vv/ pUCX plated on media containing metronidazole and niclosamide.** 17 colonies were picked from plates containing both metronidazole and niclosamide.. The colonies were then amplified by PCR using generic nitroreductase specific primers. A negative control, pUCX picked from a no drug pUCX only plate, (lane 1) and a positive control, NfsA\_Vv picked from a no drug NfsA\_Vv only plate, (lane 2) were also run. All randomly picked colonies from plates containing both niclosamide and metronidazole show the NfsA\_Vv insert.

Colonies were also picked and challenged with masked fluorophore FSL41. The colonies containing the nitroreductases were able to activate FSL41 and give off a fluorescence signal, while those not containing the nitroreductase wouldn't. All of the colonies that were picked showed fluorescence in comparison with the pUCX negative control. Fluorescence was visualised on the UV Trans-illuminator, and measured on the Enspire 2300 Multiplate Reader at ex 355 nm/ em 460 nm. Although the image taken on the UV trans-illuminator is slightly over-exposed (figure 3.24), the emission of blue fluorescence can clearly be seen from the raw fluorescence units as detected on the plate reader (figure 3.25)

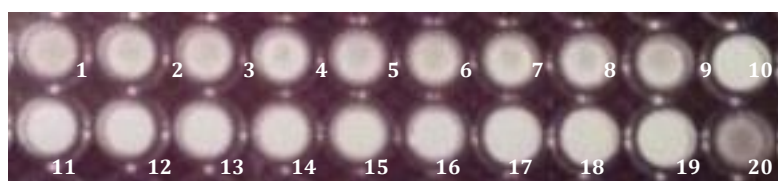


**Figure 3.24 FSL41 fluorescence visualised on UV trans-illuminator as confirmation of active nitroreductase enzymes from colonies picked from mixed culture NfsA\_Vv/ pUCX plated on media containing metronidazole and niclosamide.** 18 random colonies were picked from plates containing both metronidazole and niclosamide (wells 1-18). A negative control, pUCX picked from a no drug pUCX only plate, (well 20) and a positive control, NfsA\_Vv picked from a no drug NfsA\_Vv only plate, (well 19) were also treated with FSL41. Each colony was incubated in LB overnight, then followed the standard fluorescence screening assay (2.9.4) the following day. FSL41 was added to each well to a final concentration of 25  $\mu$ M and incubated for 4 h. Wells were then visualised under the UV trans-illuminator, with wells containing NfsA\_Vv activating FSL41 allowing the emission of blue fluorescence. The randomly picked colonies and the NfsA\_Vv positive control are emitting fluorescence, while the pUCX negative control is not, confirming that all randomly picked colonies contain NfsA\_Vv.

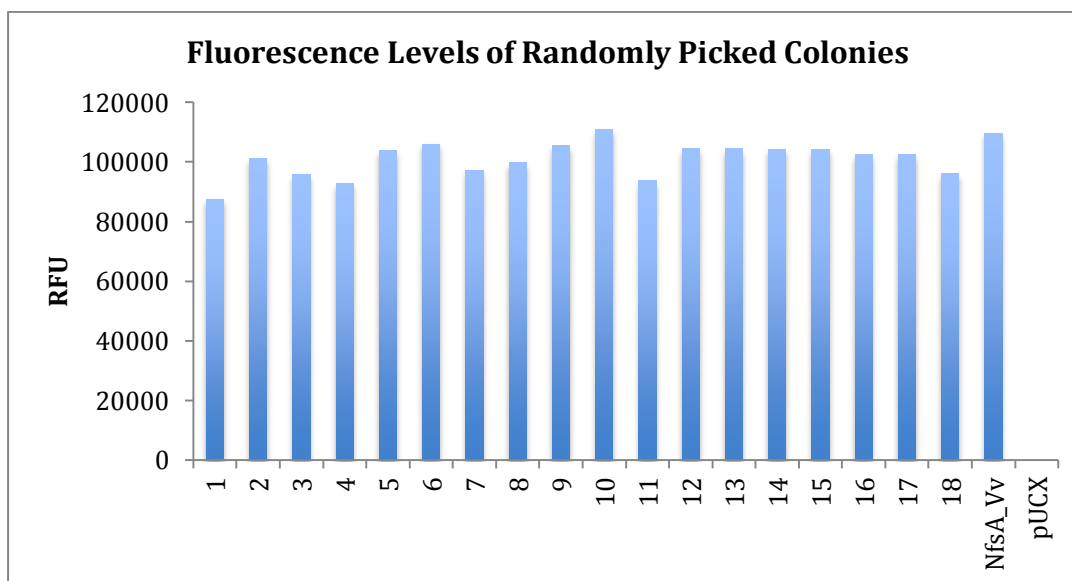


**Figure 3.25 FSL41 fluorescence plate reader ex 355 nm/ em 460 nm values as confirmation of active nitroreductase enzymes from colonies picked from mixed culture NfsA\_Vv/ pUCX plated on media containing metronidazole and niclosamide.** 18 random colonies were picked from plates containing both metronidazole and niclosamide (1-18). A negative control, pUCX picked from a no drug pUCX only plate, and a positive control, NfsA\_Vv picked from a no drug NfsA\_Vv only plate, were also treated with FSL41. Each colony was incubated in LB overnight, then followed the standard fluorescence screening assay (2.9.4) the following day. FSL41 was added to each well to a final concentration of 25  $\mu$ M and incubated for 4 h. The plate was then read on the Enspire 2300 Multiplate Reader. Wells containing NfsA\_Vv activate FSL41 allowing the emission of blue fluorescence, the background fluorescence levels from the negative pUCX control were subtracted from the final RFU of each well. All of the randomly picked colonies are emitting fluorescence, as the RFU are all around the same value as the NfsA\_Vv positive control.

### 3.3 Discussion

The screening of the 58 nitroreductase core library with the 16 nil bystander antibiotic candidates was effective in identifying which nitroreductases were capable of reducing a given nil bystander antibiotic, suggesting their possible utility as a safety mechanism in GDEPT; an FDA requirement for this technology being the ability to eliminate biological vectors from patients post-therapy or if PET imaging indicates undesirable vector localisation as pathogenic bacterium, such as *Clostridium sporogenes*, are commonly used vectors in solid tumour targeting. All but 4 of the putative nil bystander antibiotics (dimetridazole, EF5, F-misonidazole, ronidazole) screened against the 58 nitroreductase library have previously been approved for use in the clinic. Our collaborator at the Auckland Cancer Society Research Centre, Dr Adam Patterson, is currently testing several nil bystander antibiotic candidates for the ability to eliminate both *Clostridium* and adenovirus nitroreductase-labelled vectors

from human cell cultures. Clearly, it would be advantageous for any nil bystander antibiotics going forward for use in a GDEPT vector ablation system to have already made it into the clinic. From the heat-map (Figure 3.6) we can see that *N*-Benznidazole (40  $\mu$ M) exhibited 100% growth inhibition with the majority of the NfsA family, and might therefore constitute an especially promising candidate for this role. However, it would first be necessary to confirm *N*-Benznidazole is truly a nil-bystander prodrug; this could be measured in mixed multicell layers as described by Wilson *et al.*, (2002, 2003).

Of the nitroreductases that were identified as being superior at activating metronidazole to NfsB\_Ec, NfsB\_Vh had the highest growth inhibition percentage (figure 3.2), and these results were confirmed by running IC<sub>50</sub>s alongside other potential nitroreductases with higher efficacy as well as NfsB\_Ec itself (Figure 3.3). Once this had been established, the results were translated into human cells, as the technology in which this nitroreductase would be used is in eukaryotic cells. Initial results showed that the morphology of the HCT-116 cells with the NfsB\_Vh nitroreductase was compromised in the presence of metronidazole. However, challenging HCT-116: NfsB\_Vh with metronidazole at lower metronidazole concentrations, which did not compromise the morphology of the human cell line, confirmed that NfsB\_Vh was capable of efficiently ablating HCT-116 population at very low concentrations (figure 3.4). The identification of this nitroreductase with a much higher ability to activate metronidazole compared to NfsB\_Ec, and its ability to translate this effect into eukaryotic cells, could be of huge potential for the study of the role of specific cell types during development. Further testing will be required to validate this potential in developmental cell biology models, such as transgenic zebrafish lines.

The majority of studies exploiting the nitro reducing capabilities of these enzymes focus on the *E. coli* nitroreductases NfsA and NfsB, as these have the most literature available and are the most easily accessible. A useful resource has been the access to a 58 nitroreductase library that has been developed in the Ackerley laboratory as it is unique in the number and variety of nitroreductases available.

The screening of the whole 58 nitroreductase core library by growth inhibition assay enabled the identification of which nil bystander antibiotics are highly active with any individual nitroreductase. The data obtained from these early screening assays were collated into an easy to interpret colour coded heat-map (Figure 3.6). This made it simple to identify of pairs nil bystander antibiotics/ nitroreductase combinations that have opposing activation profiles. This is something that that could potentially be used in a dual targeted cell ablation system. For example, it has already been demonstrated that the beta cells of the pancreas can be specifically ablated via metronidazole treatment of transgenic zebrafish expressing NfsB\_Ec under control of an insulin promoter. This could potentially be combined with the targeting of alpha cells of the pancreas to compare and contrast the effects to the organism of knocking out these different cell types during development. Such a multiplex capability could greatly extend the power of nitroreductases as useful cell biology tools

IC<sub>50</sub> analysis of pairs of nil bystander antibiotics with opposing activation profiles also confirmed the results that had been initially observed in the growth inhibition assays. The pair that was initially given the most attention was the NfsA\_Li/ tinidazole and NfsB\_Vv/ metronidazole combination. This combination was desirable as it is an NfsA family/ NfsB family comparison (advantages of such a pairing include the existence of fluorogenic probes that can accurately discriminate the two families, as will be seen in the next chapter). Moreover, the nil bystander antibiotics that each enzyme was active with are very well studied, especially metronidazole; which is already being used in studies looking at single cell ablation in various organisms (Curado *et al.*, 2007 Pisharath *et al.*, 2009, White *et al.*, 2011).

All initial tests were performed in bacterial cells, as this allowed flexible and high throughput evaluation of nitroreductase potential. However, the intended applications of these enzyme/prodrug systems are in eukaryotic cells. It was therefore important to demonstrate that the activation profiles that had been seen in bacterial strains were readily transferable to eukaryotic cell lines. Most of the nitroreductases were transfected into HEK293 as this human cell line is well-known and easy to work in. Unfortunately due to time constraints and technical difficulties, NfsA\_Li was unable to be transfected into HEK293. It is not known if NfsA\_Li is able to be stably transfected into human cell lines, as it has been previously observed that not all

nitroreductases are able to be transfected into human cell lines with stable expression (Prosser, 2013). Instead, a HEK293: NfsA\_Pp cell line was established; this nitroreductase exhibits a similar activation profile to NfsA\_Li (i.e. high activity with tinidazole and low activity with metronidazole); and the transfected cell line was used as an opposing activation profile to partner with HEK293: NfsB\_Vv.

As was the case with HCT-116: NfsB\_Vh treated with metronidazole (Figure 3.4), the morphology of HEK293: NfsA\_Pp and HEK293 NfsB\_Vv were compromised in the presence of tinidazole and metronidazole respectively (Figures 3.17; 3.18). Looking at opposing activation profiles however had an added layer of complexity: for the technology to be feasible, HEK29: NfsA\_Pp had to not be affected by metronidazole, and HEK293: NfsB\_Vv resistant to tinidazole. Microscopy images of this (Figures 3.16; 3.17) showed that there was little effect on the cells when in the presence of the opposing nil bystander antibiotic. As a negative control HEK293 WT cells were also challenged with both metronidazole and tinidazole and visualised after a 48hr time period. Neither nil bystander antibiotic had any visible effect on the morphology of HEK293 WT (figure 3.16) confirming that the nitroreductase present was responsible for the activation of the nil bystander antibiotic and subsequent cell ablation.

All of these results were consistent with the drug activation profiles in bacterial cells and are a promising proof of principle for future dual ablation work, as well as the possibility of using this in developmental and regenerative biology studies as a novel approach to targeted cell ablation.

A different aspect of this study was that while undertaking the initial screening of the 58 nitroreductase core library against the 16 nil bystander antibiotic candidates, an anomaly was observed when niclosamide consistently showed an activation profile that was consistently the opposite of that observed with other nil bystander antibiotics. The results suggested that niclosamide has a protective role in the cell upon activation, rather than being detrimental to cell survival.

It appeared in that in the presence of niclosamide, active nitroreductases were able to grow while those with low activity weren't (Figure 3.19); the potential of this phenomenon to be exploited as a novel nitroreductase screening method was

explored. The potential to discover new nitroreductase enzymes from metagenome libraries has large implications in the use of nitroreductases as it would provide access to an even wider range of nitroreductases to work with. Functional screens of metagenome libraries are a very powerful tool to recover enzymes, and could possibly uncover previously unknown families of nitroreductases as these libraries are predicted to be comprised primarily of DNA from microbes that cannot be cultured in the lab (Vartoukian et al., 2010).

To confirm the presence of a nitroreductase in niclosamide optimisation experiments, a masked fluorophore that had been shown to be active with the majority of active nitroreductases available in the lab, FSL41, was added to the culture, the presence of fluorescence indicated the presence of a nitroreductase. However, in order for niclosamide to be applied as a positive selection agent to detect nitroreductase expression in *E. coli*, it was discovered that it was necessary for the endogenous *tolC* gene to be removed from that *E. coli* strain. It was hypothesised that in the presence of this efflux regulator, niclosamide is rapidly expelled from the bacterial cell, rendering the protective effect of an expressed nitroreductase redundant. It goes without saying, that deletion of endogenous nitroreductases from the host genome is also necessary to maximise the sensitivity of the screening system.

These are just preliminary optimisation steps as a proof of principle towards the generation of a novel system to identify new nitroreductases, or for a use in directed evolution. Future work could involve the screening of libraries available within the lab, or as a novel tool for directed evolution to decrease the efficacy of a nitroreductase with a nil bystander antibiotic for a better dual ablation opposing activation profile. This was demonstrated by validation experiments in liquid and solid media, which showed niclosamide to be a powerful tool for detection of nitroreductase activity.

## 4. Masked Fluorophores

### 4.1 Introduction

Having demonstrated in both bacterial and mammalian cells the ability of nitroreductases to metabolise nitro-quenched nil bystander antibiotics, we sought to also utilise the properties of the nitroreductases for activation of masked fluorophores. The ability of nitroreductases to activate both types of compound simultaneously would enable the development of a multiplex reporter/ target cell ablation system. This system would allow reporting of targeted cells through fluorescence visualisation, and temporal and spatial over targeted cell ablation.

The masked fluorophores used in this study are a mixture of bioreductive trigger, and nitro switch molecules as described in section 1.6. The nitro-switch quenched fluorophores have a nitro group that, upon reduction by a nitroreductase, activates the fluorescence of the fluorophore (Figure 1.7). The bioreductive trigger quenched fluorophores were developed based on the activation mechanism of other known bioreductive molecules; reduction by a nitroreductase results in an intramolecular fragmentation at a linker group which consequently results in the activation of the fluorophore (Figure 1.8). In either case, like nil bystander antibiotics, these molecules are able to exploit the capabilities of nitroreductases to reduce nitro-quenched compounds, revealing their fluorescent properties only after reduction in the presence of nitroreductases.

Teaming these with the nil bystander antibiotics would enable a system to be used in developmental and regenerative biology, whereby specific cells could be fluoresced and ablated temporally and spatially. Using this dual reporter/ ablation multiplex system, one nitroreductase would be able to activate both a nil bystander antibiotic and a masked fluorophore, while a different nitroreductase would be incapable of activating that nil bystander and masked fluorophores, but would be able to activate a different nil bystander antibiotic and masked fluorophores, which the first nitroreductase would be incapable of activating (Figure 1.11).

This would mean that the cells containing the nitroreductase would be able to be visualised upon the addition of the fluorophores, and subsequently, the addition of the nil bystander antibiotic would ablate the cells, leaving no fluorescence visible.

To test this theory, an *E. coli* 6KO library was generated, comprising of 23 nitroreductases that had potential as candidates in the dual ablation system. These nitroreductases were then screened against a range of masked fluorophores that were available in the lab to identify their activation. The masked fluorophores to be screened were chosen based on earlier screening work undertaken by a previous PhD student, Dr Horvat; those that had shown the most suitable activation profiles were re-screened against the new 6KO library.

Again, for this system to be relevant, it needed to work in mammalian cells. Once the system had been shown to be viable in bacterial cells, the nitroreductases were then transfected into human cell lines for further experimental work.

#### **4.1.1 Masked fluorophores**

The nitro-quenched masked fluorophores used in this study were developed by Dr Jeff Smaill, Dr Amir Ashoorzadeh, Dr Adam Patterson, and other researchers at the Auckland Cancer Society Research Centre and can be seen in table 2.1

The excitation/ emission wavelengths of these molecules vary, producing a wide range of emitted colours. The masked fluorophores selected for use in this study fluoresce either blue, green, or red.

#### **4.1.2 Fluorescent reporter proteins**

Currently, fluorescence reporter proteins are the standard molecular imaging tool. The green fluorescent protein (GFP) was the first to be used in this manner. It was discovered in the early 1960s when researchers studying the bioluminescent properties of *Aequorea victoria* jellyfish isolated a blue-light-emitting bioluminescent protein called aequorin, together with another protein that was eventually named the green-fluorescent protein (Kremers et al., 2011). Prasher *et al.*, (1992) first cloned the



GFP gene in 1992, after which it was used in various reporter experiments from tracking gene expression in bacteria to that of higher eukaryotes. GFP has since been engineered to yield a wide range of useful coloured fluorescing proteins, including blue, cyan, and yellow mutants (Kremers et al., 2011). Further to this, fluorescent proteins from a broad range of other species have also been identified, expanding the fluorescent colours available through to the far-red spectrum (Kremers et al., 2011). As a group, these are loosely referred to as fluorescent proteins (FPs).

Advances in fluorescent probes with red-shifted spectra has resulted in the creation of red fluorescent proteins with enhanced spectral and biochemical characteristics (Wu *et al.*, 2011). Reduced auto-fluorescence (which often interferes with GFP readings), low light scattering, and minimal absorbance at the longer wavelengths make red fluorescent proteins (RFP) superior probes for cell, tissue, and whole-body imaging, as the fluorescence is able to be visualised through several millimetres of mammalian tissue (Wu *et al.*, 2011).

#### **4.1.3 Dual ablation/ reporter system in developmental biology**

Fluorescent proteins are commonly used as reporter components in developmental and regenerative biology. Reporting on the target cell population is essential for verification of cell ablation. Techniques employing the use of a fluorescent protein/nitroreductase fusion protein under the expression of a chosen promoter have been utilised in a number of studies in the developmental and regenerative biology field (Curado et al., 2007; Kaya et al., 2012; Pisharath et al., 2009; White and Mumm 2013). It is a promising technology as no other inducible knock out system has been capable of such precision.

The characteristic promiscuity of nitroreductases allows them to reduce nitro-quenched compounds as well as prodrugs. The library of nitro-quenched masked fluorophores available in the lab (table 2.1), have previously been shown to be activated by a variety of nitroreductases in the 58 nitroreductase core library. We propose to utilise this ability by using the activated fluorescence as a reporter for targeted cell ablation in cell populations carrying a nitroreductase of choice. This will eliminate the need for a fluorescent protein/nitroreductase fusion protein, as only the

nitroreductase will be needed to be driven by a promoter for reporter and ablation properties. The ability to use just one nitroreductase to induce the properties of fluorescence, and ablation in a target population, make it a simpler and more flexible technology.

#### 4.1.4 6KO library

High levels of background fluorescence observed are observed in the SOS-R2 strain due to activation of the masked fluorophores by endogenous nitroreductases; as such, plasmids expressing any nitroreductase candidates to be screened fluorescently in bacteria first had to be transformed into the 6KO strain. The nitroreductases chosen to be transformed into the 6KO strain were those which had been identified through the growth inhibition screening process to have, or the potential to have, opposing activation profiles with nil bystander antibiotics. Due to this selection criterion, this set of nitroreductases is very heavily weighted to the *nfsA* family; while many NfsA enzymes were capable of activating a subset of nil bystander antibiotic candidates, the *nfsB* enzymes had a much broader range of activation, and there were only a few that activated a subset of nil bystander antibiotic candidates that were not readily activated by members of the *nfsA* family.

**Table 4.1 23 nitroreductase 6KO library**

#	Gene	Organism	Family	% ID/Sim
1	NfsA_Ec	<i>Escherichia coli</i>	NfsA	100/100
2	NfsA_St	<i>Salmonella enterica</i>	NfsA	87/95
3	NfsA_Ck	<i>Citrobacter koseri</i>	NfsA	86/92
4	NfsA_Kp	<i>Klebsiella pneumoniae</i>	NfsA	83/92
5	NfsA_Es	<i>Enterobacter sakazakii</i>	NfsA	82/94
6	NfsA_Ecaro	<i>Erwinia carotovora</i>	NfsA	65/82
7	NfsA_Vf	<i>Vibrio fischeri</i>	NfsA	52/68
8	NfsA_Vv	<i>Vibrio vulnificus</i>	NfsA	51/65
9	Frp1_Vh	<i>Vibrio harveyi</i>	NfsA	51/65
10	NfrA_Bs	<i>Bacillus subtilis</i>	NfsA	39/62
11	NfsA_Lw	<i>Listeria welshimeri</i>	NfsA	41/60
12	NfsA_Li	<i>Listeria innocua</i>	NfsA	39/60
13	NfsA_Bco	<i>Bacillus coagulans</i>	NfsA	38/60
14	NfsA_Np	<i>Nostoc punctiforme</i>	NfsA	38/59
15	NfsA_Bth	<i>Bacillus thuringiensis</i>	NfsA	35/58
16	NfsA_Lsak	<i>Lactobacillus sakei</i>	NfsA	40/57

17	NfsA_Pp	<i>Pseudomonas putida</i>	NfsA	35/57
18	YcnD_Bs	<i>Bacillus subtilis</i>	NfsA	35/56
19	NfsB_Ec	<i>Escherichia coli</i>	NfsB	100/100
20	NfsB_Vv	<i>Vibrio vulnificus</i>	NfsB	61/75
21	NfsB_Pp	<i>Pseudomonas putida</i>	NfsB	52/71
22	NfsB_Vh	<i>Vibrio harveyi</i>	NfsB	30/48
23	YfkO_Bs	<i>Bacillus subtilis</i>	NfsB	25/47

#### 4.1.5 Aims

The aims of this chapter were to i) Illustrate the activation profiles of the masked fluorophores with members of the 6KO 23 nitroreductase library, identifying pairs of different coloured masked fluorophores/ nitroreductases which show opposing activation profiles ii) Combine the results from (i) with results observed in chapter 3 of nil bystander antibiotics/ nitroreductases combinations with opposing activation profiles to create a multiplex reporter/ targeted cell ablation system in mixed population cells in the 6KO strain; iii) Translate the results observed in bacterial cells into human cell lines for proof of principle of use in eukaryotic models.

## 4.2 Results

### 4.2.1 Fluorescent screening in bacterial cells

Dr Horvat had previously run fluorescent screens with all 54 of the masked fluorophores available in the lab against a number of nitroreductases from the full 58 nitroreductase library in the 6KO strain, and generated a heat-map from the data obtained. The masked fluorophores that looked to be the most promising in terms of opposing activation profiles of different coloured fluorescence were identified using her heat-map. These 16 masked fluorophores (Table 2.2) were screened against the 23 nitroreductase 6KO library by fluorescence screening as described in 2.9.4 and a heat-map of the results was generated (Figure 4.1). The results of this screening confirmed the activation profiles that Dr Horvat had observed, while adding additional information for some NfsA family members that were not available during Dr Horvat's research. The results can be seen in figure 4.4.

While a lot of masked fluorophores are either active with the majority of nitroreductases, or show little to no activity with the majority of the nitroreductases, it is clear to see that some masked fluorophores are more active with a related group of nitroreductases. For example, the blue fluorophores FSL162, FSL163, FSL175, FSL176 can clearly be seen to have high activity with the majority of the NfsB enzymes present, while there is little to no activity with the NfsA family enzymes. What is more interesting however, is the clear preference of the activation of the two green fluorophores, FSL76 and FSL150 with the NfsA family enzymes, while the red masked fluorophore, FSL178, appears to have a clear activation preference with the NfsB family fluorophores. These observations make a good basis for future experimentation of a multiplex reporter system.

	25	48	59	61	95	111	162	163	169	170	171	175	176	76	150	178
NfsA_Ec	2326	14421	11798	12053	4747	14114	2835	2675	7905	1362	16430	398	448	4399	2554	0
NfsA_St	4285	11087	12764	13672	9276	15174	2783	1394	6754	3787	15873	865	986	2623	3286	116
NfsA_Ck	4865	3987	12937	13654	3789	2876	2364	1784	8753	8992	3027	385	249	2098	649	5
NfsA_Kp	789	12766	13654	12998	4989	16389	789	657	7584	376	3762	379	346	3004	2868	132
NfsA_Es	797	3971	13199	10264	577	17498	1124	1240	8383	4609	22993	983	826	3120	394	0
NfsA_Ecaro	781	4973	13284	12066	50	17123	958	1748	6576	3139	19959	863	953	2544	439	0
NfsA_Vf	4296	3627	654	453	11976	643	876	2098	8450	412	16938	374	401	2435	735	8
NfsA_Vv	7893	9873	9765	8754	3892	9866	1678	2763	6890	8726	17986	484	389	2098	2657	157
Frpl_Vh	876	9862	9862	7845	4091	8753	567	548	8456	2093	2864	386	397	2140	2186	6
NfrA_Bs	638	8762	356	463	436	367	687	1409	7854	378	19863	487	635	3264	986	20
NfsA_Lw	4547	4203	11261	10744	2097	1346	879	1596	4154	2035	21264	115	176	3814	328	0
NfsA_Li	4793	4098	11466	10848	2919	1842	1909	1117	7421	9796	20249	497	800	3513	482	0
NfsA_Bco	652	2567	12683	11875	2987	3291	754	647	3962	3092	3674	476	376	2987	364	7
NfsA_Np	875	3676	15638	14678	355	16739	354	537	4672	456	19853	326	475	1537	482	0
NfsA_Bth	763	4437	2859	13780	653	2876	577	378	2498	3289	2075	397	377	354	427	100
NfsA_Lsak	659	2335	13787	13247	322	12973	584	436	3974	356	254	6087	765	325	367	34
NfsA_Pp	4457	10973	12840	12893	4921	12665	765	856	9836	4209	17634	421	633	454	1758	80
YcnD_Bs	857	276	367	456	265	3782	349	453	543	234	378	532	329	493	375	384
NfsB_Ec	687	8275	9836	12896	654	14672	4378	4326	10897	356	16397	9635	3987	264	653	289
NfsB_Vv	9635	7626	17223	13179	6138	16662	12063	9017	12650	4971	18200	5095	3286	1118	387	591
NfsB_Pp	3362	8546	18572	15523	2515	19280	3903	7954	12387	3769	21319	3127	3531	80	548	220
NfsB_Vh	3873	2989	452	14563	356	463	10758	8025	11866	643	20186	235	327	120	742	9
YfkO_Vh	2789	6532	3782	3267	245	14097	3094	645	10973	237	20754	345	266	352	485	325

**Figure 4.1 Heat-map of 23 nitroreductase 6KO library with different masked fluorophores.** The heat-map was generated from fluorescence averages from 5 independent assays. Fluorescence is expressed as the raw fluorescent units measured after subtraction of endogenous auto-fluorescence observed in the empty plasmid control strain. All fluorophores were added to a final concentration of 50  $\mu$ M, and fluorescence was measured at one of three different excitation/ emission settings according to the emission colour of the unmasked fluorophore; red fluorescence (ex 645/ em 660), green fluorescence (ex 405/ em 585), or blue fluorescence (ex 355/ em 460). The colour of the cells in the first row indicates the colour of fluorescence that each unmasked fluorophore emits. In this heat-map, the green squares denote nitroreductase enzymes that have high activity with the given nil bystander antibiotic, orange some activity, and red no activity. For high, activity, some activity, and low activity ranges were specified as follows; blue fluorescence >5000, 1000-4999, >1000; green fluorescence >2000, 1000-1999, >1000; red fluorescence >200, 100-199, >100 respectively.

### 4.2.2 Combined fluorescence reporting and cell ablation

Initial experiments to demonstrate dual fluorescence and ablation capabilities were undertaken using the nitroreductases that showed promising opposing activation profile combinations in chapter 3. As FSL41 has been shown previously by Dr Horvat to be highly active with most nitroreductases, this masked fluorophore was used to identify the presence of nitroreductases during the initial optimisation.

Day cultures of 200  $\mu$ L were inoculated with 15  $\mu$ L of an overnight culture and grown for three hours prior to the addition of 25  $\mu$ M FSL41. After a further four hour incubation period, fluorescence was recorded qualitatively on the UV trans-illuminator as illustrated in Figure 4.2. In parallel, replicate cultures were treated at the 3 h timepoint not only with 25  $\mu$ M FSL41, but also with the nil bystander antibiotic they had demonstrated high activity with in figure 3.6. Again, fluorescence and turbidity were measured four hours post-challenge. Quantitative analysis on the Enspire 2300 Multiplate Reader confirmed the presence or absence of fluorescence and cell density (not shown).

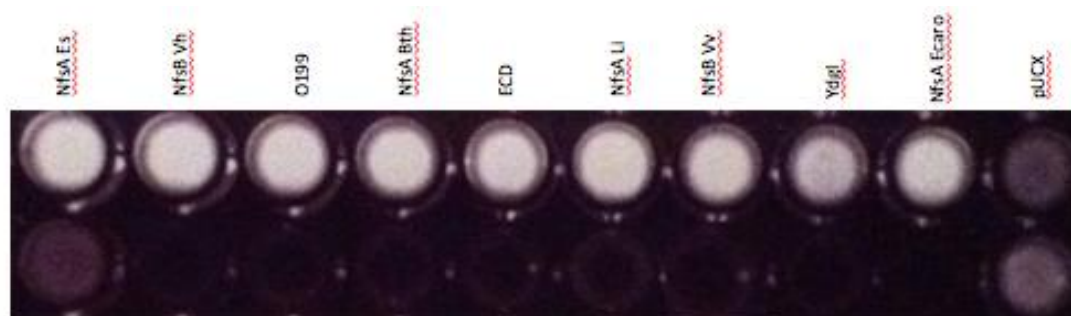


**Figure 4.2 UV Trans-illuminator image of FSL41-treated cultures of *E. coli* 6KO over-expressing different candidate nitroreductases, with (top) or without (bottom) antibiotic challenge.**

Fluorescence was visualised directly on a UV trans-illuminator 4 h post-addition of FSL41. The top row shows the unmasking of FSL41 fluorescence by cultures of 6KO cells over-expressing candidate nitroreductases (as labelled), in the absence of antibiotic challenge. In contrast, the bottom row shows the absence of fluorescence when a strongly activated nil-bystander antibiotic is present as well as FSL41 (Nil bystander antibiotics in each well from left to right are as follow; EF5 (130  $\mu$ M), metronidazole (50  $\mu$ M), EF5 (130  $\mu$ M), F-misonidazole (130  $\mu$ M), tinidazole (75  $\mu$ M), tinidazole (75  $\mu$ M), metronidazole (50  $\mu$ M), metronidazole (50  $\mu$ M), tinidazole (75  $\mu$ M), metronidazole (50  $\mu$ M) (Here, the pUCX empty plasmid control strain was challenged with metronidazole; but has previously been shown to be resistant to all nil bystander antibiotics at the concentrations used).

These cultures were also imaged using a confocal microscope. After the 4 h FSL41 incubation period, samples from each culture were mixed at a 1:1 ratio with 4% paraformaldehyde (to fix the bacteria) before being placed on a microscope slide. An

Olympus FV1000 confocal microscope with 100x lens was used to image each slide. Settings for each laser remained the same between samples of the same excitation wavelength. Representative results for the empty plasmid control strain, and for the NfsB\_Vh over-expressing strain in the absence or presence of metronidazole challenge, are depicted in Figures 4.3 4.4 and 4.5, respectively.

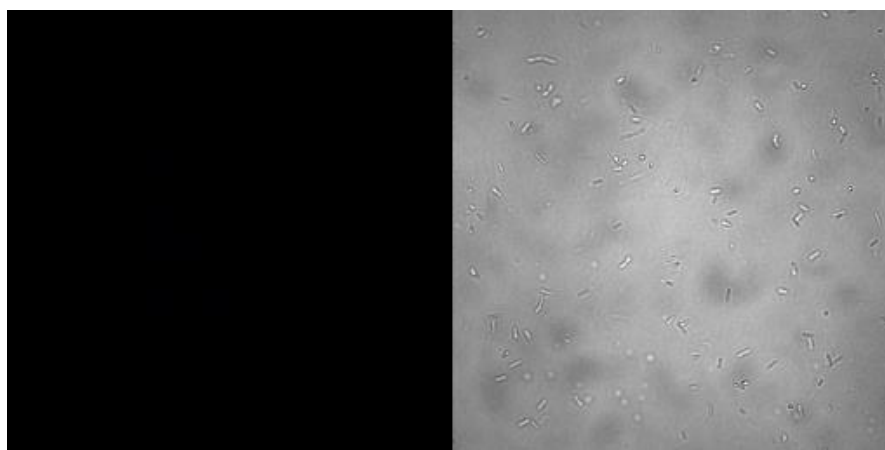


**Figure 4.3 6KO *E. coli* empty plasmid (pUCX) control strain treated with FSL41.** Cultures over-expressing empty pUCX were treated with 25  $\mu$ M FSL41 and incubated for 4 h. Cultures were fixed to slides using 4% paraformaldehyde then imaged on an Olympus FV1000 confocal microscope using the 100x lens, at settings of 405 laser 5%, HV 700 V, Offset 10% and Gain 1x. The left side of this image shows no fluorescence produced, as there is no nitroreductase present to metabolise FSL41 to its active form. The right side shows the same bacteria under transmitted light.

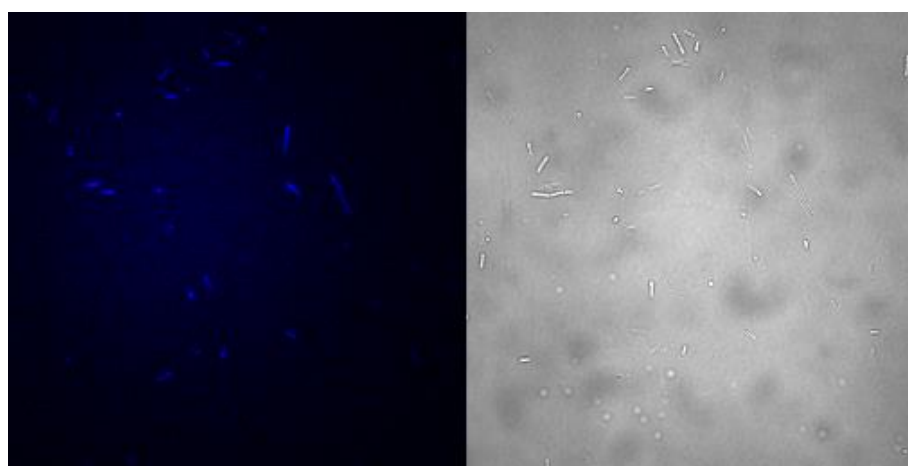


**Figure 4.4 6KO *E. coli* over-expressing NfsB\_Vh, treated with FSL41.** Cultures over-expressing nitroreductase NfsB\_Vh were treated with 25  $\mu$ M FSL41 and incubated for 4 h. Cultures were fixed to slides using 4% paraformaldehyde then imaged on an Olympus FV1000 confocal microscope using the 100x lens, 405 laser, at settings of 5%, HV 700 V, Offset 10% and Gain 1x. The left side of this image shows the fluorescence produced by FSL41 being metabolised in the presence of NfsB\_Vh, the right hand shows the same bacteria under transmitted light.

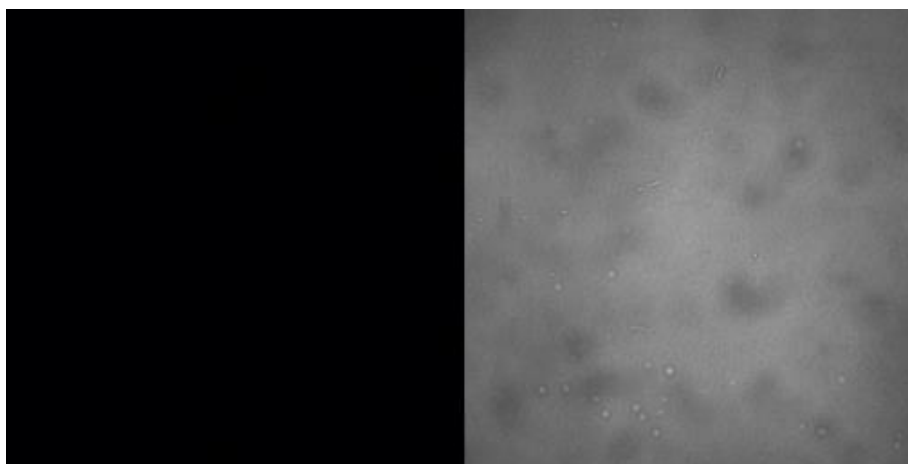


**Figure 4.5 6KO *E. coli* over-expressing NfsB\_Vh treated with FSL41 and metronidazole.** Cultures over-expressing nitroreductase NfsB\_Vh were treated with 25  $\mu$ M FSL41 and challenged with 50  $\mu$ M metronidazole and incubated for 4 h. Cultures were fixed to slides using 4% paraformaldehyde then imaged on an Olympus FV1000 confocal microscope using the 100x lens, 405 laser at settings of 5%, HV 700 V, Offset 10% and Gain 1x. The right hand side of this image shows the disappearance of fluorescence indicating that the cells are dying due to the presence of metronidazole. This is confirmed by the image on the right hand side, the bright field image of the same area, consistent with complete cell ablation.

Together, these results confirm the ability of each nitroreductase candidate to utilise a combination of nil bystanders and nil bystander antibiotics as an effective reporter/ablation system in *E. coli* cells. Whereas fluorescence is clearly visible in nitroreductase-expressing cell cultures treated with FSL41 in the absence of antibiotic, post-antibiotic challenge no fluorescence is seen. The OD600 measurements taken on the Enspire 2300 Multiplate Reader confirm that the loss of fluorescence is due to ablation of the cell population (not shown).

The next step was to demonstrate that these results could be translated to eukaryotic cells. This was first tested using the stable HCT116: NfsB\_Vh cell line that had previously been established by Dr Horvat (Section 3.2.1). These cells were seeded at a 5 million cell density into duplicate 35mm fluorodishes and grown overnight. The following day, 150  $\mu$ M metronidazole was added to one of the cell populations and incubated for an hour. 25  $\mu$ M FSL41 was then added to both the challenged and unchallenged cell populations, which were then incubated for a further hour. The cells were then visualised on an Olympus FV1000 confocal microscope.

The results mirrored those observed in bacterial cells, with HCT116: NfsB\_Vh found to be capable of activating the fluorescence of FSL41 (Figure 4.8). Upon addition of



metronidazole, however, the fluorescence disappears due to the ablation of the cell population (Figure 4.9).

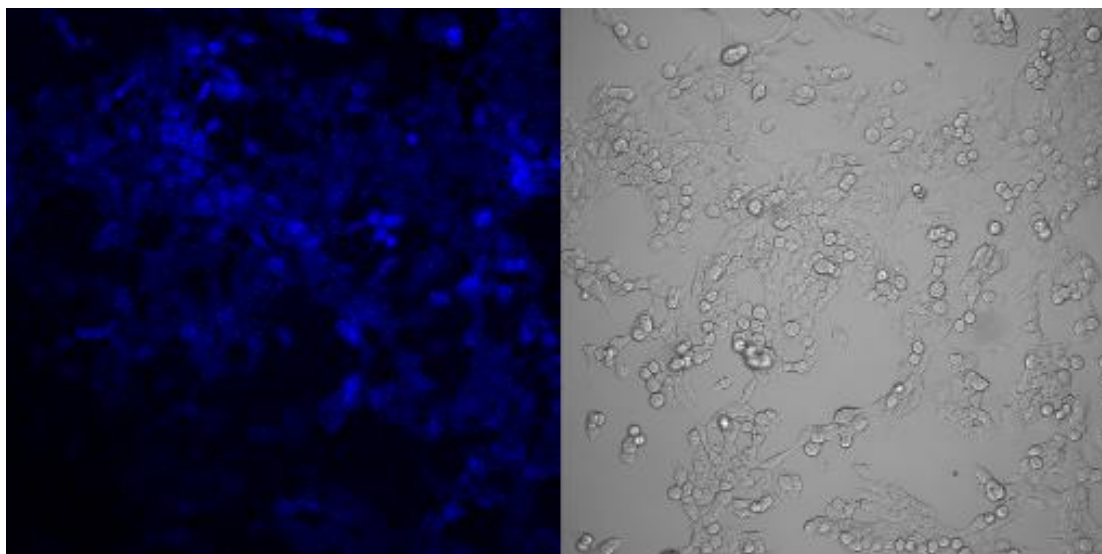


**Figure 4.6 HCT116: NfsB\_Vh treated with FSL41.** Cultures of HCT-116 over-expressing nitroreductase NfsB\_Vh were treated with 25  $\mu$ M FSL41 and incubated for 1 h. Cultures were then visualised on an Olympus FV1000 confocal microscope using the 20x lens, 405 laser at settings of 5%, HV 700 V, Offset 10% and Gain 1x. The left hand side of this image shows the fluorescence produced by FSL41 being metabolised in the presence of NfsB\_Vh, the right hand side of the image shows the same HCT116 cells under transmitted light.

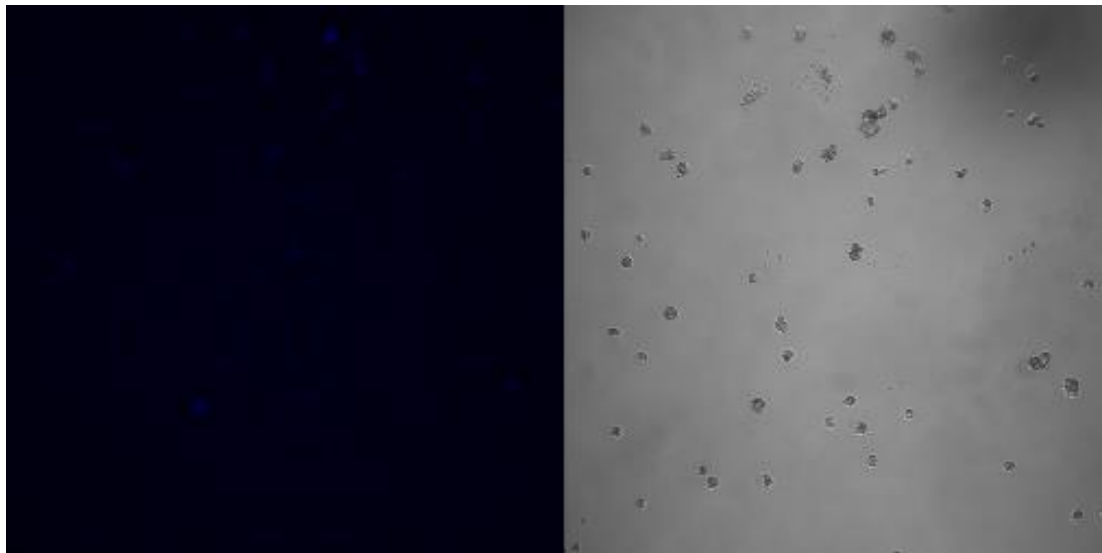


**Figure 4.7 HCT116: NfsB\_Vh treated with FSL41 and challenged with metronidazole.** Cultures of HCT-116 over-expressing nitroreductase NfsB\_Vh were treated with 5  $\mu$ M metronidazole and incubated for 1 h. 25  $\mu$ M FSL41 was added and the cells were incubated for a further hour. Cultures were then visualised on an Olympus FV1000 confocal microscope using the 20x lens, 405 laser at settings of 5%, HV 700 V, Offset 10% and Gain 1x. The left side of this image shows the disappearance of fluorescence indicating that the cells are dying due to the presence of metronidazole. This is confirmed by the image on the right side, the bright field image of the same area, which shows that the cell morphology has changed and they no longer look healthy, as well as a reduced cell population.

### 4.2.3 Dual fluorophore screening in bacterial cells

Following confirmation of the ability to use fluorescence reporting in a single nitroreductase cell ablation system, we next wanted to determine if selective imaging could be observed in a mixed population nitroreductase setting, with two nil bystander antibiotics and two masked fluorophores present; each nitroreductase active with only one masked fluorophore, and one nil bystander antibiotic. This was first tested in *E. coli* cells.

For the reporter system to be useful, two masked fluorophores that emitted fluorescence at different wavelengths needed to be used, to be able to distinguish between cell populations. The ideal fluorophores to be used in this setting would be green and red, as they have the longest wavelengths of the available fluorophores. This makes them the most relevant for *in vivo* imaging as they are the most able to penetrate tissue (Bhaumik, 2011). These two colours also don't have any crossover of wavelengths so no false positive fluorescence would be observed. This is not the case with blue and green fluorescence, for which there is some overlap in the wavelengths; this can be problematic when trying to distinguish cell populations. Moreover, blue fluorophores emit at a wavelength similar to cellular auto-fluorescence, so will have to contend with high background fluorescence (Bhaumik, 2011).

From the results of the nil bystander antibiotic and the masked fluorophore screening, two nitroreductases were selected as the best option for this analysis; NfsA\_Pp and NfsB\_Vv. NfsA\_Pp is active with tinidazole and the green fluorophore FSL76 while NfsB\_Vv is active with metronidazole and the red fluorophore FSL178. Again, NfsA\_Li would have been preferred over NfsA\_Pp for this analysis, but as described in section 3.2.3 it was unable to be transfected into human cell lines within the timeframe of this research. As NfsA\_Pp showed very similar activation profiles to NfsA\_Li with both nil bystander antibiotics and masked fluorophores, it was an acceptable substitute for these proof-of-principle experiments. Figure 4.10 shows the opposing activation profiles of NfsA\_Pp and NfsB\_Vv, with pairs of nil bystander antibiotics and masked fluorophores.

	NfsA_Pp	NfsB_Vv
FSL76/ tinidazole		
FSL178/ metronidazole		

**Figure 4.8 Identification of candidate nitroreductase enzymes that exhibit opposing activation profiles for two nil bystander antibiotics, and two masked fluorophores.** Results summarised from combined nil bystander antibiotic and masked fluorophore screening heat-maps (Figures 3.6 and 4.1), where green indicates high activity with the compounds, while red indicates little to no activity. NfsA\_Pp is capable of activating the green fluorophore FSL76, but not the red fluorophore FSL178; and is also capable of activating the nil bystander antibiotic tinidazole, but not metronidazole. NfsB\_Vv shows the opposite activation profile to this, activating the red fluorophore FSL178, but not the green fluorophore FSL76; and the nil bystander antibiotic metronidazole, but not tinidazole.

Replicate 200  $\mu$ L cultures of 6KO strains over-expressing either NfsA\_Pp or NfsB\_Vv were established by inoculation with 15  $\mu$ L of an overnight culture and then grown for three hours prior to the addition of masked fluorophores (final concentration of 25  $\mu$ M). Cells were then mixed at a 1:1 ratio with 4% paraformaldehyde before being placed on a microscope slide. An Olympus FV1000 confocal microscope was used to image slides using the 100x lens. Settings for each laser remained the same between samples of the same excitation wavelength.

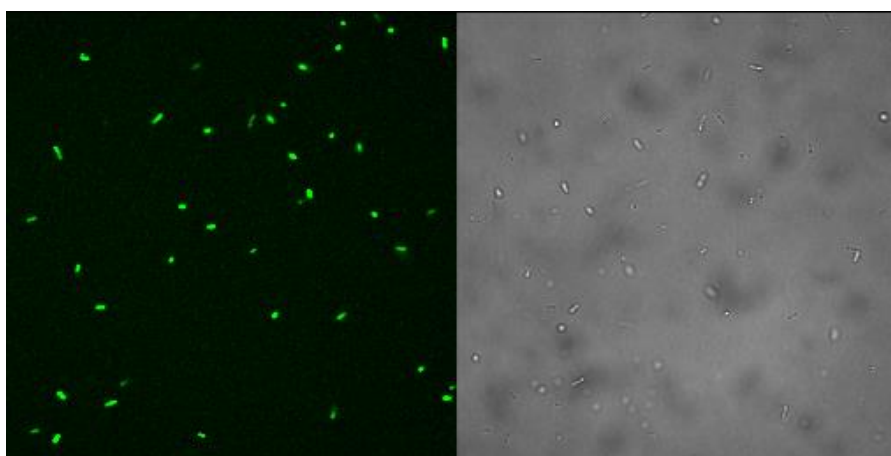


**Figure 4.9 6KO *E. coli* over-expressing NfsA\_Pp treated with FSL76.** Cultures over-expressing nitroreductase NfsA\_Pp were treated with 25  $\mu$ M FSL76 and incubated for 4 h. Cultures were fixed to slides using 4% paraformaldehyde then imaged on an Olympus FV1000 confocal microscope using the 100x lens, 488 laser at settings of 5%, HV 700 V, Offset 10% and Gain 1x. The left side of this image shows the fluorescence produced by FSL76 being metabolised in the presence of NfsA\_Pp, the right hand shows the same bacteria under transmitted light.

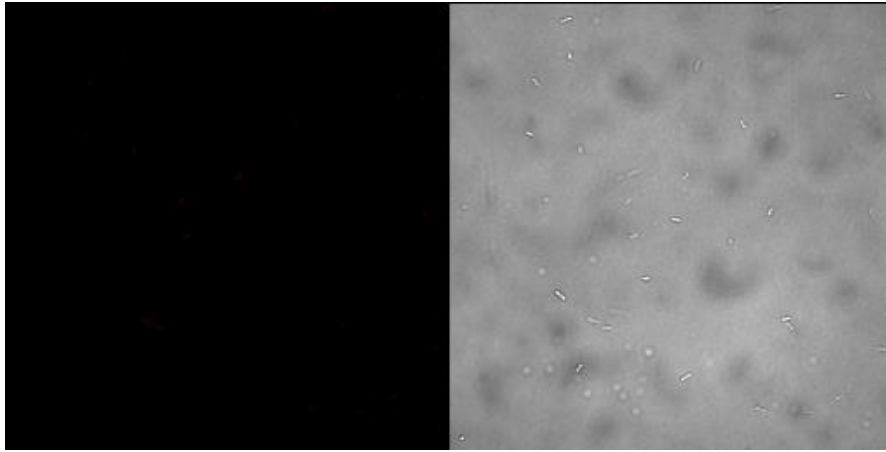


**Figure 4.10 6KO *E. coli* over-expressing NfsA\_Pp treated with FSL178.** Cultures over-expressing nitroreductase NfsA\_Pp were treated with 25  $\mu$ M FSL178 and incubated for 4 h. Cultures were fixed to slides using 4% paraformaldehyde then imaged on an Olympus FV1000 confocal microscope using the 100x lens, 647 laser at settings of 5%, HV 700 V, Offset 10% and Gain 1x. The right hand side of this image shows that NfsA\_Pp is incapable of activating FSL178 therefore no fluorescence is produced, the right hand shows the same bacteria under transmitted light.

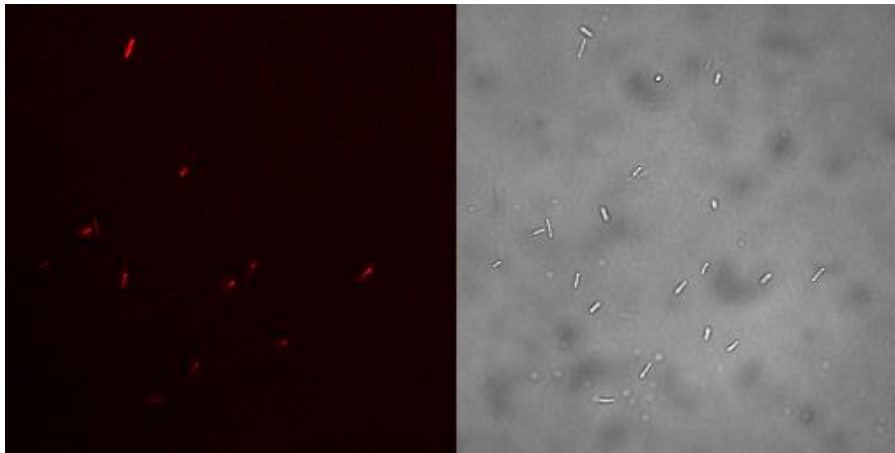


**Figure 4.11 6KO *E. coli* over-expressing NfsB\_Vv treated with FSL178.** Cultures over-expressing nitroreductase NfsB\_Vv were treated with 25  $\mu$ M FSL178 and incubated for 4 h. Cultures were fixed to slides using 4% paraformaldehyde then imaged on an Olympus FV1000 confocal microscope using the 100x lens 647 laser, at settings of 5%, HV 700 V, Offset 10% and Gain 1x. The left side of this image shows the fluorescence produced by FSL178 being metabolised in the presence of NfsB\_Vv, the right hand shows the same bacteria under transmitted light.

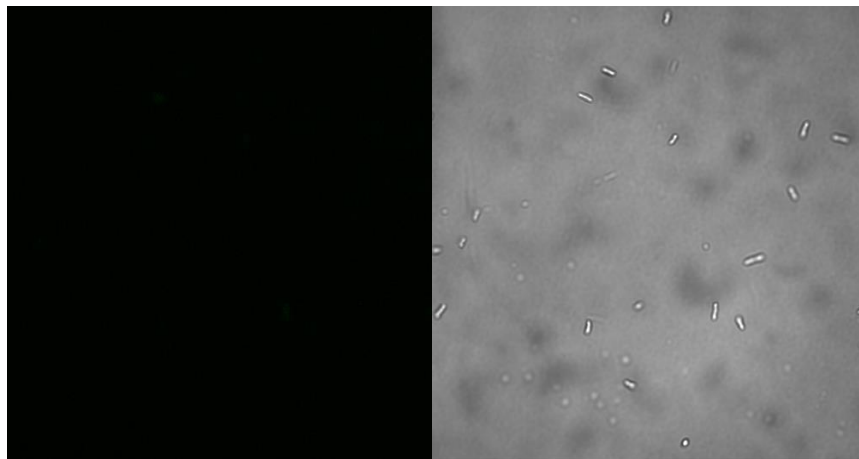


**Figure 4.12 6KO *E. coli* over-expressing NfsB\_Vv treated with FSL76.** Cultures over-expressing nitroreductase NfsB\_Vv were treated with 25  $\mu$ M FSL76 and incubated for 4 h. Cultures were fixed to

slides using 4% paraformaldehyde then imaged on an Olympus FV1000 confocal microscope using the 100x lens 488 laser, at settings of 5%, HV 700 V, Offset 10% and Gain 1x. The left of this image shows that NfsB\_Vv is incapable of activating FSL178 therefore no fluorescence is produced, the right hand shows the same bacteria under transmitted light.

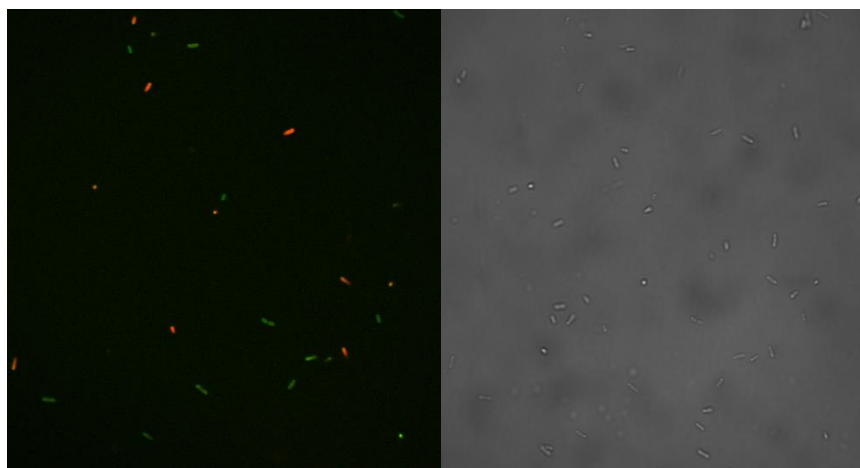


**Figure 4.13 6KO *E. coli* mixed culture multiplex fluorescence imaging.** A mixed population culture containing 6KO *E. coli* over-expressing NfsB\_Vv and NfsA\_Pp was treated with both FSL76 and FSL178 and incubated for 4 h. Cultures were fixed to slides using 4% paraformaldehyde then imaged on an Olympus FV1000 confocal microscope using the 100x lens ,488 laser at settings of 5%, HV 700 V, Offset 10% and Gain 1x, and 647 laser at settings of 5%, HV 700 V, Offset 10% and Gain 1x. The left side of this image shows two distinct cell populations, NfsA\_Pp causing the green fluorescence of FSL76 and NfsB\_Vv causing the red fluorescence of FSL178. The right image shows the same bacteria under transmitted light.

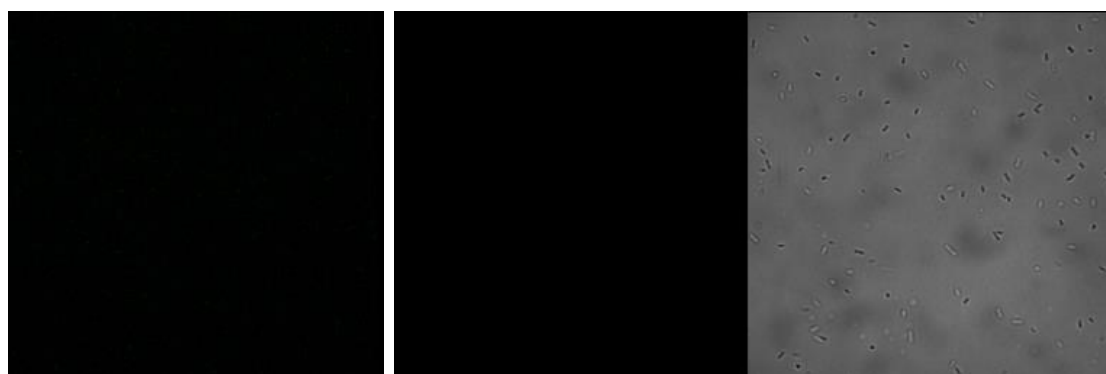


**Figure 4.14 6KO *E. coli* pUCX treated with FSL76 and FSL178.** Cultures over-expressing empty pUCX were treated with either 25  $\mu$ M FSL76 or FSL178 and incubated for 4 h. Cultures were fixed to slides using 4% paraformaldehyde then imaged on an Olympus FV1000 confocal microscope using the 100x lens, 488 laser at settings of 5%, HV 700 V, Offset 10% and Gain 1x, for FSL76 and 647 laser at settings of 5%, HV 700 V, Offset 10% and Gain 1x for FSL178. The far left image and the centre image show no fluorescence produced, as there is no nitroreductase present to metabolise FSL76 (far left) or FSL178 (centre) to their active forms. The right hand shows the same bacteria under transmitted light.

The results of confocal imaging of the *E.coli* 6KO strains were consistent with the initial fluorophore screening (figure 4.1). Cultures over-expressing NfsA\_Pp were capable of activating FSL76 (figure 4.9), but not FSL178 (figure 4.10). Cultures over-expressing NfsB\_Vv had the opposite activation profile, activating FSL178

(figure 4.11), but not FSL76 (4.12). A mixed population of cells over-expressing either NfsA\_Pp or NfsB\_Vv showed distinct fluorescence activation in individual cells (figure 4.13). A negative control with cultures over-expressing pUCX, confirmed that the presence of an over-expressed nitroreductase was necessary for the activation of fluorescence (figure 4.14).

#### **4.2.4 Dual fluorophore screening in human cell lines**

In mammalian cells, newly generated transfections into HEK293 cell lines were confirmed by addition of FSL41, as it had previously been shown that active nitroreductases are generally capable of reducing FSL41. All transfected cell lines were grown in DMEM + 2% HEPES, 10% FCS, and 2% Penicillin/Streptomycin, 2  $\mu$ M puromycin. Each transfected cell line had been subcultured at least 3 times in DMEM containing puromycin, the selection for cells containing the F279/ V5 plasmid used in the creation of Gateway<sup>TM</sup> plasmids, after the initial transfection.

For fluorescence screening in HEK293 for confirmation of stable transfected cell lines, cells were seeded at 5 million cell density into 35mm fluoro dishes and left to grow overnight. The following day FSL41 was added to a final concentration of 25  $\mu$ M and incubated for a further 2 h.

After this 2 h time period, cells were visualised on an Olympus FV1000 confocal microscope using the 20x lens. Blue fluorescence confirmed that transfections had been successful for HEK293: NfsB\_Ec (figures 4.16) HEK293: NfsB\_Vv (figure 4.17), and HEK293: NfsA\_Pp (figure 4.18). Negative controls with untransfected HEK293 WT cells confirmed that cells which aren't carrying a nitroreductase are incapable of activating fluorescence (figure 4.15).

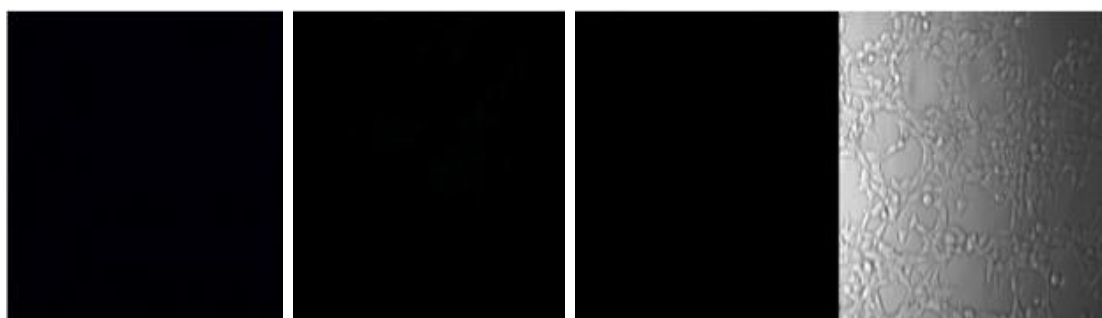


**Figure 4.15 HEK293 WT cells treated with either FSL41, FSL76, or FSL178.** HEK293 WT cultures were treated with 25  $\mu$ M of either FSL41, FSL76, or FSL178 and incubated for 1 h. Cultures then imaged on an Olympus FV1000 confocal microscope using the 100x lens at settings of 405 laser 5%, HV 700 V, Offset 10% and Gain 1x, 488 laser 5%, HV 700 V, Offset 10% and Gain 1x, for FSL76 and 647 laser 5%, HV 700 V, Offset 10% and Gain 1x for FSL178. The far left image, centre left image, and the centre right image show no fluorescence, as there is no nitroreductase present to metabolise FSL41 (far left) FSL76 (centre left), or FSL178 (centre right) to their active forms. The right hand image shows the same cells under transmitted light.

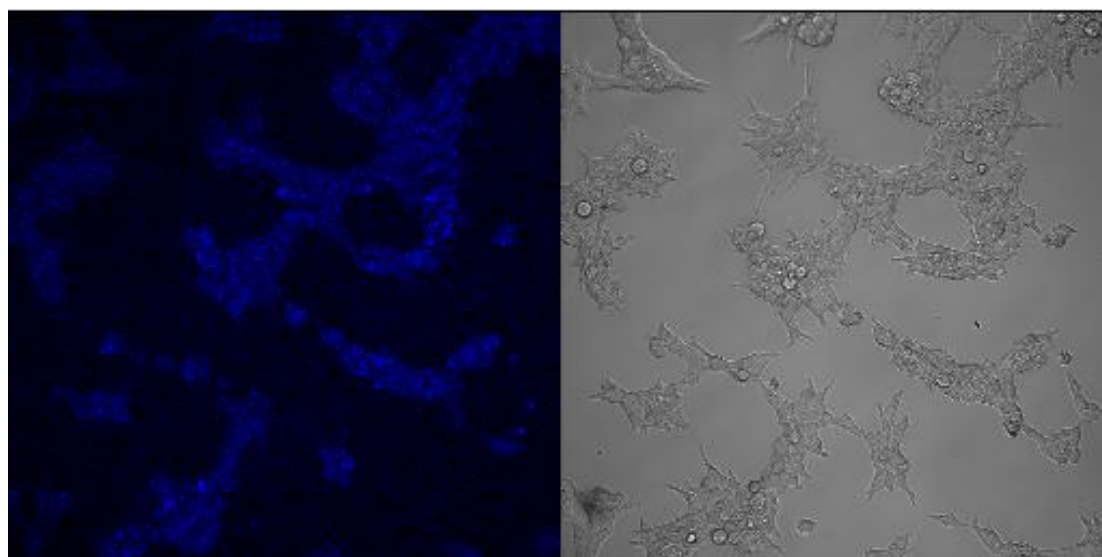


**Figure 4.16 HEK293: NfsB\_Ec treated with FSL41.** Cultures over-expressing nitroreductase NfsB\_Ec were treated with 25  $\mu$ M FSL41 and incubated for 1 h. Cultures were then visualised on an Olympus FV1000 confocal microscope using the 20x lens, 405 laser at settings of 5%, HV 700 V, Offset 1% and Gain 1x. The left image shows the fluorescence produced by FSL41 being metabolised in the presence of NfsB\_Ec, the right shows the same cells under transmitted light. The activation of FSL41 confirms that this is a stably transfected cell line.



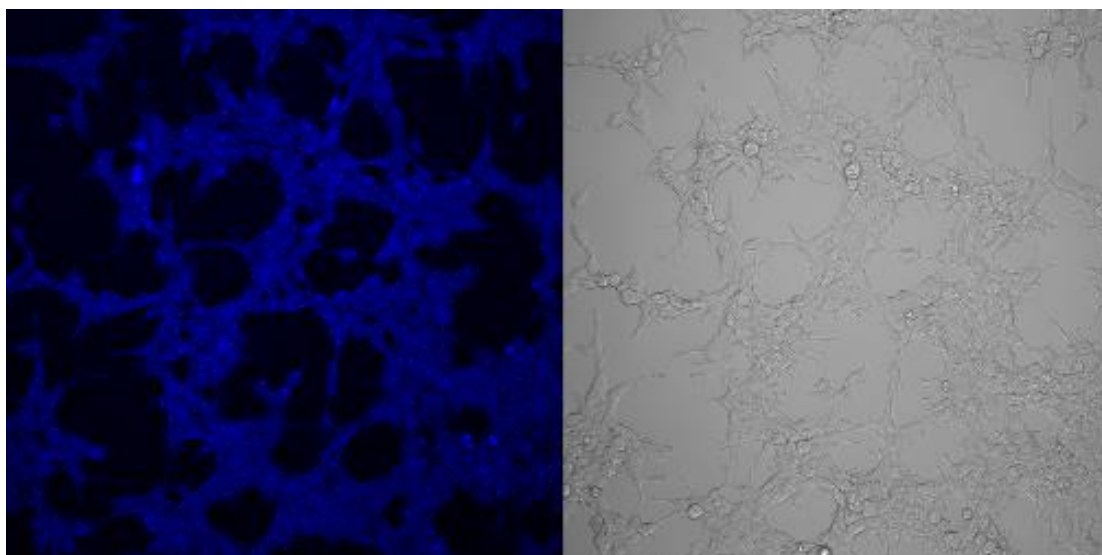


**Figure 4.17 HEK293: NfsB\_Vv treated with FSL41.** Cultures over-expressing nitroreductase NfsB\_Vv were treated with 25  $\mu$ M FSL41 and incubated for 1 h. Cultures were then visualised on an Olympus FV1000 confocal microscope using the 20x lens, 405 laser at settings of 5%, HV 700 V, Offset 10% and Gain 1x. The left side of this image shows the fluorescence produced by FSL41 being metabolised in the presence of NfsB\_Vv, the right shows the same cells under transmitted light. The activation of FSL41 confirms that this is a stably transfected cell line.

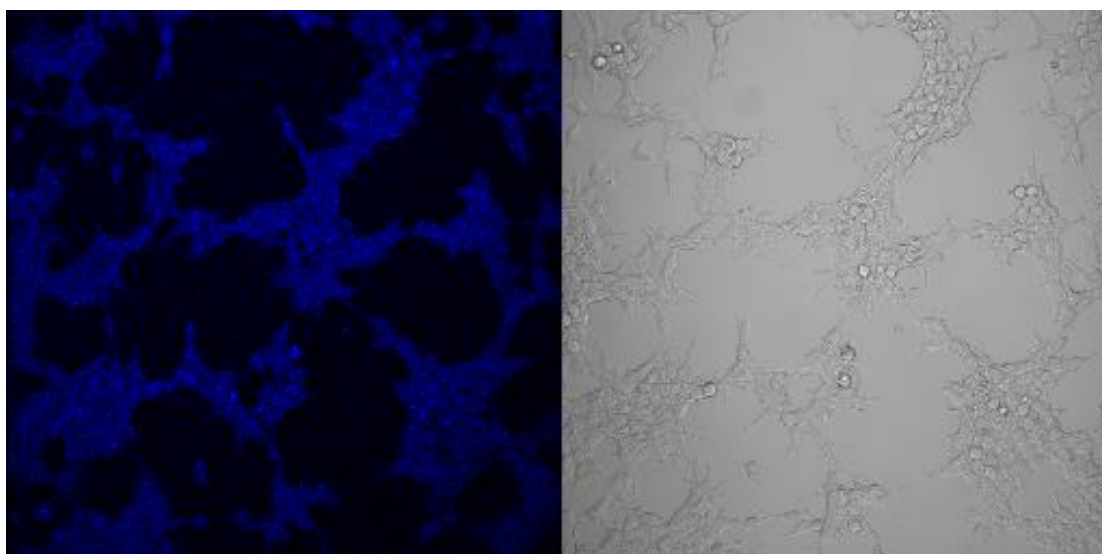


**Figure 4.18 HEK293: NfsA\_Pp treated with FSL41.** Cultures over-expressing nitroreductase NfsA\_Pp were treated with 25  $\mu$ M FSL41 and incubated for 1 h. Cultures were then visualised on an Olympus FV1000 confocal microscope using the 20x lens, 405 laser at settings of 5%, HV 700 V, Offset 10% and Gain 1x. The left side of this image shows the fluorescence produced by FSL41 being metabolised in the presence of NfsA\_Pp, the right shows the same cells under transmitted light. The activation of FSL41 confirms that this is a stably transfected cell line.

HEK293 cells transfected with either NfsA\_Pp or NfsB\_Vv, demonstrated the same ability to activate masked fluorophores in human cells as they had in bacterial cells.

HEK293: NfsA\_Pp is capable of activating FSL76 (figure 4.19), but not FSL178 (figure 4.20), while HEK293: NfsB\_Vv is capable of activating FSL178 (figure 4.21), but not FSL76 (figure 4.21). In a mixed cell population of HEK293: NfsA\_Pp and



HEK293: NfsB\_Vv, distinct cell populations were seen to fluoresce dependent on what nitroreductase they were carrying (figures 4.25).

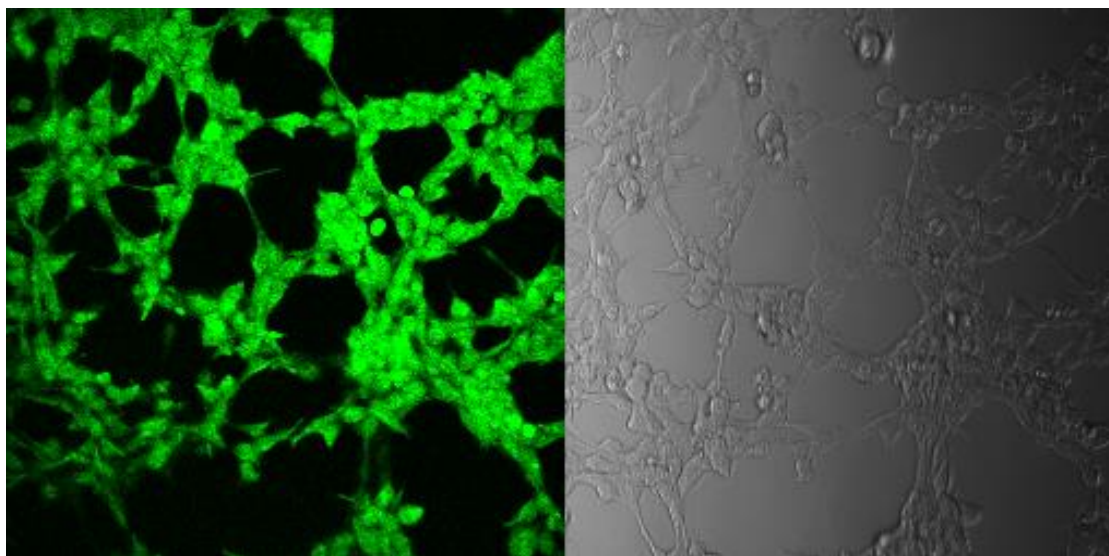


**Figure 4.19 HEK293: NfsA\_Pp treated with FSL76.** Cultures over-expressing nitroreductase NfsA\_Pp were treated with 25  $\mu$ M FSL76 and incubated for 1 h. Cultures were then visualised on an Olympus FV1000 confocal microscope using the 20x lens, 488 laser at settings of 5%, HV 700 V, Offset 10% and Gain 1x. The left side of this image shows the fluorescence produced by FSL76 being metabolised in the presence of NfsA\_Pp, the right shows the same cells under transmitted light.

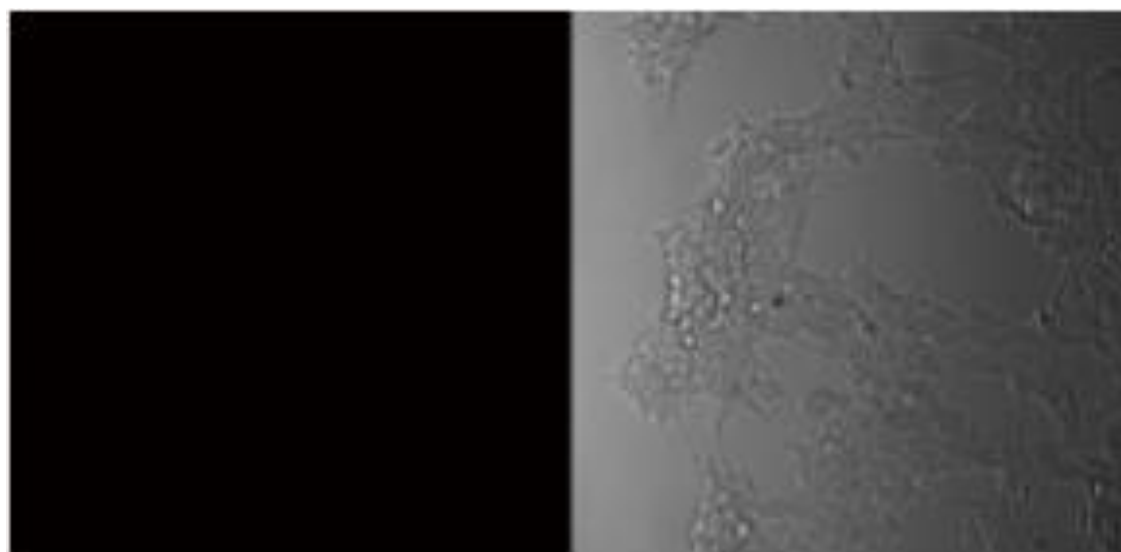


**Figure 4.20 HEK293: NfsA\_Pp treated with FSL178.** Cultures over-expressing nitroreductase NfsA\_Pp were treated with 25  $\mu$ M FSL178 and incubated for 1 h. Cultures were then visualised on an Olympus FV1000 confocal microscope using the 20x lens, 647 at settings of laser 5%, HV 700 V, Offset 10% and Gain 1x. The left side of this image shows NfsA\_Pp is incapable of activating FSL178 as there is no fluorescence observed, the right shows the same cells under transmitted light.

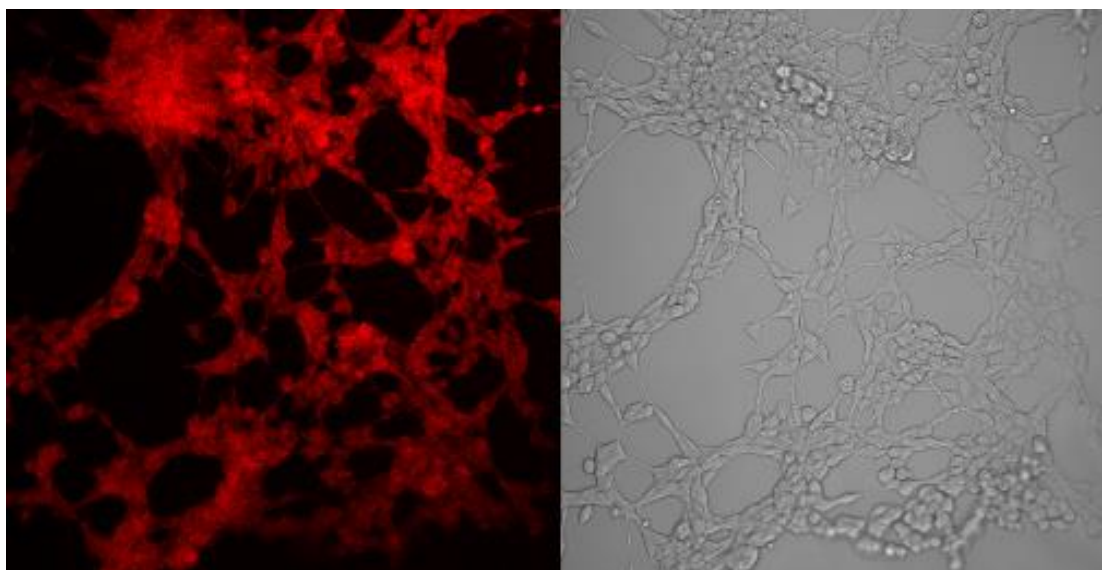


**Figure 4.21 HEK293: NfsB\_Vv treated with FSL178.** Cultures over-expressing nitroreductase NfsB\_Vv were treated with 25  $\mu$ M FSL178 and incubated for 1 h. Cultures were then visualised on an Olympus FV1000 confocal microscope using the 20x lens, 647 laser at settings of 5%, HV 700 V, Offset 10% and Gain 1x. The left side of this image shows the fluorescence produced by FSL178 being metabolised in the presence of NfsB\_Vv, the right shows the same cells under transmitted light.

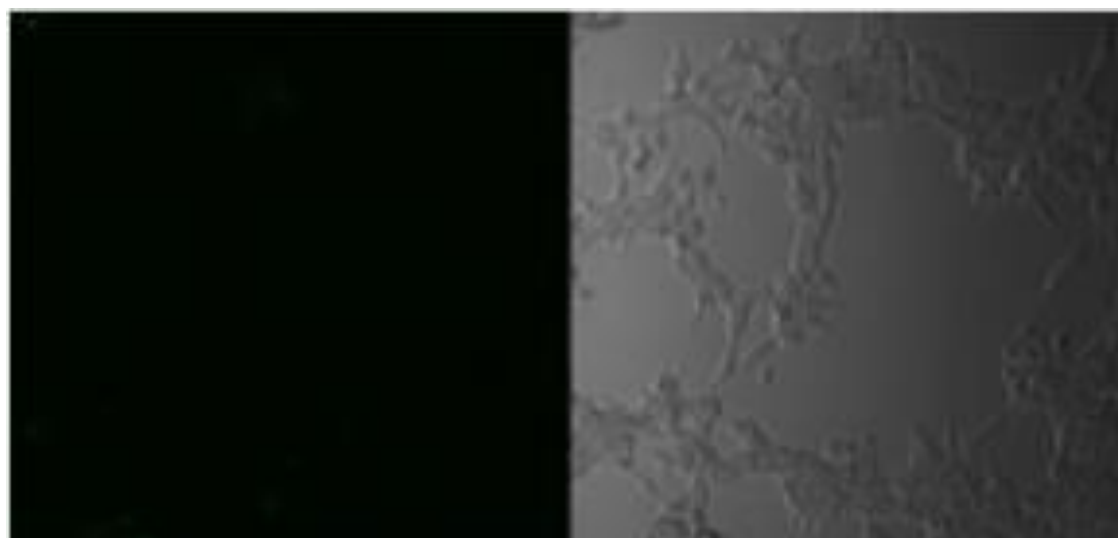


**Figure 4.22 HEK293: NfsB\_Vv treated with FSL76.** Cultures over-expressing nitroreductase NfsB\_Vv were treated with 25  $\mu$ M FSL76 and incubated for 1 h. Cultures were then visualised on an Olympus FV1000 confocal microscope using the 20x lens, 488 laser at settings of 5%, HV 700 V, Offset 10% and Gain 1x. The left side of this image shows NfsB\_Vv is incapable of activating FSL76 as there is no fluorescence observed, the right shows the same cells under transmitted light.

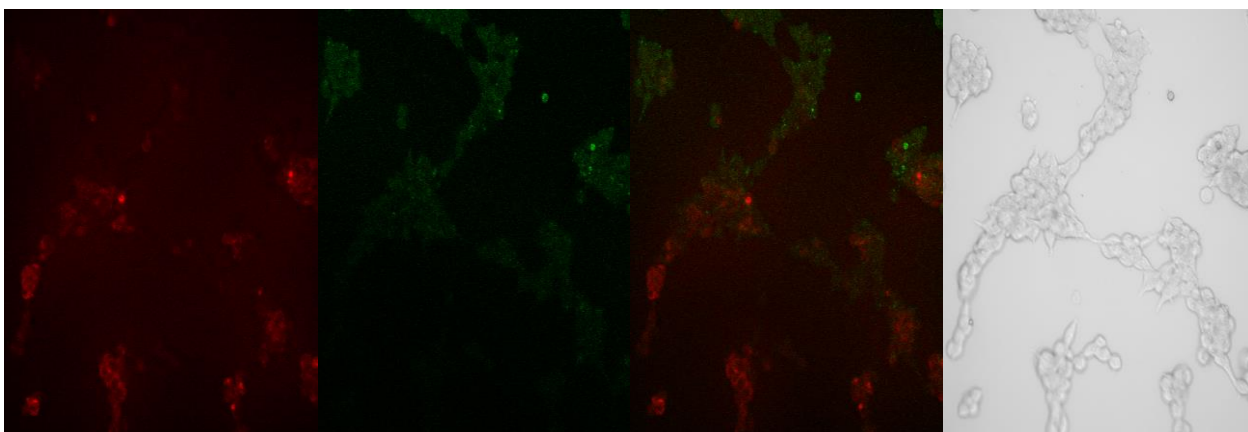


**Figure 4.23 HEK293 mixed culture multiplex fluorescence imaging.** A mixed population culture containing HEK293: NfsB\_Vv and HEK293: NfsA\_Pp was treated with both FSL76 and FSL178 and incubated for 1 h. Cultures were then visualised on an Olympus FV1000 confocal microscope using the 100x lens, laser 647 at settings of laser 5%, HV 700 V, Offset 10% and Gain 1x (far left) 488 laser at settings of 5%, HV 700 V, Offset 10% (centre left) and Gain 1x, and The far left image shows distinct areas of FSL178 activation while the centre left image shows distinct areas of FSL76 activation. The centre right image shows these two images superimposed on top of each other, while the far right image shows the same cells under transmitted light.

#### **4.2.5 Dual fluorescence reporting/ nil bystander antibiotic targeted cell ablation**

Having confirmed that NfsA\_Pp and NfsB\_Vv exhibited opposing activation profiles with the green probe FSL76 and the red probe FSL178, it was next tested whether these selective fluorescence capabilities could be combined with the selective ablation capabilities demonstrated in chapter 3. This was first evaluated in *E. coli* 6KO cells.

Initial experiments undertaken tested the ablation (figures 4.25; 4.27) or retention (Figures 4.24; 4.26) of fluorescence in single nitroreductase populations challenged with either metronidazole or tinidazole. In a culture over-expressing NfsA\_Pp treated with FSL76 and challenged with metronidazole, green fluorescence is clearly visible (figure 4.24). In a culture over-expressing NfsB\_Vv treated with FSL178 and challenged with tinidazole, red fluorescence is clearly visible (figure 4.26). However, in a culture over-expressing NfsA\_Pp treated with FSL76 and challenged with tinidazole, green fluorescence is not visible, and the cell population is seen to have decreased (figure 4.25). In a culture over-expressing NfsB\_Vv treated with FSL178 and challenged with metronidazole, red fluorescence is not visible, and the cell population is seen to have decreased (figure 4.27). These results had been expected from the growth inhibition and fluorescence screening (figure 4.10).

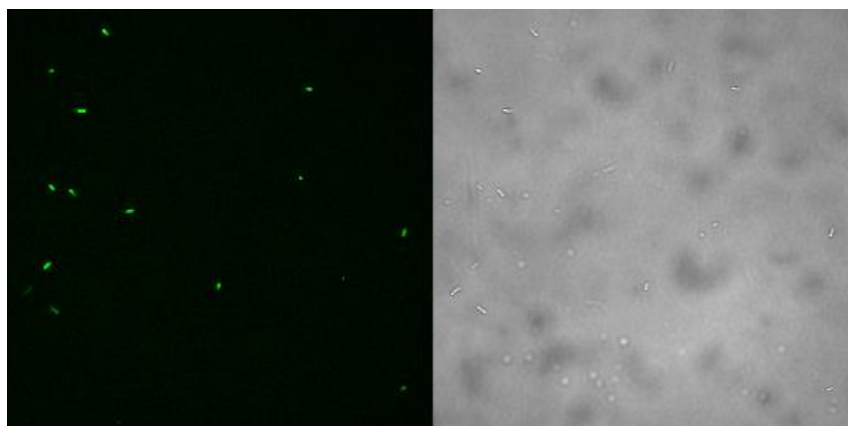


**Figure 4.24 6KO *E. coli* over-expressing NfsA\_Pp treated with FSL76 and challenged with metronidazole.** Cultures over-expressing nitroreductase NfsA\_Pp were treated with 25  $\mu$ M FSL76 and 50  $\mu$ M metronidazole and incubated for 4 h. Cultures were fixed to slides using 4% paraformaldehyde then imaged on an Olympus FV1000 confocal microscope using the 100x lens, 488 laser at settings of 5%, HV 700 V, Offset 10% and Gain 1x. NfsA\_Pp activates FSL76 to produce green fluorescence (left panel), because the cells over-expressing this nitroreductase are unaffected by metronidazole. The right shows the same bacteria under transmitted light.

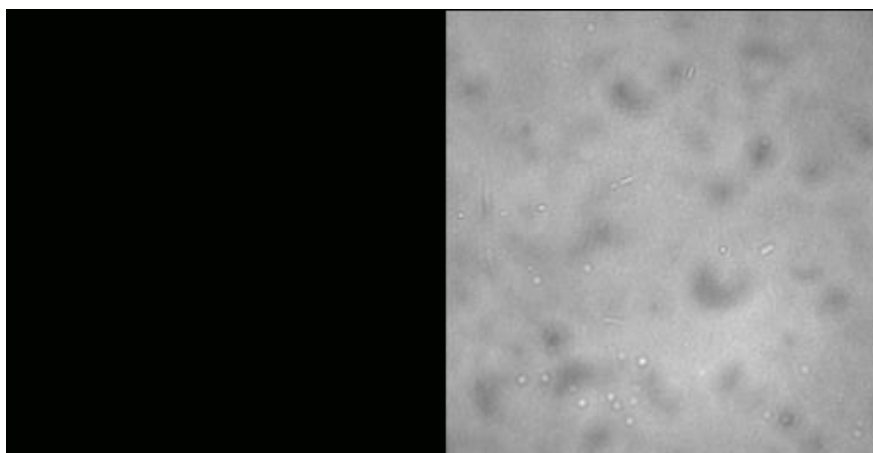


**Figure 4.25 6KO *E. coli* over-expressing NfsA\_Pp treated with FSL76 and challenged with tinidazole.** Cultures over-expressing nitroreductase NfsA\_Pp were treated with 25  $\mu$ M FSL76 and 50  $\mu$ M tinidazole and incubated for 4 h. Cultures were fixed to slides using 4% paraformaldehyde then imaged on an Olympus FV1000 confocal microscope using the 100x lens, 488 laser at settings of 5%, HV 700 V, Offset 10% and Gain 1x. Although NfsA\_Pp activates FSL76, green fluorescence is not visible, shown on the left, as the nitroreductase also activates tinidazole which ablates the cell population as can be seen on the right.

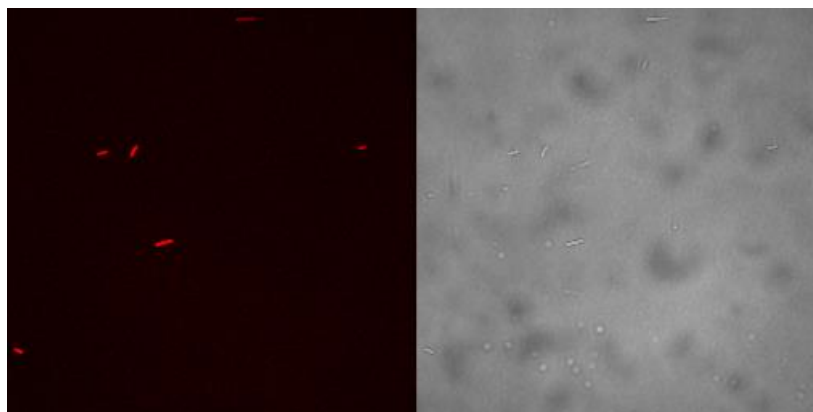


**Figure 4.26 6KO *E. coli* over-expressing NfsB\_Vv treated with FSL178 and challenged with tinidazole.** Cultures over-expressing nitroreductase NfsB\_Vv were treated with 25  $\mu$ M FSL178 and

challenged with 75  $\mu$ M tinidazole and incubated for 4 h. Cultures were fixed to slides using 4% paraformaldehyde then imaged on an Olympus FV1000 confocal microscope using the 100x lens, 647 laser at settings of 5%, HV 700 V, Offset 10% and Gain 1x. NfsB\_Vv activates FSL178 to produce red fluorescence. As NfsB\_Vv is incapable of activating tinidazole, the fluorescence is still visible in its presence. This can be seen on the left. The right hand shows the same bacteria under transmitted light.

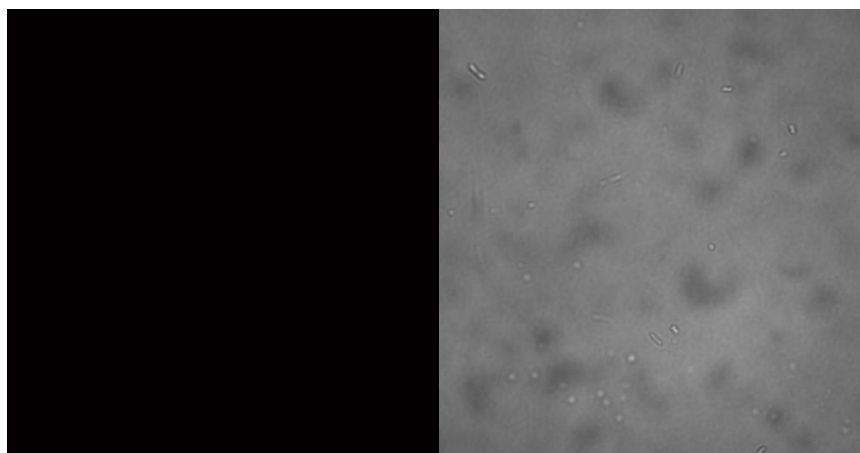


**Figure 4.27 6KO *E. coli* over-expressing NfsB\_Vv treated with FSL178 and challenged with metronidazole.** Cultures over-expressing nitroreductase NfsB\_Vv were treated with 25  $\mu$ M FSL178 and challenged with 50  $\mu$ M metronidazole and incubated for 4 h. Cultures were fixed to slides using 4% paraformaldehyde then imaged on an Olympus FV1000 confocal microscope using the 100x lens, 647 laser at settings of 5%, HV 700 V, Offset 10% and Gain 1x. Although NfsB\_Vv activates FSL178, red fluorescence is not visible, shown on the left, as the nitroreductase also activates metronidazole which ablates the cell population as can be seen on the right.

As dual opposing fluorophore and antibiotic activation profiles had been demonstrated for NfsA\_Pp and NfsB\_Vv, replicate cultures of cells expressing either nitroreductase were mixed, then treated with both fluorophores (FSL76 and FSL178) together, followed by challenge with either 75  $\mu$ M tinidazole or 50  $\mu$ M metronidazole. In mixed cell populations the masked fluorophores and nil bystander antibiotics behaved as had been expected as well, with the presence of both NfsA\_Pp and NfsB\_Vv and FSL76 and FSL178 challenged with metronidazole showing only green fluorescence, as the red fluorescing population also activates metronidazole therefore eliminating the cell population (figure 4.31). The opposite was seen in the same mixed population of both NfsA\_Pp and NfsB\_Vv and FSL76 and FSL178 when challenged with tinidazole, showing only red fluorescence, as the green fluorescing population also activates tinidazole therefore eliminating the cell population (figure 4.32).



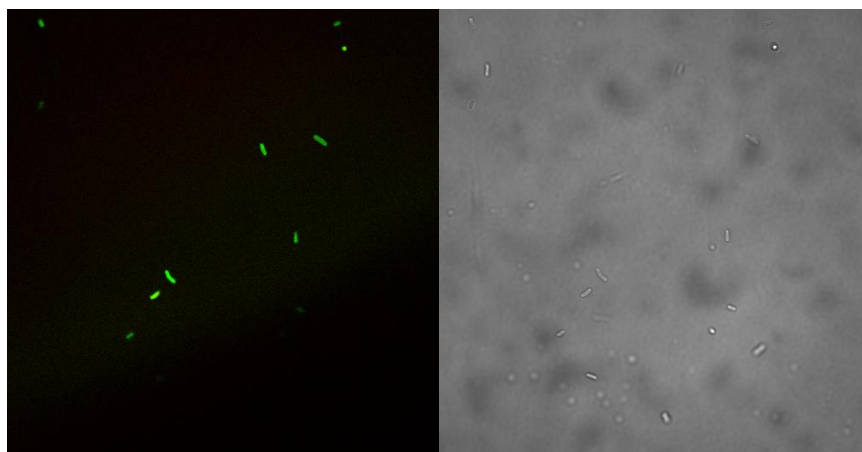


**Figure 4.28 6KO *E. coli* mixed culture multiplex fluorescence imaging and ablation challenged with metronidazole.** A mixed population culture containing 6KO *E. coli* over-expressing NfsB\_Vv and NfsA\_Pp was treated with both FSL76 (25  $\mu$ M) and FSL178 (25  $\mu$ M) and metronidazole (50  $\mu$ M) and incubated for 4 h. Cultures were fixed to slides using 4% paraformaldehyde then imaged on an Olympus FV1000 confocal microscope using the 100x lens, 488 laser at settings of 5%, HV 700 V, Offset 10% and Gain 1x, and 647 laser at settings of 5%, HV 700 V, Offset 10% and Gain 1x. Although NfsB\_Vv activates FSL178 to produce red fluorescence, none can be seen as the bacterial population has been ablated due to the ability of NfsB\_Vv to activate metronidazole. NfsA\_Pp activates FSL76 to produce green fluorescence, as it is incapable of activating metronidazole, the green fluorescence is still visible in its presence as the NfsA\_Pp bacterial population has not been ablated. This can be seen on the left. The right hand shows the same bacteria under transmitted light.

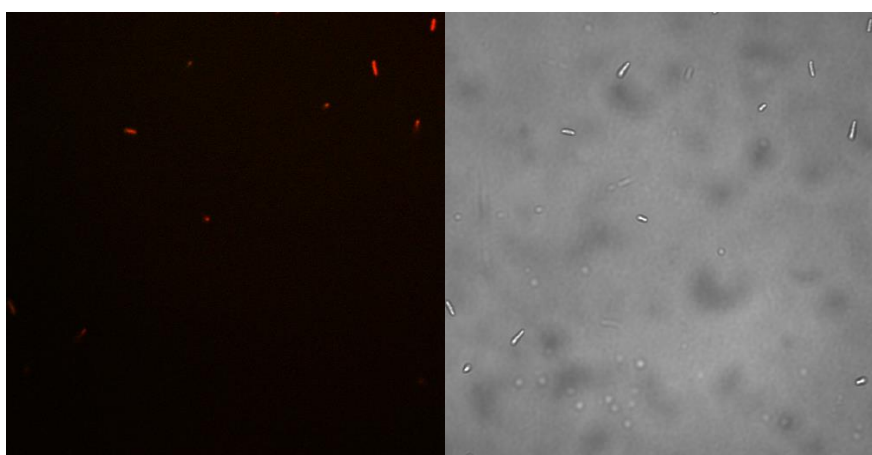


**Figure 4.29 6KO *E. coli* mixed culture multiplex fluorescence imaging and ablation challenged with tinidazole.** A mixed population culture containing 6KO *E. coli* over-expressing NfsB\_Vv and NfsA\_Pp was treated with both FSL76 and FSL178 and tinidazole and incubated for 4 h. Cultures were fixed to slides using 4% paraformaldehyde then imaged on an Olympus FV1000 confocal microscope using the 100x lens, 488 laser at settings of 5%, HV 700 V, Offset 10% and Gain 1x, and 647 laser at settings of 5%, HV 700 V, Offset 10% and Gain 1x. Although NfsA\_Pp activates FSL76 to produce green fluorescence, none can be seen as the bacterial population has been ablated due to the ability of NfsA\_Pp to activate tinidazole. NfsB\_Vv activates FSL178 to produce red fluorescence, as it is incapable of activating tinidazole, the red fluorescence is still visible in its presence as the NfsB\_Vv bacterial population has not been ablated. This can be seen on the left. The right hand shows the same bacteria under transmitted light.

Finally, when cultures of *E. coli* strains over-expressing either NfsA\_Pp or NfsB\_Vv were mixed and then challenged with both 75  $\mu$ M tinidazole and 50  $\mu$ M metronidazole, complete cell elimination and disappearance of any fluorescence was observed (figure 4.30).

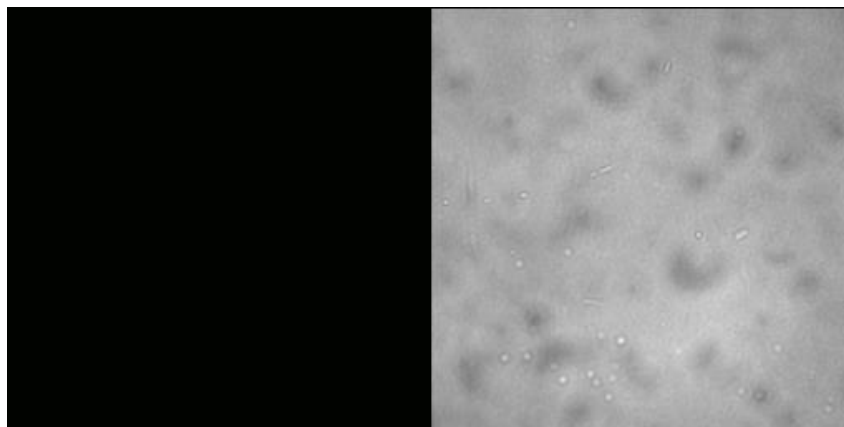


**Figure 4.30 6KO *E. coli* mixed culture multiplex fluorescence imaging challenged with metronidazole and tinidazole.** A mixed population culture containing 6KO *E. coli* over-expressing NfsB\_Vv and NfsA\_Pp was treated with both FSL76 and FSL178 and metronidazole 50  $\mu$ M and tinidazole 75  $\mu$ M and incubated for 4 h. Cultures were fixed to slides using 4% paraformaldehyde then imaged on an Olympus FV1000 confocal microscope using the 100x lens, 488 laser at settings of 5%, HV 700 V, Offset 10% and Gain 1x, and 647 laser at settings of 5%, HV 700 V, Offset 10% and Gain 1x. Although NfsA\_Pp activates FSL76 to produce green fluorescence, and NfsB\_Vv activates FSL178 to produce red fluorescence, neither can be seen as both bacterial populations have been ablated due to the ability of NfsA\_Pp to activate tinidazole and the ability of NfsB\_Vv to activate metronidazole. This can be seen on the left. The right images the same area under transmitted light, and confirms the bacterial population has been ablated.

The dual fluorescence reporter/ cell ablation system showed the same effect in human cells as in bacterial cells. The addition of 150  $\mu$ M tinidazole to HEK293: NfsA\_Pp cells treated with FSL76 showed ablation of the cell population, and almost complete disappearance of fluorescence (figure 4.31), while the addition of 150  $\mu$ M metronidazole to HEK293: NfsB\_Vv cells treated with FSL178 showed ablation of the cell population, and almost complete disappearance of fluorescence (figure 4.32).

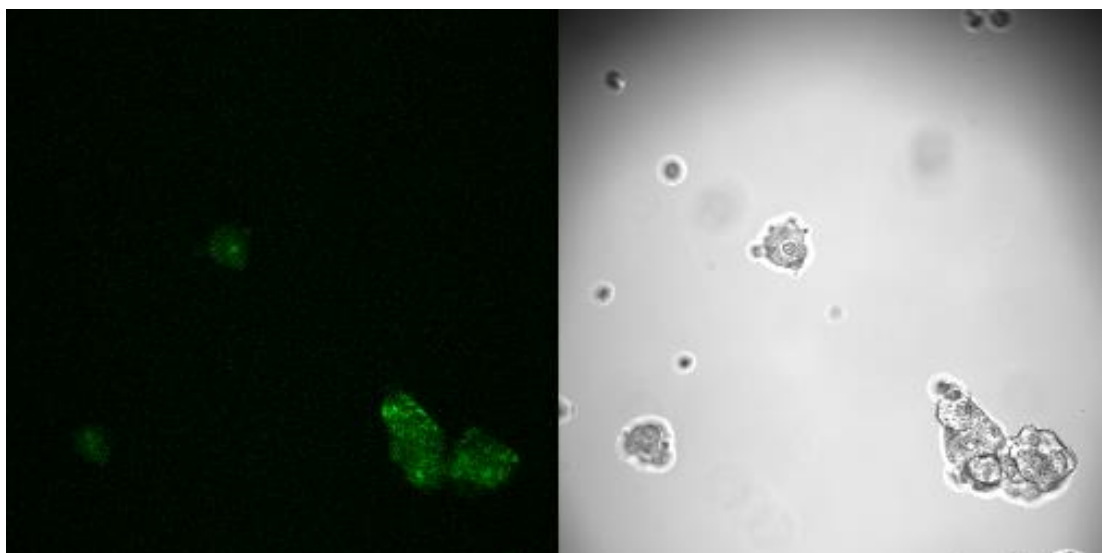


**Figure 4.31 HEK293: NfsA\_Pp treated with FSL76 and challenged with tinidazole.** HEK293: NfsA\_Pp cultures were treated with 25  $\mu$ M FSL76 and challenged with 150  $\mu$ M tinidazole and incubated for 1 h. Cultures were then imaged on an Olympus FV1000 confocal microscope using the 20x lens, 488 laser at settings of 5%, HV 700 V, Offset 10% and Gain 1x. NfsA\_Pp activates FSL76 to produce fluorescence, and tinidazole which ablates the cell population. As can be seen under transmitted light on the right hand side, the cell morphology has deteriorated, and the cell population has been ablated. The left side shows that there is still a small amount of green fluorescence visible, implying that full cell death has not occurred.

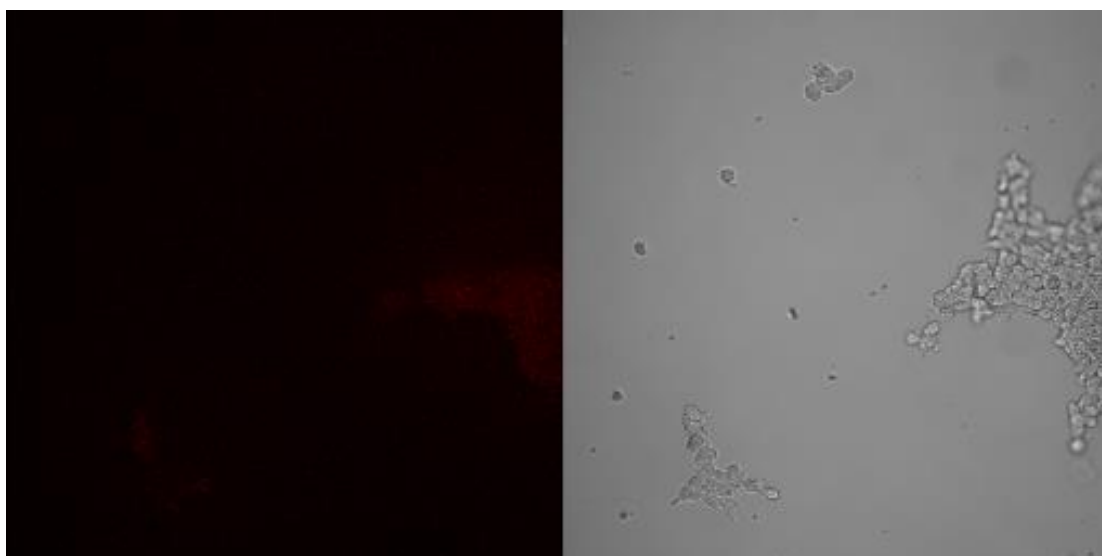


**Figure 4.32 HEK293: NfsB\_Vv treated with FSL178 and challenged with metronidazole.** HEK293: NfsB\_Vv cultures were treated with 25  $\mu$ M FSL178 and challenged with 150  $\mu$ M metronidazole and incubated for 1 h. Cultures were then imaged on an Olympus FV1000 confocal microscope using the 20x lens, 647 laser at settings of 5%, HV 700 V, Offset 10% and Gain 1x. NfsB\_Vv activates FSL178 to produce red fluorescence, and metronidazole which ablates the cell population. As can be seen under transmitted light on the right hand side, the cell morphology has deteriorated, and the cell population has been ablated. The left side shows that there is little to no fluorescence visible, confirming near-complete cell death.

Results from bacterial cells were again mirrored in human cell lines in mixed culture populations. When a co-culture of HEK293: NfsA\_Pp and HEK293: NfsB\_Vv was



incubated with both FSL76 and FSL178, and challenged with 50  $\mu\text{M}$  metronidazole, only green fluorescence was observed. This is because the red fluorescing HEK293: NfsB\_Vv population also activates metronidazole, leading to its clean ablation from the co-culture (Figure 4.33). The opposite phenotype was seen in a replicate co-culture incubated with both masked fluorophores and challenged with 75  $\mu\text{M}$  tinidazole; only red fluorescence was observed, as the green fluorescing HEK293: NfsA\_Pp population also activates tinidazole, leading to ablation (Figure 4.34).

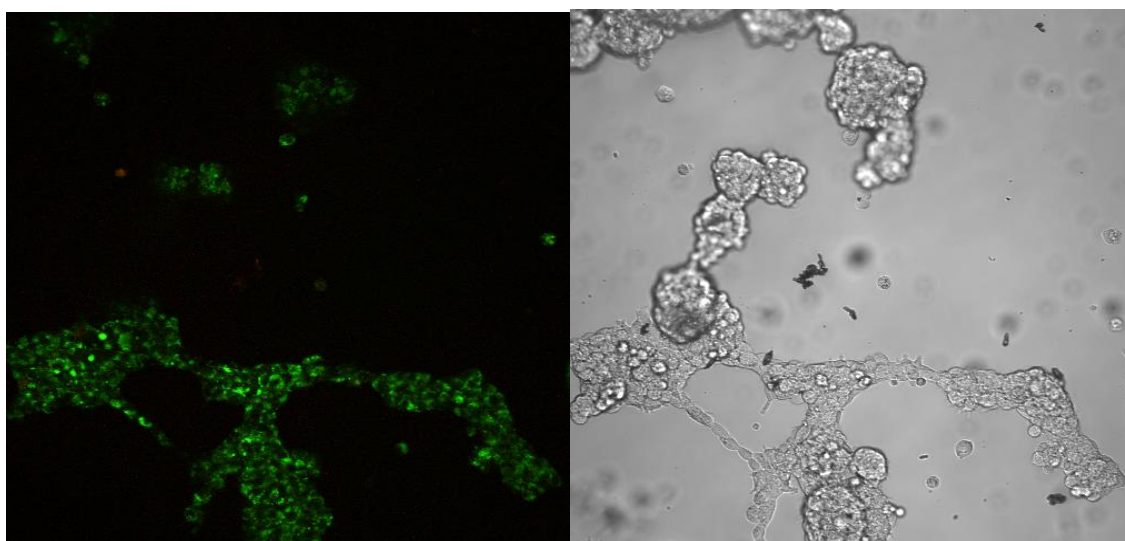


**Figure 4.33 HEK293 mixed culture multiplex fluorescence imaging and ablation challenged with metronidazole.** A mixed population culture containing HEK293: NfsB\_Vv and HEK293: NfsA\_Pp was treated with both FSL76 (25  $\mu\text{M}$ ) and FSL178 (25  $\mu\text{M}$ ) and metronidazole (150  $\mu\text{M}$ ) and incubated for 1 h. Cultures were then imaged on an Olympus FV1000 confocal microscope using the 100x lens, 488 laser at settings of 5%, HV 700 V, Offset 10% and Gain 1x, and 647 laser at settings of 5%, HV 700 V, Offset 10% and Gain 1x. Although NfsB\_Vv activates FSL178 to produce red fluorescence, none can be seen as the cell population has been ablated due to the ability of NfsB\_Vv to co-activate metronidazole, NfsA\_Pp activates FSL76 to produce green fluorescence, and as it is incapable of co-activating metronidazole, the green fluorescence is still visible. This can be seen on the left. The right hand shows the same area under transmitted light.

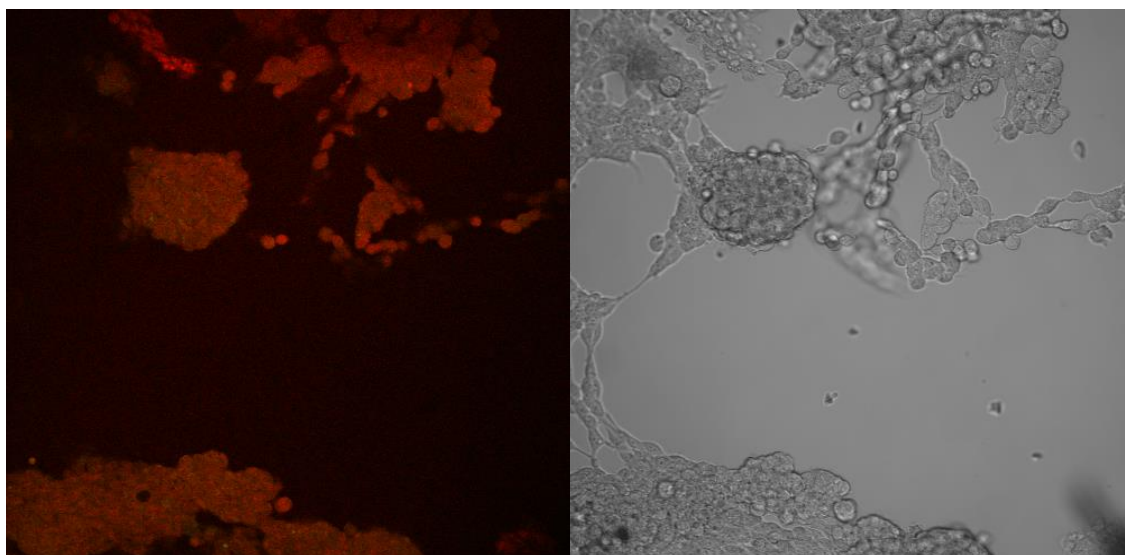


**Figure 4.34 HEK293 mixed culture multiplex fluorescence imaging and ablation challenged with tinidazole.** A mixed population culture containing HEK23: NfsB\_Vv and HEK293: NfsA\_Pp was treated with both FSL76 and FSL178 and tinidazole and incubated for 4 h. Cultures were then imaged on an Olympus FV1000 confocal microscope using the 100x lens, 488 laser at settings of 5%, HV 700 V, Offset 10% and Gain 1x, and 647 laser at settings of 5%, HV 700 V, Offset 10% and Gain 1x. Although NfsA\_Pp activates FSL76 to produce green fluorescence, none can be seen as the cell population has been ablated due to the ability of NfsA\_Pp to co-activate tinidazole. NfsB\_Vv activates FSL178 to produce red fluorescence, as it is incapable of activating tinidazole, the red fluorescence is still visible. This can be seen on the left. The right hand shows the same area under transmitted light.

### 4.3 Discussion

The previous fluorescence screening work by Dr Horvat made the choice of masked fluorophores to be rescreened in the 6KO library easy to narrow down. The selections were based on masked fluorophores that had previously shown high activity with nitroreductases chosen for their selective prodrug and fluorophore activation profiles. Dr Horvat's work also helped establish FSL41 as a general indicator of nitroreductase activity; this enabled the initial optimisation experiments with alternative fluorescent probes (figure 4.9-4.14) to be run with confidence, and allowed for the functional validation of successful transfection; with the presence of fluorescence in the human cell line populations providing proof that the nitroreductase is present and active (figures 4.16; 4.17; 4.18).

Although targeted cell ablation systems using fluorescent proteins as reporter systems are in current use in the field of developmental biology, there would be advantages in reporting directly on the nitroreductase as opposed to a bicistronic fluorescent reporter

protein. Bicistronic systems have been shown to have caused delayed replication time of transfected cells, and to produce less protein than monocistronic systems (Schaller *et al.*, 2007). These disadvantages could be overcome by the use of masked fluorophores, thereby negating the need for the use of a bicistronic system for reporting on targeted cell ablation.

These initial optimisation protocols enabled an investigation into the ablation of fluorescence for developmental biology, first utilising the nitroreductase which had been identified as having the most efficacy with metronidazole in chapter 3, NfsB\_Vh. The results of this study demonstrate that when bacteria over-expressing NfsB\_Vh are treated only with FSL41, there is a high level of fluorescence, and the growth of the cell population appears to remain unaltered (figure 4.4). When a cell population containing NfsB\_Vh treated with FSL41 was challenged with metronidazole, however, the fluorescence levels and the corresponding cell density levels also decreased (figure 4.5), confirming that the addition of a nil bystander antibiotic was responsible for the decline in cell population, and consequently the disappearance of fluorescence. These results were mirrored in experiments carried out in transfected HCT-116 human cell lines (figures 4.6; 4.7). This was important as it has been previously shown that not all nitroreductases behave the same in human cells as bacterial cells, and this technology is aimed to be used within the field of developmental biology in eukaryotic cells.

With the basic dual imaging and ablation tools validated it was next sought to determine whether these could be expanded into a multiplex system of nil bystander antibiotics and masked fluorophores, which might provide dual ablation/ reporter capabilities in a mixed cell population. Results from chapter 3, and from the fluorescence screening indicated that the two most promising nitroreductases for this were NfsA\_Li, and NfsB\_Vv. As has been stated, NfsA\_Pp was used for these experiments in the place of NfsA\_Li, as NfsA\_Li was unable to be taken through to human cell line stage due to technical difficulties and time constraints. NfsA\_Pp is capable of activating the nil bystander antibiotic tinidazole and the masked fluorophore FSL76, which NfsB\_Vv is not, and exhibits at most low-level activity with the nil bystander antibiotic metronidazole and the masked fluorophore FSL178,

which NfsB\_Vv does activate. These capabilities were found to translate consistently from individual bacterial (figures 4.9-4.13) to human (figures 4.19-4.22) cell cultures.

The next step to validate this dual reporter/ ablation system was to test these techniques in mixed culture populations. In both bacterial cells, and human cell lines distinct populations in mixed cultures are observed either enabling the fluorescence of FSL76 or FSL 178 (figures 4.13; 4.25). Upon the addition of tinidazole to these mixed cultures, the population of green fluorescing cells disappeared while the red fluorescing cells remained (figures 4.29, 4.34), as would be expected given that NfsA\_Vv is resistant to tinidazole but can activate FSL178. In contrast, upon the addition of metronidazole to the mixed cultures, the population of red fluorescing cells disappeared while the green fluorescing cells remained (Figures 4.28, 4.33). Again, this is what would be expected as NfsB\_Pp is resistant to metronidazole, but can activate FSL76. This result confirms the ability of initial testing of nitroreductase systems to be undertaken in bacterial systems, and provides strong evidence that a multiplexed dual reporter/ ablation system should be possible *in vivo*.

Thus, these results give a comprehensive proof of principle that the combination of masked fluorophores and nil bystander antibiotics used in conjunction with nitroreductases with opposing activation profiles have the potential to be utilised in developmental and regenerative biology studies for the purpose of a multiplexed dual reporter/ ablation system. Developmental and regenerative biology studies have already employed the use of a single nitroreductase (*E. coli* NfsB\_Ec), exploiting its nitro-reducing capabilities for targeted cell ablation in individual cell types using built in fluorescent proteins as reporters (White and Mumm, 2013). The expanded approach presented in this chapter, however, could enable a temporal and spatial reporter/ ablation system targeted to two different cell types in the same organism, with increased sensitivity and flexibility.

## 5. Summary, Conclusions, and Future Directions

### 5.1 Research motivation

#### 5.1.1 GDEPT

The ability of nitroreductases to reduce a range of nitroquenched compounds has offered potential for an all-encompassing GDEPT system, whereby a single nitroreductase is able to activate a PET imaging agent to confirm localisation of the vector carrying the therapeutic gene, a prodrug for the treatment of cancer, and a nil bystander antibiotic as a safety mechanism to eliminate of the delivery vector.

GDEPT is a fast developing and promising field of research into cancer treatment, the development of which is being boosted by clinical advances and mainstream acceptance of next-generation tumour-targeting viral vectors ([Schmidt, C. 2011](#)) The discovery of nitroreductases and their ability to reduce nitroquenched compounds has been exploited to activate numerous clinically advanced prodrug combinations that were originally developed to be reduced by hypoxic regions of cancerous tumours (Brown, 2007; Patterson et al., 2007, Denny, 2003; Singleton et al., 2007). The imaging of the distribution and magnitude of the therapeutic gene expression is an important component of GDEPT; it enables visualisation of the vector to ensure it has localised to the tumour and is viable throughout the treatment process. The development of fluorescent imaging methods to detect the gene expression could enable this to be a possibility, providing information on the optimal time and duration for prodrug administration (Singleton *et al.*, 2007). Another highly valuable use of this technology would be to monitor real time expression of therapeutic gene expression in the presence of a prodrug throughout therapy, trumping current methodology which focuses on the size of the tumour post treatment to evaluate drug efficacy. Nitroreductases that are capable of activating masked fluorophores are a promising tool, as there are currently only a small number of reporter systems that can be used in a non-invasive manner to directly report on enzyme activity. Importantly, this approach removes the need to introduce a secondary reporter gene to the system.

Another important step in the development of a GDEPT system is the need to eliminate the vector used to deliver the therapeutic gene, post therapy. This is

extremely important to qualify for FDA approval, as many of the vectors used are either viruses or bacteria of pathogenic origin due to the efficiency from their natural life cycle as viruses, are capable of effectively invading human cells and expressing their genes within the cell. For elimination of viral vectors in particular, it is likely to be essential that the ablating nitroreductase is expressed early in the life cycle, and that it is highly active at converting a nil-bystander antibiotic into a potent cytotoxin. The identification in this thesis of several nitroreductases that are far more active than *E. coli* NfsB with metronidazole, as well as several new and promising nitroreductase/antibiotic combinations, will provide fertile ground for further development of systems to efficiently eliminate labelled viruses from human cells, either *in vitro* or *in vivo*.

The addition of imaging agents to confirm the localisation of the vector containing the therapeutic gene and at which point there is the highest gene expression in these cells but not surrounding healthy cells, combined with a mechanism to void the system of the vector post treatment, could greatly advance the development of GDEPT as a viable tool for the treatment of a wide range of solid tumour cancers.

### **5.1.2 Novel developmental biology tools**

The ability of nitroreductases to activate nil bystander antibiotics that ablate only the target cells where the nitroreductase is present, leaving surrounding cells untouched, has also been exploited in the fields of developmental and regenerative biology.

These fields exploit the ability of nitroreductases to act as suicide genes that can ablate a specific cell population. In the case of developmental biology, these capabilities can help identify key functions the target cells have in the developing organism, and what diseases may result when an organism lacks the target cell type. In regenerative studies, the ability to ablate a specific cell population can enable inferences as to whether that cell population is capable of regenerating, and what biological factors are essential for this to take place. The added bonus of having the nitroreductase system in place instead of a gene knockout, is that the specific cell type that is targeted can be ablated at any time during development; therefore enabling the study into the effect of ablation at different time points during development rather

than just one.

A handful of contemporary studies have exploited the ability of nitroreductases to reduce nil bystander antibiotics for targeted ablation of a specific cell population. To do this, a fluorescent reporter and a nitroreductase, NfsB\_Ec, are fused to a promoter of interest. Upon the addition of the nil bystander antibiotic metronidazole, the cell population containing the nitroreductase fusion molecule are ablated, and surrounding cells are left untouched. Transparent organisms such as *Xenopus* and zebrafish are ideal models for reporting on the ablation via a fluorescent fusion protein.

The Ackerley lab's access to nitro-quenched masked fluorophores as well as numerous nitro-quenched nil bystander antibiotics, has enabled us to propose advancing on existing capabilities via integration of only a nitroreductase in place of the gene of interest; i.e. no accompanying fluorescent protein, these being functionally replaced by the masked fluorophore substrates. This would have the same visual effect as the GFP/ nitroreductase system, with the absence of fluorescence after the addition of the nil bystander antibiotics indicating ablation of the cells expressing the nitroreductase protein.

The ability to report on the cell population using fluorescent imaging is important, as it allows the area to be ablated to be visualised prior to addition of the nil bystander antibiotic, ensuring that expression of the nitroreductase gene is exclusive to the target tissue. It also enables the efficacy of ablation to be evaluated directly, post-addition of the nil bystander antibiotic.

Expanding on the basic scenario, we have proposed a two way reporter/ ablation system; wherein one nitroreductase is active with a specific masked fluorophore and nil bystander antibiotic, and inactive with a different masked fluorophore and nil bystander antibiotic combination, while a second nitroreductase exhibits the opposing activation profile, being inactive with the first masked fluorophore/ nil bystander combination, and active with the other.

This system would allow the study of multiple cell types at once, with the ability to study the effect of ablating two different cell types at specific times during

development; either simultaneously or subsequently. Although complete ablation of the target cell population is not currently achievable, the identification in this thesis of nitroreductases with superior metronidazole activation to *E. coli* NfsB, as well as other promising nitroreductase/ nil bystander antibiotic combinations may make this goal a reality.

## **5.2 Key Findings**

### **5.2.1 Identification of nitroreductases active with nil bystander antibiotics**

The 58 nitroreductase core library in the Ackerley lab (table 1.1) is the default library used to screen for nitroreductases that are active with nil bystander antibiotics. The core library contains 13 different families of enzymes, with the majority being from either the NfsA and NfsB families. The screening of this library with the 16 nil bystander antibiotic candidates (table 2.1) by growth inhibition assays (2.9.2) enabled the profiling of all nitroreductase/ nil bystander antibiotic combinations, and identification of combinations of nitroreductases and nil bystander antibiotics that might be useful for targeted cellular ablation.

### **5.2.2 Identification of nitroreductases superior to NfsB\_Ec for metronidazole activation**

The established applications of nitroreductases in developmental and regenerative biology led us to seek a better nitroreductase/ nil bystander antibiotic combination for targeted cell ablation.

Currently these studies employ the nitroreductase NfsB\_Ec, and the nil bystander antibiotic metronidazole. The concentrations of metronidazole being used in these systems however, are extremely high and often toxic to the system, therefore finding a nitroreductase that has greater activity with metronidazole would be beneficial. Initial growth inhibition screens indicated that many nitroreductases in the 58 nitroreductase library had a much higher efficacy with metronidazole than NfsB\_Ec which, at the lowest concentrations used, had essentially no effect.



More detailed IC<sub>50</sub> analyses indicated that NfsB\_Vh had the best efficacy with metronidazole of all the nitroreductase candidates in our 58 nitroreductase library. Expression of NfsB\_Vh in HCT-116 cells showed that this activated cell ablation capability was transferrable to mammalian cells.

The addition of FSL41, one of the masked fluorophores available in the lab, allowed fluorescence imaging of the cells containing NfsB\_Vh. In both bacterial and mammalian cells, FSL41 was shown to be present in cell populations unchallenged with metronidazole, but upon the addition of metronidazole, and the subsequent ablation of the cell population, the fluorescence disappeared. This confirmed that we are able to use masked fluorophores to report on a cell population before and after the addition of a nil bystander antibiotic.

### **5.2.3 Combined dual reporter/ ablation system**

The success of using a solely nitroreductase based system for the imaging/ ablation of a single cell population lead to the idea of a dual imaging/ ablation system – targeting two distinct populations of cells via two distinct nitroreductases, each able to activate one of two nil bystander antibiotics, and one of two masked fluorophores, with opposing activation profiles.

The complete screening of the 58 nitroreductase library against 16 nil bystander antibiotic candidates of interest enabled the generation of a colour coded heat-map to identify potential combinations for a more detailed evaluation by IC<sub>50</sub> assays. Promising nitroreductases identified via this screening method were then able to be screened with masked fluorophores to identify any that could be used in a multiplex reporter/ cell ablation system.

Growth inhibition assays undertaken in bacterial cells confirmed the identification of nitroreductases with opposing activation profiles. For example, the nitroreductases NfsA\_Li, NfsA\_Pp, and NfsA\_Ecaro are capable of activating tinidazole but not metronidazole, while NfsB\_Vv is capable of activating metronidazole, but not tinidazole. The IC<sub>50</sub> analysis of these nitroreductases with either tinidazole or metronidazole, indicated that NfsA\_Li was the most effective activator of tinidazole,

while at the same time having little to no ability to activate metronidazole. These results were the basis for selecting NfsA\_Li and tinidazole in combination with NfsB\_Vv and metronidazole as a promising dual nitroreductase ablation system. Unfortunately due to technical difficulties and time constraints, NfsA\_Li was unable to be transfected into HEK293 cells. The IC<sub>50</sub> analyses indicated that the next most effective activator of tinidazole that also exhibited minimal activation of metronidazole was NfsA\_Pp.

The addition of metronidazole and tinidazole to HEK293 cells expressing either NfsB\_Vv or NfsA\_Pp mirrored the results that were observed in bacterial cells; this was a pleasing outcome, as not all nitroreductases are capable of being stably transfected and expressed in mammalian cells (Prosser *et al.*, 2010; Prosser *et al.*, 2013). The success of these two nitroreductases in activating distinct nil bystander antibiotics without substantial overlap, show a promising proof of principle that they will be able to be utilised for experimental work in mammalian based research – although this has only been tested at a single cellular level it is a positive outcome likely to have practical applications in eukaryotic systems, especially zebrafish or *Xenopus* models.

The initial validation of a dual nitroreductase ablation system in both bacterial and mammalian cells led to the next step; adding a second factor to the system, a masked fluorophore, for imaging and reporting on ablation. Fluorophore screening was undertaken with a selection of masked fluorophores identified on the basis of previous work undertaken by Dr Horvat.

Again the initial screening was undertaken in bacterial cells, and promising combinations carried over into human cells. Results were consistent over both cell types. The nitroreductases that had initially indicated promise in terms of presenting opposing activation profiles with the nil bystander antibiotics, again showed opposing activation profiles to each other with masked fluorophores of different colours. The nitroreductases NfsA\_Li and NfsA\_Pp were identified as being capable of activating a green probe, FSL76 but not a red probe, FSL178; whereas NfsB\_Vv was capable of activating FSL178, but not FSL76.

Using a mixed population, mixed fluorophore model, and adding just one of the two possible nil bystander antibiotics, we observed that the masked fluorophores could report on the presence or absence (i.e. ablation) of cell populations expressing each nitroreductase. Thus, it appears that selective imaging and/or ablation of specific cells in a 2-way multiplexed nitroreductase expression system should be achievable in animal models.

#### **5.2.4 Niclosamide**

An interesting side story developed while screening the 58 nitroreductase library with the 16 nil bystander antibiotic candidates, when an anomaly in the activation profile of niclosamide was observed. In cell populations containing nitroreductases which are highly active with a particular prodrug, the population should be ablated upon the addition of that prodrug. Niclosamide however showed minimal growth inhibition with the most active nitroreductases in the library, and most tellingly, complete cell death with the empty pUCX plasmid. It appeared that the nitroreductases were conferring a protective effect on the cells.

Further investigation established that this protective effect was contingent on the *E. coli* host strain having its TolC exporter pump knocked out. Based on this observation, proof of principle experiments were conducted using solid media to show that niclosamide could be used to specifically select colonies over-expressing a functional nitroreductase enzyme. This interesting observation suggests that a single nitroreductase gene can act not only as a negative selection agent, but also a positive one, capable of defending the host cell against an otherwise toxic nitroaromatic insult. Possible applications of this technology are discussed in the following section.

### **5.3 Future Directions**

#### **5.3.1 GDEPT**

The ablation of a tumour-targeting vector used in the proposed three-step approach to GDEPT is the final step in what could potentially be a ground-breaking new therapy for the treatment of cancer. It is an essential step as many of the proposed vectors for this technology are of pathogenic origin, making their ablation post treatment an essential step for FDA approval.

This research has identified a number of lead nitroreductase/ nil bystander antibiotic combinations that could be tested for superior activity to NfsB\_Ec/ metronidazole. For example, a lot of NfsA family members showed very high levels of activity with *N*-benznidazole. Future experiments that could test the utility of these nitroreductase/ nil bystander antibiotic combinations for elimination of GDEPT vectors could be carried out in tumour xenograft models, using nitroreductase labelled bacterial or viral vectors, to confirm whether or not effective ablation of the vector can be achieved. If successful, this technology might have applications in other scenarios where an effective suicide gene is desirable as a safety control, for example in stem cell transplants, where the transplanted cell population could be rapidly ablated upon observing an adverse patient response.

### **5.3.2 Developmental and regenerative biological studies**

The nitroreductase based reporter/ ablation systems tested in this thesis could also have numerous applications in developmental and regenerative biology. The ability to use these in a multiplex fashion potentially adds another layer of complexity, providing the ability to selectively target multiple cell types at any chosen time during development, either simultaneously or successively, and with the added advantage that is not present with gene knock out technology; the potential for reversal of the ablation after the removal of the nil bystander antibiotic in regenerative models.

The results obtained in this study are still preliminary. The system has shown very promising results in both bacterial and human cell populations, with initial proof of principle experiments carried out in bacterial cells and the results observed to generally be translatable into human cells. The next step for this work is to apply the same parameters in whole model organisms. The most obvious choices for this would either be in *Xenopus* or zebrafish, as these have already been explored for single cell population ablation in promoter driven nitroreductase / fluorescent protein systems.

### 5.3.3 Niclosamide as a tool for directed evolution

The identification of a nil bystander antibiotic that had the opposite activation profile to that normally seen with nitroaromatic molecules – certainly to that observed with all other nil bystander antibiotics - led to the proposal of its use in the lab as a novel identifier of active nitroreductases, or its possible use as a tool for directed evolution. One application that is currently being investigated in the Ackerley lab is as a high throughput positive selection for identification of nitroreductases in metagenomic libraries (i.e. libraries of randomly purified and cloned DNA fragments sourced from a particular environment, e.g. soil). These libraries provide access to enzymes from the estimated 99% of microbes that cannot currently be cultured in the lab environment (Vartoukian *et al.*, 2010).

A dual niclosamide and antibiotic prodrug selection could also allow the directed evolution of nitroreductases for loss of activity with that prodrug, while still retaining generic nitroreductase activity (i.e. the ability to protect the host cell against niclosamide). This could prove especially useful for tailoring the activity of nitroreductases to be used in the dual reporter/ ablation system. For example, whereas NfsB\_Vv was strongly selective for metronidazole over tinidazole, NfsA\_Pp was less selective for tinidazole over metronidazole (Figure 3.7), and thus was an imperfect partner for the dual ablation scenario. To eliminate this residual activity with metronidazole, one approach could be to use error-prone PCR to generate a large library of *nfsA\_Pp* gene variants, to clone this library into a *tolC* deleted strain of *E. coli*, to select for clones that can grow in the presence of both metronidazole and niclosamide, and finally to then screen these clones to identify individual mutants that have lost activity with metronidazole but can still activate tinidazole effectively.

### 5.4 Concluding remarks

Nitroreductases have proven to be versatile enzymes, capable of being used for a range of different activities, and in various fields through their unique ability to metabolise a vast range of nitro-quenched compounds.

This study has built upon previous work in the Ackerley lab undertaken to exploit nitroreductases for their ability to activate nitro-quenched compounds, and has developed three novel ideas; a dual ablation/ reporter system for use in developmental and regenerative biological studies based solely around the activation properties of nitroreductases; a possible 2-way multiplex scenario, utilising two nitroreductases with opposing nil-bystander antibiotic/ masked fluorophore activation profiles; and a high throughput screening method utilising the anomaly observed in the activation profile of niclosamide.

Nitroreductases capable of superior activation of metronidazole to NfsB Ec, which is currently set as the ‘gold-standard’ of nitroreductase induced cell ablation in developmental biology studies, were identified. Likewise, promising candidates for activation of other nitro-quenched nil bystander antibiotics of interest, were uncovered. These results will help the expansion of nitroreductases for use in targeted cell ablation in both developmental biology, and a possible vector ablation system in GDEPT.

While these are the specific fields that this thesis has focused on, these results could have much further reaching impacts on various areas of research that utilise efficient nitroreductase catalysis.

The ability to partner masked fluorophores and nil bystander antibiotics both metabolised by the same nitroreductase will expand the utility of nitroreductases for targeted cell ablation, adding a built in reporter capability.

Niclosamide’s positive selection for active nitroreductases has led to the possibility of developing a high throughput screening method to identify nitroreductases that are currently not accessible, due to the inability of their host organisms to be cultured in the lab. This could further expand the repertoire of nitroreductases available to different fields of science.

In summary, this thesis has demonstrated the catalytic flexibility of nitroreductase enzymes, as well as their potential to have a beneficial impact on numerous fields of science and medicine, most prominently GDEPT and developmental biology.

## References

### Websites

<http://www.drugbank.ca/drugs/DB00916>, accessed 20.08.2013

<http://www.drugbank.ca/drugs/DB00911> accessed 20.08.2013)

<http://www.cancer.gov/drugdictionary?cdrid=39504> accessed 20.08.2013

<http://www.cancer.gov/drugdictionary?cdrid=458064> accessed 20.08.2013

<http://imaging.cancer.gov/programsandresources/fmiso-documentation> accessed 02.09.2013

<http://www.drugbank.ca/drugs/DB00614> accessed 20.08.2013

<http://www.drugbank.ca/drugs/DB06803> accessed 20.08.2013

<http://www.cancer.gov/clinicaltrials/search/view?cdrid=586650&version=HealthProfessional> accessed 20.08.2013

<http://www.drugbank.ca/drugs/DB00698> accessed 20.08.2013

<http://www.drugbank.ca/drugs/DB00336> accessed 20.08.2013

[www.invitrogen.com/content/sfs/manuals/gatewayman.pdf](http://www.invitrogen.com/content/sfs/manuals/gatewayman.pdf) accessed 29.09.2013

### Articles

Barak, Y., Thorne, S.H., Ackerley, D.F., Lynch, S.V., Contag, C.H., and Matin, A. New enzyme for reductive cancer chemotherapy, YieF, and its improvement by directed evolution. *Molecular Cancer Therapeutics* (2006). 5: 97–103

Basu, P.P. Rifaximin therapy for metronidazole-unresponsive *Clostridium difficile* infection: a prospective pilot trial. *Therapeutic advances in Gastroenterology* (2010) 4: 221-225

Benkli, K., Karaburun, A.C., Gundogdu-Karaburun, N., Demirayak, S., Guven, K., et al Synthesis and antimicrobial activities of some new nitroimidazole derivatives. *Archives of Pharamacal Research* (2003) 10: 773-777

Bhaumik, S., and Gambhir, S.S. Optical imaging of Renilla luciferase reporter gene expression in living mice (2002). *PNAS* 99: 377–382.

Bhaumik, S., Sekar, T.V., Depuy, J., Klimash, J., and Paulmurugan, R. Noninvasive optical imaging of nitroreductase gene-directed enzyme prodrug therapy system in living animals. (2011). *Gene Therapy*

Bremner, J.C Assessing the bioreductive effectiveness of the nitroimidazole RSU1069 and its prodrug RB6145: with particular reference to in vivo methods of evaluation. *Cancer Metastasis Reviews* (1993) 12: 177–193.

Brindle, K. New Approaches for Imaging Tumour Responses to Treatment. *Nature Reviews* (2008) 8: 94-107

Brown, J.M. Tumor hypoxia in cancer therapy. *Methods in Enzymology* (2007) 435:297-321

Bryant, D.W., McCalla, D.R., Leeksa, M., and Laneuville, P. Type I nitroreductases of *Escherichia coli*. *Canadian Journal of Microbiology* (1981) 27, 81–86.

Brown, J.M., Giaccia, A.J. The Unique Physiology of Solid Tumors: Opportunities (and Problems) for Cancer Therapy. *Cancer Research* (1998) 58: 1408

Brown, J. M., Wilson, W. R. Exploiting Tumour Hypoxia in Cancer Treatment. *Nature Reviews* (2004) 4: 437-447



Castro, J.A., Diaz de Toranzo, E.G. Toxic effects of nifurtimox and benznidazole, two drugs used against American trypanosomiasis (Chagas' disease). *Biomedical and Environmental Sciences* (1988) 1: 19-33

Chen, Y., Hu, L. Design of anticancer prodrugs for reductive activation. *Medicinal Research Reviews* (2009) 29: 29-64

Chen, S., Knox, R., Wu, K., Deng, P., S., Zhou, D., Bianchet, M. A., Amzel, L. M. Molecular Basis of the Catalytic Differences among DT-diaphorase of Human, Rat, and Mouse. *The Journal of Biological Chemistry* (1997) 272: 1437–1439.

Christofferson, A, Wilkie. J Mechanism of CB1954 reduction by *Escherichia coli* nitroreductase. *Biochemical Society Transactions* (2009) 37: 413

Croce, C.M. Molecular Origins of Cancer Oncogenes and Cancer. *The New England Journal of Medicine* (2008) 358: 502-511

Curado S, Stainier DY, Anderson RM: Nitroreductase-mediated cell/tissue ablation in zebrafish: a spatially and temporally controlled ablation method with applications in developmental and regeneration studies. *Nature protocols* (2008) 3(6):948-954

Curado, S., Anderson, R.M., Jungblut, B., Mumm, J., Schroeter, E., Stainer, Y.R., Conditional Targeted Cell Ablation in Zebrafish: A New Tool for Regeneration Studies. *Developmental Dynamics* (2007) 236: 1025–1035

Dachs, G. U., Hunt, M. A., Syddall, S., Singleton, D. C., Patterson A. V. Bystander or No Bystander for Gene Directed Enzyme Prodrug Therapy. *Molecules* (2009) 14: 4517-4545

Davison JM, Akitake CM, Goll MG, Rhee JM, Gosse N, Baier H, Halpern ME, Leach SD, Parsons MJ: Transactivation from Gal4-VP16 transgenic insertions for tissue-specific cell labeling and ablation in zebrafish. *Developmental biology* (2007) 304(2):811-824.

Deacon, J.M., Holliday, S.B., Ahmed, I., Jenkins, T.C. Experimental pharmacokinetics of RSU-1069 and its analogues: high tumor/plasma ratios (1986) International journal of radiation oncology, biology, physics 12: 1087-1090

Denny, W.A. The role of hypoxia-activated prodrugs in cancer therapy. The Lancet Oncology (2000). 1: 25–29.

Denny, W.A. Prodrugs for Gene-Directed Enzyme-Prodrug Therapy (Suicide Gene Therapy). Journal of Biomedical Biotechnology (2003) 1: 48-70

Denny WA, Wilson WR. Considerations for the Design of Nitrophenyl Mustards as Agents with Selective Toxicity for Hypoxic Tumor Cells. Journal of Medicinal Chemistry (1986) 29: 879-887

DeVita, V. T., Chu, E. A History of Cancer Chemotherapy. Cancer Research (2008) 68: 8643-8653

Greco, O., Dachs, G. U., Gene Directed Enzyme/Prodrug Therapy of Cancer: Historical Appraisal and Future Prospectives. Journal of Cell Physiology (2001) 187: 22–36

Gunay, N.S., Capan, G., Ulusoy, N., Ergenc, N., Otuk, G., Kaya, D. 5-Nitroimidazole derivatives as possible antibacterial and antifungal agents. Farmaco (1999) 54: 826-831

Hartley, J.L., Temple, G.F., Brasch, M.A. DNA cloning using in vitro site-specific recombination. Genome Research (2000) 10: 1788–1795

Kaya, F., Mannioui, A., Chesneau, A., Sekizar, S., Maillard, E., Ballagny, C., Houel-Renault, L., Dupasquier, D., Bronchain, O., Holtzmann, I., Desmazieres, A., Thomas, J.L., Demeneix, B.A., Brophy, P.J., Zalc, B., Mazabraud, A.. Live imaging of targeted cell ablation in *Xenopus*: a new model to study demyelination and repair. *The Journal of Neuroscience* (2012) 37: 12885-12895

Kennedy AS, Raleigh JA, Perez GM, Calkins DP, Thrall DE, Novotny DB, Varia MA. Proliferation and Hypoxia in Human Squamous Cell Carcinoma of the Cervix: First Report of Combined Immunohistochemical Assays. *International Journal of Radiation Oncology, Biology, Physics* (1997) 37: 897-905

Komar, G., Seppanen, M., Eskola, O., Lindholm, P., Gronroos, T. J., Forsback, S., Sipila, H., Evans, S. M., Solin, O., Minn, H.  $^{18}\text{F}$ -EF5: a new PET tracer for imaging hypoxia in head and neck cancer. *Journal of Nuclear Medicine* (2008) 49: 1944-1951

Koronakis, V., Eswaran, J., Hughes, C. Structure and function of TolC: the bacterial exit duct for proteins and drugs. *Annual Review of Biochemistry* (2004) 73: 467–489

Kremers, G.J., Gilbert, S.G., Cranfill, P.J., Davidson, M.W., Piston, D.W. Fluorescent proteins at a glance. *Journal of Cell Science* (2011) 124: 157-160

Löfmark, S., Edlund, C., Nord, C.E. Metronidazole Is Still the Drug of Choice for Treatment of Anaerobic Infections. *Clinical Infectious Diseases* (2010) 50: S16-S23

McCormick, F. Cancer Gene Therapy: Fringe or Cutting Edge? *Nature Reviews* (2001) 1: 130-141

Moreno, S.N., Docampo, R. Mechanism of toxicity of nitro compounds used in the chemotherapy of trichomoniasis. *Environmental Health Perspectives* (1985) 64: 199-208

Muller, M. Mode of action of metronidazole on anaerobic bacteria and protozoa. *Surgery* (1983) 93: 165-171

Osada, T., Chen, M., Yang, X.Y., Vandeusen, J.B., Hsu, D., Clary, B.M., Clary, T.M., Chen, W., Morse, M.A., Lyster, H.K., Antihelminth Compound Niclosamide Downregulates Wnt Signaling and Elicits Antitumor Responses in Tumors with Activating APC Mutations (2011) *Cancer Research* 12: 4172-4182

Padera, T., Stoll, B., Tooredman, J., Capen, D., di Tomaso, E., Jain, R. Pathology: Cancer Cells Compress Intratumour Vessels. *Nature* (2004) 427: 695

Parkinson, G.N., Skelly, J.V., Neidle, S. Crystal structure of FMN-dependent nitroreductase from *Escherichia coli* B: a prodrug-activating enzyme. *Journal of Medicinal Chemistry* (2000) 43: 3624-3631

Paterson, E.S., Boucher, S.E., Lambert, I.B. Regulation of the *nfsA* Gene in *Escherichia coli* by SoxS. *Journal of Bacteriology* (2002) 1: 51-8

Patridge, E.V., Ferry, J.G. WrbA from *Escherichia coli* and *Archaeoglobus fulgidus* is an NAD(P)H:quinone oxidoreductase. *Journal of bacteriology* (2006) 188: 3498-3506

Patterson, A.V., Ferry, D.M., Edmunds, S.J., Gu, Y., Singleton, R. S., Patel, K., Pullen, S. M., Hicks, K. O., Syddall, S. P., Atwell, G. J., Yang, S., Denny, W. A., Wilson, W. R. Cancer Therapy: Preclinical Mechanism of Action and Preclinical Antitumor Activity of the Novel Hypoxia-Activated DNA Cross-Linking Agent PR-104. *Clinical Cancer Research* (2007) 13: 3922-3932

Thanabalu T., Koronakis E., Hughes C., Koronakis V. Substrate-induced assembly of a contiguous channel for protein export from *E.coli*: Reversible bridging of an inner-membrane translocase to an outer membrane exit pore. *EMBO Journal* (1998) 17: 6487–6496

Theys, O Pennington' L Dubois' G Anlezark, T Vaughan' A Mengesha' W Landuyt, J Anne, P J Burke, P Dûrre, B G Wouters, N P Minton and P Lambin Repeated cycles of *Clostridium*-directed enzyme prodrug therapy result in sustained antitumour effects in vivo *British Journal of Cancer* (2006) 95: 1212–1219.

Pisharath, P., Parsons, M.J., Lieschke, G.J., Nitroreductase-Mediated Cell Ablation in Transgenic Zebrafish Embryos (2009) *Zebrafish, Methods in Molecular Biology*, vol. 546

Prasher, D.C., Eckenrode, V.K., Ward, W.W., Prendergast, F.G., Cormier, M.J. Primary structure of the *Aequorea victoria* green-fluorescent protein. *Gene* (1992) 111: 229-233

Prosser, G.A., Copp, J. N., Mowday, A.M., Guise, C.P., Syddall, S.P., Williams, E.M., Horvat, C. N., Swe, P.M., Ashoorzadeh, A., Denny, W. A., Smaill, J. B., Patterson, A. V., Ackerley, D.F. Creation and screening of a multi-family bacterial oxidoreductase library to discover novel nitroreductases that efficiently activate the bio-reductive prodrugs CB1954 and PR-104A. *Biochemical Pharmacology* (2013) 85: 1091-1103

Prosser, G. A., Copp, J. N., Syddall, S. P., Williams, E.M., Smaill, J. B., Wilson, W.R., Patterson, A.V., Ackerley, D. F. Discovery and Evaluation of *Escherichia coli* Nitroreductases that Activate the Anti-cancer Prodrug CB1954. *Biochemical Pharmacology* (2010b) 79: 678–687

Prosser, G. A., Patterson, A. V., Ackerley, D. F. UvrB Gene Deletion Enhances SOS Chromotest Sensitivity for Nitroreductases that Preferentially Generate the 4-hydroxylamine Metabolite of the Anti-cancer Prodrug CB1954. *Journal of Biotechnology* (2010a) 150: 190–194

Rainov, N. G. A Phase III Clinical Evaluation of Herpes Simplex Virus Type 1 Thymidine Kinase and Ganciclovir Gene Therapy as an Adjuvant to Surgical Resection and Radiation in Adults with Previously Untreated Glioblastoma Multiforme. *Human Gene Therapy* (2000) 11: 2389–2401

Sack, U., Walther, W., Scudiero, D., Selby, M., Kobelt, D., Lemm, M., Fichtner, I., Schlag, P.M., Shoemaker, R. H., Stein, U. Novel Effect of Antihelminthic Niclosamide on S100A4-Mediated Metastatic Progression in Colon Cancer. *Journal of the National Cancer Institute* (2011) 13: 1018-36

Sasaki, Y., Sone, T., Yoshida, S., Yahata, K., Hotta, J., Chesnut, J.D., Honda, T., Imamoto, F. Evidence for high specificity and efficiency of multiple recombination signals in mixed DNA cloning by the Multisite Gateway system. *Journal of Biotechnology* (2004) 107: 233-243

Sawyer, P.R., Brogden, R.N., Pinder, R.M., Speight, T.M., Avery, G.S., Tinidazole: A Review of its Antiprotozoal Activity and Therapeutic Efficacy. *Drugs* (1976) 6: 423-40

Schaller, T., Appel, N., Koutsoudakis, G., Kallis, S., Lohmann, V., Pietschmann, T., Bartenschlager, R. Analysis of Hepatitis C Virus Superinfection Exclusion by Using Novel Fluorochrome Gene-Tagged Viral Genomes *Journal of Virology* (2007) 9: 4591-4603

Schmidt, C. Amgen spikes interest in live virus vaccines for hard-to-treat cancers. *Nature Biotechnology* (2011) 29(4):295-296

Siim BG, Denny WA, Wilson WR. Nitro reduction as an electronic switch for bioreductive drug activation. *Oncology Research* (1997) 9(6-7):357-369

Singleton, D.C., Li, D., Bai, S.Y., Syddall, S.P., Smaill, J.B., Shen, Y., Denny, W.A., Wilson, W.R., Patterson, A.V. The Nitroreductase Prodrug SN 28343 Enhances the Potency of Systemically Administered Armed Oncolytic Adenovirus ONYX-411NTR. *Cancer Gene Therapy* (2007) 14: 953–967

Steib, A., Jacobberger, B., Von Bandel, M., Beck, F., Beller, J.P., Boudjema, K., Koffel, J.C., Otteni, J.C. Concentrations in plasma and tissue penetration of ceftriaxone and ornidazole during liver transplantation. *Antimicrobial Agents and Chemotherapy* (1993) 37: 1873-1876

Streker, K., Freiberg, C., Labischinski, H., Hacker, J., Ohlsen, K.. *Staphylococcus aureus* NfrA (SA0367) is a flavin mononucleotide-dependent NADPH oxidase involved in oxidative stress response (2005) 187: 2249-2256

- van Rossum, T., Kengen, S.W., van der Oost, J. Reporter-based screening and selection of enzymes *FEBS Journal* (2013) 13: 2979-2996
- Vartoukian SR, Palmer RM, Wade WG. Strategies for culture of 'unculturable' bacteria *Federation of European Microbiological Societies Microbiology Letters* (2010) 309:1-7.
- Vass, S.O., Jarrom, D., Wilson, W.R., Hyde, E.I., and Searle, P.F. *E. coli* NfsA: an alternative nitroreductase for prodrug activation gene therapy in combination with CB1954 (2009) *British Journal of Cancer* 100, 1903–1911.
- White, D.T. Mumm, J, S. The nitroreductase system of inducible targeted ablation facilitates cell-specific regenerative studies in zebrafish. *Methods* (2013) pub. Online March 2013. In Press.
- White, Y.A.R., Woods, D.C., Wood, A.W., A transgenic zebrafish model of targeted oocyte ablation and de novo oogenesis. *Developmental Dynamics* (2011) 240: 1929-1937
- Whiteway, J., Koziarz, P., Veall, J., Sandhu, N., Kumar, P., Hoecher, B., Lambert, I.B. Oxygen-Insensitive Nitroreductases: Analysis of the Roles of nfsA and nfsB in Development of Resistance to 5-Nitrofurantoin Derivatives in *Escherichia coli*. *Journal of Bacteriology* (1998) 21: 5529-5539
- Wilson, W.R., Pullen, S.M., Hogg, A., Helsby, N.A., Hicks, K.O., Denny, W.A. Quantitation of bystander effects in nitroreductase suicide gene therapy using three-dimensional cell cultures *Cancer Research* (2002) 5: 1425-32
- Wu, B., Piatkevich, K.D., Lionnet, T., Singer, R.H., Verkhusha, V.V. Modern Fluorescent Proteins and Imaging Technologies to Study Gene Expression, Nuclear Localization, and Dynamics. *Current Opinion in Cell Biology* (2011) 23: 310-317
- Zenno, S., Koike, H., Tanokura, M., Saigo, K. Gene cloning, purification, and

characterisation of NfsB, a major oxygen-insensitive nitroreductase from *Escherichia coli*, similar in biochemical properties to FRaseI, the major flavin reductase in *Vibrio fischeri*. *Journal of Biochemistry* (1996) 120: 736-744

Zhao XF, Ellingsen S, Fjose A. Labelling and targeted ablation of specific bipolar cell types in the zebrafish retina. (2009) *BMC Neuroscience* 10: 107